Ecophysiological modelling of the exchanges of CO18O and COS in terrestrial ecosystems: applications to the estimation of photosynthetic and respiratory fluxes at continental and global scales

Jérôme Ogée

Mémoire présenté à l'**Université de Bordeaux**
(école doctorale *Sciences et Environnements*)
Par **Jérôme Ogée**
Pour obtenir l'**Habilitation à Diriger des Recherches**
(Spécialité *Physique de l'Environnement*)

Modélisation éco-physiologique des échanges de $C^{18}OO$ et COS dans les écosystèmes terrestres: application à l'estimation des flux de photosynthèse et respiration aux échelles continentales et planétaires

Illustration humoristique de l'abstraction scientifique: vache sphérique, sur la Lune.
(https://fr.wikipedia.org/wiki/Vache_sphérique).

Soutenu devant le jury composé de :

Philippe Bousquet, Professeur, Université Versailles Saint Quentin, HDR (président)
Dani Or, Professeur, Université ETH Zürich (rapporteur)
Pierre Friedlingstein, Professeur, Université Exeter (rapporteur)
Philippe Peylin, Directeur de Recherche, CNRS, HDR (rapporteur)
Bernard Genty, Chargé de Recherche, CNRS (examinateur)
Yves Brunet, Directeur de Recherche, INRA (examinateur)

Table of Contents

Foreword

This manuscript presents a synthesis of the research I have conducted over the past 12 years in the "Functional Ecology and Environmental Physics" unit (EPHYSE) and, since 2014, in the "Soil-Plant-Atmosphere Interactions" unit (ISPA). The year 2007 is when I became "senior researcher" (CR1) at INRA. More importantly, it corresponds to the launch of my first multi-partner research project as principal investigator, the ANR-funded project MIST ("Modelling Isotope Signals in Tree-rings", 2007-2011). Thus 2007 marks well the beginning of my activities of "direction of research".

Over those 12 years, my research has been organised around 4 general themes, rapidly summarised in the Appendix I of this document. The core of the manuscript focuses on one of these research themes: the **development of multi-tracer approaches to predict with better accuracy photosynthetic and respiratory fluxes over land**. The tracers of interest here are the oxygen isotope composition of CO_2 ($C^{18}OO$) as well as carbonyl sulphide (COS). This activity around these two complementary tracers of the C cycle consumed a large part of my recent years of research and involves the work of many collaborators and students. There was thus plenty of material for a thesis, and allowed me to go more deeply into the subject.

In **chapter 1**, I give a brief historical overview of our understanding of the contemporary global C cycle and its link to the climate of the Earth. This naturally sets the rationale behind the on-going international effort to improve our predictions of the land C sink. It also naturally introduces the principles of using $C^{18}OO$ and COS as tracers of photosynthetic and respiratory fluxes over land as well as their pros and cons with respect to other approaches.

In **chapter 2**, I review in more details the recent (last 10 years) literature on the exchange of $C^{18}OO$ and COS between soils and the atmosphere. By doing so, I also summarise results from several articles that I co-authored recently on the subject and indicate how I envisage incorporating this new knowledge into land surface models for global scale applications. I close this chapter with a priority list of remaining questions to be addressed and future directions to be taken.

In **chapter 3**, I review our most recent understanding of the exchange of $C^{18}OO$ and COS between foliage and the atmosphere. This chapter also summarises results from several articles that I co-published recently on the subject. I also present unpublished results to illustrate how these new theories of COS and $C^{18}OO$ fluxes from foliage can be simplified and incorporated into global land surface models, using readily available parameters such as the maximum carboxylation rate of each plant functional type. I finally close the chapter listing remaining questions to be addressed.

Writing this memoire gave me the occasion to think more deeply about the motivations that push me and my colleagues to develop these multi-tracer approaches and what needed to be done to better promote them amongst the global C cycle research community. These ideas are developed in chapter 1 and briefly summarised in **chapter 4** in the light of the results presented in chapters 2 and 3.

Acknowledgements

First of all, I would like to thank Philippe Bousquet, Pierre Friedlingstein, Dani Or, Philippe Peylin, Bernard Genty and Yves Brunet for having accepted to be in my jury and spend time evaluating this work with their own eyes and expertise. The topic of the thesis can seem extremely focused from the outset but is actually very broad in reality, and many different expertise had to be gathered. I realised that some sections or chapters may seem too general to some, and too detailed to others. I tried to keep it balanced between the two extremes but the exercise was not always easy. I genuinely hope that each of you find something of interest in parts of this thesis.

The work presented here would have not been possible without the contributions of many great and enthusiastic people. I would like to acknowledge them here and thank them once again for their high-quality work. I particularly thank 'mister loud' Steven Wohl and 'mister cool' Régis Burlett, for their incredible ingenuity and both technical and ecological knowledge that they applied with enthusiasm to answer the research questions we wanted to address; 'mister stoic' Sam Jones for thinking so deeply on these soil microcosm experiments and water extraction lines and for always anticipating the next question; 'team players' Joana Sauze and Teresa Gimeno, for their positive spirit and sense of teamwork, and for responding always present for running new experiments; 'community planner' Aurore Kaisermann, for her contagious enthusiasm to work on this exotic gas COS and her planning skills for conducting experiments (and keeping offices and labs tidy!); 'witty' Jason West, for his great spirit and sense of humour, even when working on week-ends; 'intrepid' Laura Meredith, for her openness in sharing data and ideas with us, and her bravery and vision in tackling gas exchange and meta-genomics data at the same time.

The person who had the vision, it is first and foremost my main colleague, supportive partner and beautiful wife Lisa Wingate, as she imagined bringing this team around us and made it happen with so much energy and dedication. I remember Lisa, one of the first times we met in 2004, talking to me with so much excitement about micro-algae in soils and asking me why everybody working on $C^{18}OO$ ignored their existence. I thought at the time she was charming but a bit crazy too, and would have never imagined that 15 years later I would be sharing her enthusiasm and would have spent all this time helping her, with my humble physics and chemistry background, implement parameterisations of how these little soil bugs modify the $C^{18}OO$ and COS in the atmosphere.

This work would have not been possible without the continuous input and support from key colleagues, and most notably Alexandre Bosc, for his great input when we initiated the first gas exchange systems; Matthias Cuntz, for his incredible computing skills and his broad understanding of large-scale C cycle modelling, and Valérie Savornin, for her patience and dedication in managing the budgets and administration of our team. I would like to acknowledge here Bernard Genty again, not as a jury member but as a friend and great scientist, for all the long conversations we had, his great sense of humour and continuous stimulation. The work presented here and especially in chapter 3 has greatly benefited from his immense expertise in experimental and theoretical plant physiology.

It was a real pleasure to work with this young team of scientists. We had true moments of laughter thinking how much brain cells we were dedicating to understand the drivers of COS and $C^{18}OO$ exchange in soils. "Who cares about these tracers?" we were asking ourselves, realising how nerdy we were. However, by writing this thesis I realised how much progress we have made thanks to all these nerdy brain cells. There are always more things to be learnt and understood, but I can see that our understanding is now mature enough to be integrated into large-scale

models and applications. It would be a real shame if all this new knowledge that we have gained over the last few years on processes regulating atmospheric $C^{18}OO$ and COS does not benefit the larger community working on the contemporary global C cycle model. Having key players of this scientific community in my jury is a real honour and a chance to make this happen.

Chapter 1 – Historical overview and rationale

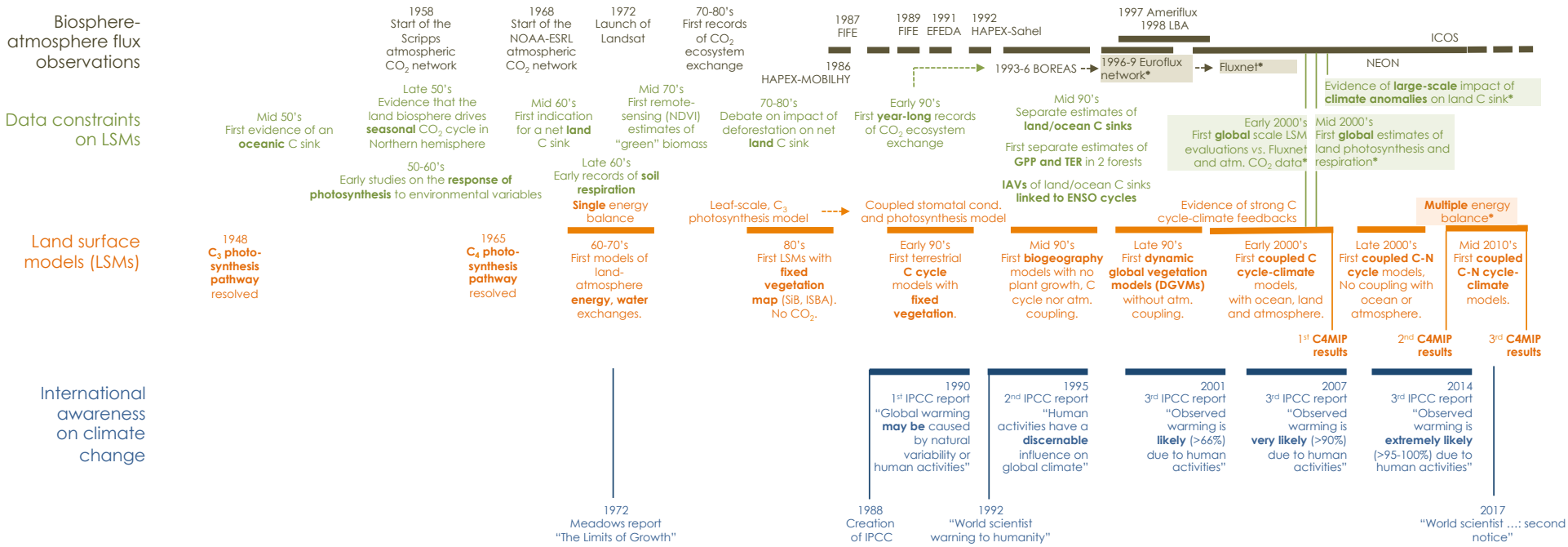

Figure 1.1 | Timeline of key breakthroughs related to the study of the contemporary C cycle over land and its feedbacks on climate, declined in 3 categories (biosphere-atmosphere flux observations, land surface modelling and their evaluation using large-scale datasets). I also added a fourth category (international awareness of climate change) to set these studies into a broader context. Shaded boxes with asterisks indicate the activities that I have contributed to. LSM: land surface model; GPP: gross primary production (i.e. gross photosynthesis); TER: total ecosystem respiration; C4MIP: coupled climate-carbon cycle models inter-comparison project; IAV: inter-annual variability; ENSO: El Niño Southern Oscillation.

1.1 History of the study of the contemporary global C cycle

Introduction

The study of the C cycle and its feedbacks on the climate of the Earth has been an ever-growing field of research, notably because of its relevance to address climate change and ecological questions. When I started my scientific career in 1997 as a PhD student and later postdoctoral fellow, the research community studying the C cycle was already well structured and a growing number of international programmes to monitor continuously the land-atmosphere exchanges of CO_2 and also water and energy were being launched (Fig. 1.1). To start this thesis, I thus felt important to go a little back in time and give a brief historical overview of our understanding of the contemporary global C cycle and its link to the climate of the Earth. This overview is clearly not exhaustive as the aim was mainly to present key studies that seemed relevant for introducing the atmospheric tracers of interest here ($C^{18}OO$ and COS).

1900-1950: early records of atmospheric CO_2 and recognition of the ocean sink

In the early 1900s, the greenhouse effect of atmospheric CO_2 was already recognised. Chamberlin in 1899 and Arrhenius in 1903 had even suggested that climatic changes must be in part related to changes in the CO_2 content in the air (see Revelle & Suess, 1957). It was also recognised that fossil fuel burning was probably impacting CO_2 levels in the atmosphere, but it was difficult to verify to what extent, as we did not have enough records of atmospheric CO_2 concentrations.

Atmospheric CO_2 concentration was also recognised to be highly variable, in contrast to oxygen, nitrogen and the rare gasses, and this variation was largely unexplained. In the late 1930's, initial observations of a slight increase of average temperature in the northern hemisphere led Callendar (1938) to conclude that all the excess CO_2 from fossil fuel must have remained in the atmosphere. In the mid 1950s, Callendar's conclusions were subsequently questioned, notably because the few records of CO_2 concentrations available at the time were not standardised, nor very accurate. A strong selection of the data had therefore to be done and could equally indicate a lack of any trend in atmospheric CO_2 since the 19th century (Slocum, 1955). Based on radiocarbon (^{14}C) measurements in wood (originating from atmospheric CO_2) and marine carbonate (from dissolved CO_2), Revelle and Suess estimated a mean residence time of CO_2 in the atmosphere before it is dissolved into the sea of *ca.* 10 years, suggesting that a large part of the excess CO_2 from fossil fuel must have already been transferred to the ocean (Revelle & Suess, 1957). They also recognised that atmospheric CO_2 could increase more rapidly in future decades if industrial fuel combustion continued to rise exponentially. 1957 was the launch of the International Geophysical Year. Revelle and Suess took this opportunity to call for more calibrated and standardised data collection of atmospheric CO_2 mixing ratio and isotope abundances in order to predict more accurately future changes in this important greenhouse gas.

60-70's: recognition of the land imprint on atmospheric CO_2

In 1955, Charles David (Dave) Keeling started collecting air samples in the atmospheric boundary layer at various locations in California far away from anthropogenic sources, and measured their CO_2 mixing ratios and isotopic abundances ($^{13}C/^{12}C$ and $^{18}O/^{16}O$) with high accuracy (Keeling, 1958). He first found large diurnal variations in the CO_2 mixing ratio, even at high elevations, with maximum values at night and early morning (Fig. 1.2). He also found that the $^{13}C/^{12}C$ and $^{18}O/^{16}O$ ratios of air CO_2 were related to the inverse of the CO_2 mixing ratio, the so-called 'Keeling plot' (Fig. 1.2). He explained this as a mixing of two CO_2 pools, one from the free atmosphere and one coming locally from a local source. The Keeling plot allowed him to identify the $^{13}C/^{12}C$ ratio of this local source and it fell well within the range of plant organic matter, which led him to

conclude that the diurnal variations that he recorded were caused by ^{13}C-depleted plant-respired CO_2 building up in the shallow atmospheric boundary layer at night. He also noticed that the CO_2 mixing ratio was always the same every afternoon even at distant locations. This was because the atmospheric boundary layer in mid afternoon usually mixes well with the free atmosphere. Dave Keeling was measuring the CO_2 mixing ratio in the free troposphere, whose value does not depend on local sources or sinks. He also recognised that the oxygen isotope abundances of CO_2 was close to that "in chemical equilibrium with average ocean water, but individual samples showed variations that generally did not correlate with changes in concentration in air and were as yet unexplained."

After setting up an observatory network of atmospheric CO_2 stations and aircraft measurements, including the famous one at Mt. Mauna Loa in Hawaii, Dave Keeling found that tropospheric CO_2 was variable but mainly in the Northern Hemisphere, and followed a clear seasonal cycle. Combined with the $^{13}C/^{12}C$ ratio data, it was concluded that vegetation mainly drove these seasonal variations of CO_2 in the Northern Hemisphere (Keeling, 1960). This was a real milestone in our understanding of the role played by vegetation in the carbon cycle. Dave Keeling also observed that, at the South Pole, the CO_2 concentration had increased by about 1.3 ppm per year which corresponded roughly to what was "expected from the combustion of fossil fuel (1.4 pmm) if no removal from the atmosphere was taking place" (Keeling, 1960). The study concluded that the ocean was a small CO_2 sink or that the land biosphere had counteracted the ocean sink.

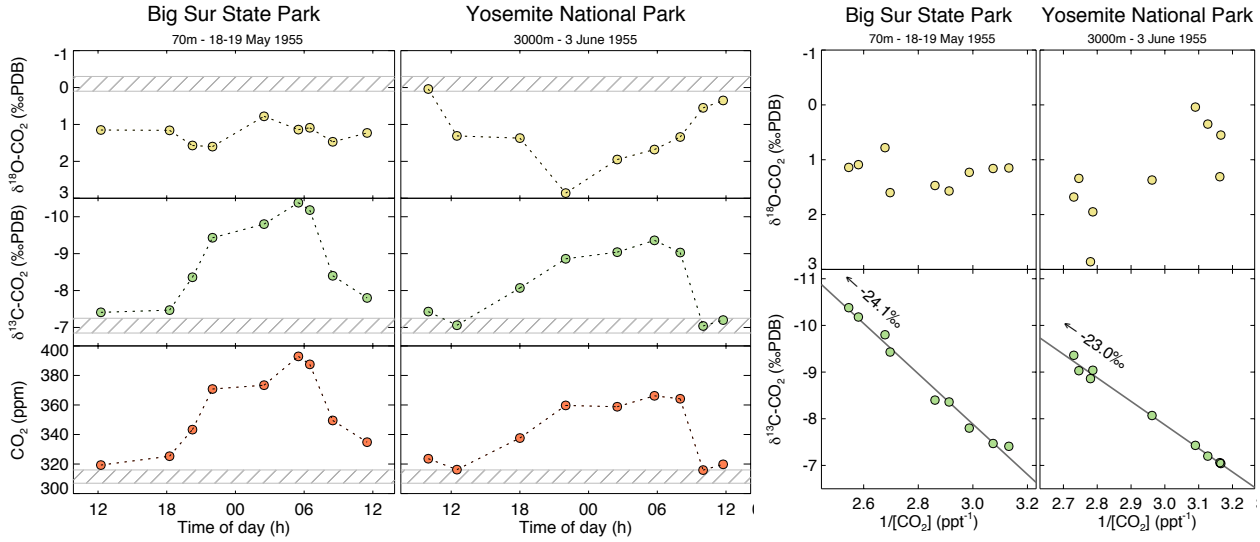

Figure 1.2 | Early records of CO_2 mixing ratios and stable isotope abundances ($^{13}C/^{12}C$ and $^{18}O/^{16}O$) in rural areas in California. Shaded areas correspond to the estimated tropospheric values. Redrawn from Keeling (1958).

Using longer records and seasonally-detrended Mauna Loa data, Bolin and Keeling later revised the increase rate to a lower value of about +0.72ppm per year (Bolin & Keeling, 1963). They concluded that anthropogenic CO_2 emissions (re-estimated around +1.6 ppm per year) were being absorbed, in large part ("probably between 50 and 60 per cent") in the oceans. This study was also the first observation-driven latitudinal distribution of CO_2 sources and sinks at the Earth's surface. Regrouping the CO_2 data into latitudinal regions and a simple 1D atmospheric transport model, Bolin and Keeling estimated a net transfer of CO_2 into the sea in each hemisphere above 30° and a net release in tropical regions. The land vegetation north of 45°N was also found "responsible for a net consumption of carbon dioxide of about 15Gt of CO_2 [4GtC] during the vegetation period in summer". However, the partitioning between land and ocean fluxes was

mostly driven by assumptions based on qualitative observations of the latitudinal CO_2 gradient and the distribution of land and ocean, and with limited knowledge of the atmospheric transport across latitudes.

70-80's: debate on the land biosphere contribution and initial bottom-up estimates

Until the 1970s, the land biosphere was recognised to influence greatly the seasonality of CO_2 in the northern hemisphere (Keeling, 1960; Bolin & Keeling, 1963), but it was still unclear if it acted as a net sink or a net source of atmospheric CO_2. This was partly because most studies at the time were so-called 'top-down' approaches, based on atmospheric concentration measurements and transport. The contribution of the land biosphere could not be easily separated from those of the oceans and fossil fuel emissions, and was thus deduced as a residual term, with very little constraints on the other terms and the atmospheric transport.

In the late 70's and early 80's a debate started about the impact of deforestation on the land C sink. Several research groups reported the land biosphere as a C source due to deforestation. Using agricultural and forestry statistics to estimate the rate of land use change, and estimates of the amounts of organic carbon within an ecosystem following forest harvest, the land biosphere was estimated to be a net source of atmospheric CO_2, greater than fossil fuel emission since 1960 and in the range of 1.8-4.7 GtC by 1980 (Houghton *et al.*, 1983). This result from one of the first 'bottom-up' approach was a real milestone but could not be easily reconciled with our understanding of the atmospheric CO_2 budget. For example, Broecker *et al.* (1979), reviewing results from recent models of atmospheric and ocean CO_2 budget were finding "no compelling evidence (…) that the terrestrial biomass ha[d] decreased at a rate comparable to that of fossil fuel combustion over the last two decades".

The 1970s was also the time when the general public started to become aware that human activities in general, and fossil fuel emissions in particular, were possibly affecting the Earth's climate worldwide. The Meadows report "The limits of growth" was published in 1972 (my year of birth…) and advocated the need to reduce human population and economic growths to better manage natural resources. The report also recognised that "it was not known how much CO_2 or thermal pollution could be released without causing irreversible changes in the Earth's climate" and that "this ignorance about the limits of the Earth's ability to absorb pollutants should be reason enough for caution in the release of polluting substances" (Meadows *et al.*, 1972).

Motivated by the increasing need in crop production, plant physiologists were also making great progress in the understanding and modelling of plant photosynthesis. The development of portable leaf cuvette and infrared gas analysers simplified the study of leaf photosynthesis and its response to environmental conditions. This led to the emergence of various forms of biochemical models of leaf photosynthesis (see Caemmerer *et al.*, 2009 for a review). In particular, the model of Farquhar, von Caemmerer and Berry (1980) became a real landmark in linking plant primary productivity to environmental conditions such as light, temperature and nutrient availability. It also formed the basis for our current understanding of carbon isotope discrimination during photosynthesis (Farquhar *et al.*, 1982). However, because it required knowledge of enzyme-kinetics parameters that were not well documented at the time, this photosynthetic model was still considered a research tool difficult to use in field-scale applications. Instead, simpler and empirical forms such as the light-use efficiency canopy photosynthesis model that relates gross primary productivity to the total sunlight absorbed by the canopy was proposed and tested (Monteith, 1977), sometimes with a separated treatment of the sunlit and shaded parts in the canopy (Sinclair *et al.*, 1976).

In 1972, the launch of the Earth Resources Technology Satellite 1 (ERTS-1, later called Landsat 1) opened a new era in the monitoring of the land biosphere. This satellite was monitoring the entire Earth and equipped with multispectral sensors notably in the red and near infrared (NIR) bands. Rouse *et al*. (1973) used the now-famous normalized difference vegetation index (NDVI), defined as the ratio of the difference in the NIR and red bands to their sum, and found a strong correlation between this new spectral index and green biomass over the Great Plains. This demonstrated how remote-sensing products could be used to monitor crop yield or vegetation biomass at the large scale.

The 1970's also witnessed the first records of energy, water and CO_2 ecosystem exchanges over crops (see Baldocchi *et al.*, 2001 for a review). The method used at the time was not mature enough to allow continuous measurements, nor reliable to measure fluxes over tall vegetation such as forest canopies. It is not until the late 1980s, when technological advances in sonic anemometry, infrared spectrometry, and digital computers were made, that land-atmosphere exchanges could be reported more routinely over agricultural and natural vegetation, in various atmospheric conditions. This led to the launch of regional scale experiments that measured fluxes of energy, water and sometimes CO_2 over land such as HAPEX-MOBILHY in southwest of France or FIFE in Kansas, USA.

The 70-80s were clearly a unique period during which different disciplines, from remote sensing and plant physiology to agronomy and micrometeorology, were integrated towards quantifying global photosynthesis over land. Yet, by the end of these two decades, it was still not clear whether the terrestrial biosphere acted as a sink or a source of atmospheric CO_2. This period also coincides with the creation of the International Panel on Climate Change (IPCC) in 1988 and the release of the first IPCC report in 1990. In this report, evidence for global warming was given but it could not be concluded yet that this warming was attributed to human activities rather than to natural climate variability.

90's: towards a consensus that the contemporary land biosphere is a C sink

Until the 1990s, global-scale land surface models (LSMs) were developed mostly for meteorological applications and described only energy, momentum and water exchanges at the land surface. These models did not describe the C cycle over land but were forced by fixed vegetation maps to represent different land surfaces characterized mostly by their roughness and leaf area and their ability to control water losses *via* stomata (see Sellers *et al.*, 1997a for a review).

In the early 1990s several groups started to integrate the leaf-level photosynthesis model of Farquhar *et al*. (1980) into a canopy radiative transfer model designed for large scale applications using satellite remote sensing data (Bonan, 1991; Sellers *et al.*, 1992). Global-scale biogeochemical models of the C turnover in soils were also being developed (e.g. Schimel *et al.*, 1994). In parallel, growing records of remote-sensing images revealed that deforestation rates in the Amazon, previously taken from forest inventories, had been overestimated (e.g. Skole & Tucker, 1993). The combination of these new land C cycle models with satellite images opened new avenues for obtaining independent, 'bottom-up' estimates of the land-atmosphere CO_2 fluxes.

An increasing number of programs monitoring CO_2 in the ocean boundary layer across the globe also helped refined our estimates of ocean-atmosphere CO_2 fluxes. Combining this new knowledge and budget of atmospheric CO_2, Tans and colleagues concluded that a large amount of the CO_2, of the order of 2-2.7 GtC yr^{-1}, must be absorbed in the northern hemisphere (NH) by terrestrial ecosystems (Tans *et al.*, 1990). It first came out as a surprise because there was virtually

no other direct evidence at that time for such a strong C uptake by northern ecosystems. A follow-up study reported that this NH C sink had a strong inter-annual variability (Conway *et al.*, 1994). These studies relied mostly on atmospheric CO_2 measurements and were not without uncertainties. However, additional evidence for the existence of a large land C sink in the northern hemisphere came a few years later from concurrent measurements of atmospheric O_2/N_2 ratios (Keeling *et al.*, 1996) and $^{13}C/^{12}C$ ratios of CO_2 (Ciais *et al.*, 1995).

The newly-developed models of canopy photosynthesis (Sellers *et al.*, 1992) and soil C turnover (Schimel *et al.*, 1994) were combined with the carbon isotope photosynthetic discrimination model of Farquhar *et al*. (1982) to disentangle the CO_2 flux over the vegetation from that over the ocean or from fossil fuel emissions (Ciais *et al.*, 1995). The atmospheric data was first used to estimate the surface fluxes of total CO_2 and $^{13}CO_2$ in each latitudinal band. The atmospheric transport of the two tracers was inverted using a model that had been previously validated against measurements of trichlorofluoromethane and ^{85}Kr, a constraint that did not exist in earlier studies (e.g. Bolin & Keeling, 1963). For each latitudinal region, the net fluxes of CO_2 and $^{13}CO_2$ were then "de-convoluted" in terms of land, ocean and fossil fuel fluxes using estimated values of their carbon isotope 'signatures' (I.e. the ratio of the $^{13}CO_2$ flux to the CO_2 flux). The global-scale photosynthesis and soil respiration models could have been used to compute the land CO_2 flux directly but were used here only to estimate the isotopic signature of that flux. It is because the isotopic disequilibrium between fossil fuel, ocean or land fluxes was expected to be strong enough to provide robust de-convoluted fluxes from atmospheric data, even with large errors associated to the isotopic signatures (Ciais *et al.*, 1995). The results confirmed those of Tans *et al*. (1990) that the land biosphere, especially in the northern hemisphere, was acting as a net sink for CO_2. For 1992 this land sink was estimated at 1.5 GtC globally, and as high as 3.5 GtC in the northern temperate and boreal regions, while the tropical regions were found to be a CO_2 source of about 2 GtC (Ciais *et al.*, 1995). The main source of uncertainty was found to be associated with the atmospheric sampling, in the order of ±1 GtC, or even more if other sources of uncertainties were accounted for (but see also Keeling *et al.*, 2017). Ten years of AVHRR NDVI data between 1981 and 1991 later supported the idea that plant growth had been occurring in northern latitudes during that decade (Myneni *et al.*, 1997).

Two seminal studies, combining also atmospheric CO_2 and $^{13}C/^{12}C$ ratio measurements to disentangle ocean from land CO_2 fluxes, found the first evidence that the large inter-annual variability of the global ocean and land C sinks was strongly associated to the El Niño/Southern Oscillation (ENSO) cycles (Francey *et al.*, 1995; Keeling *et al.*, 1995). Globally, It was found that the oceans were typically larger sinks during El Niño events, whereas the terrestrial biosphere was the reverse (Francey *et al.*, 1995; Keeling *et al.*, 1995).

The first year-long records of net CO_2 ecosystem exchange started in 1991 at Harvard forest in Massachusetts (Goulden *et al.*, 1996) and in 1994 during the large scale experiment BOREAS in Canada (Sellers *et al.*, 1997b). Both studies showed that those forests acted as a net CO_2 sink, between 1.4-2.8 tC ha^{-2} yr^{-1} at Harvard forest and 0.9-1.2 tC ha^2 yr^{-1} at the black spruce forest in Canada. These early eddy covariance measurements were instrumental in the launch of eddy covariance 'flux tower' networks worldwide such as Euroflux in Europe, Ameriflux in North America or LBA in the Amazon basin (Fig. 1.3).

As estimates of the net CO_2 flux over land were getting more and more precise, several research groups attempted to estimate process-level fluxes such as photosynthesis and respiration, with the idea to test newly-developed models of these gross CO_2 fluxes at local to global scales (Williams *et al.*, 1997; Sellers *et al.*, 1997b). Having continuous sub-hourly measurements of the

net ecosystem exchange allowed to study separately ecosystem respiration and gross photosynthesis. Nocturnal CO_2 fluxes measured during windy nights were used to develop a respiration versus temperature relationship for the forest that was then applied at other periods to separate the net exchange into gross photosynthesis and respiratory fluxes. Maximum rates of photosynthesis were much higher at Harvard forest than at the boreal site (Sellers *et al.*, 1997b). At comparable light levels, photosynthesis was also higher in cloudy conditions than under clear sky. These partitioning algorithms still form today the basis of flux-based, global-scale estimates of land photosynthesis (Reichstein *et al.*, 2005; Beer *et al.*, 2010; Lasslop *et al.*, 2010).

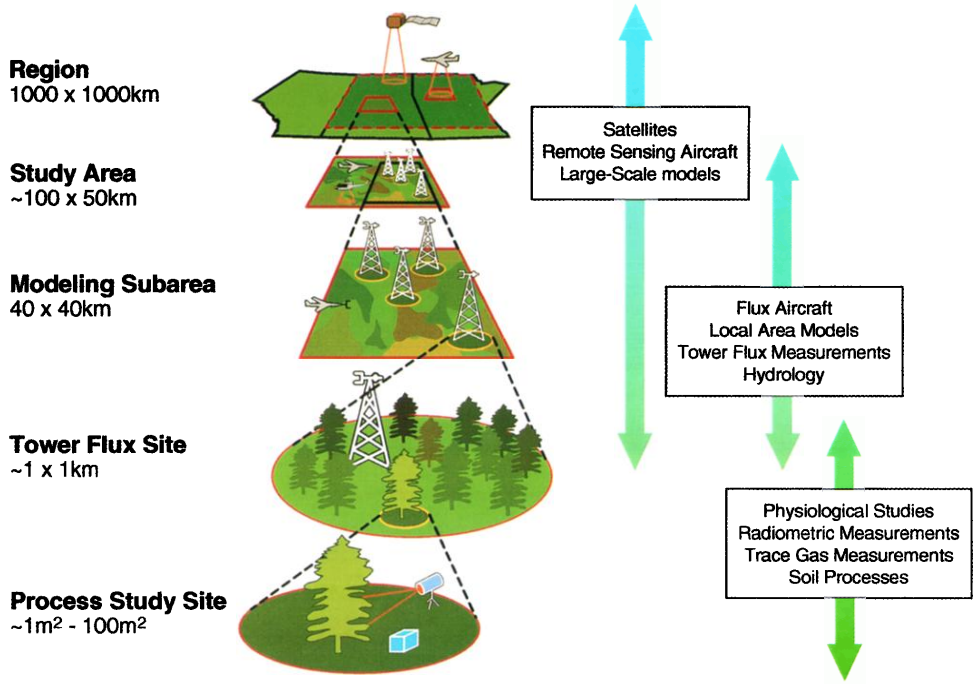

Figure 1.3 | Multiscale measurement strategy used in BOREAS (1993-1996) and in later programs (e.g. LBA or the Regional Experiment of CarboEurope-IP). Taken from Sellers *et al.* (1997b).

90's: $C^{18}OO$ identified as a large scale tracer of photosynthesis over land

Although eddy covariance measurements of the net CO_2 ecosystem exchange were rapidly spreading across ecosystems, they were still too sparse to estimate photosynthesis and respiration at scales larger than the ecosystem. On the other hand, the oxygen isotope composition[1] of atmospheric CO_2 had been identified as a potential tracer to disentangle photosynthesis and respiration at continental and global scales.

From the ever-growing atmospheric CO_2 flask network, it was getting clearer that the $\delta^{18}O$ of CO_2 displayed a strong north-south gradient (Fig. 1.4) that involved very large CO_2 fluxes over land (Francey & Tans, 1987). Francey and Tans argued that this "enormous" North-South gradient reflected "the oxygen isotope ratio in ground water, *via* mechanisms involving gross catalysed CO_2 exchange with leaf (and possibly) soil water." Using a simple 2-box model for the Northern Hemisphere, each box containing 175GtC (i.e. a quarter of the atmosphere), but with ground

[1] Following international practices, we will express the isotope composition of CO_2 or water as a deviation to an international standard (VPDBg for CO_2 and VSMOW for water). For example, the oxygen isotope composition of CO_2 is: $\delta^{18}O = R_{CO2}/R_{VPDBg} - 1$, where R_{CO2} denotes the $^{18}O/^{16}O$ ratio of CO_2 and $R_{VPDBg} = 0.002088349077$ is the $^{18}O/^{16}O$ ratio of the international standard VPDBg. To a good approximation, R_{CO2} can be estimated as $0.5[C^{18}OO]/[CO_2]$ where the brackets denote dry-air mixing ratios.

water pools differing by 10‰ (taken from the latitudinal gradient in precipitation, see Rozanski *et al.*, 1992) and an exchange time between the two boxes of 0.25 yr, they estimated that, to create an average gradient of 1.2‰ (the average difference between Mauna Loa, Hawaii, and Point Barrow, Alaska, in 1984-1985), fluxes of the order of 200 GtC yr^{-1} were required[2].

From the work of Mills and Urey (1940) on un-catalysed CO_2-H_2O isotopic exchange kinetics, they estimated that such a large flux could not be the result of an isotopic exchange with ocean waters (too slow and in the opposite direction as the atmospheric gradient) or with water droplets in clouds (too slow as well). They also estimated that fossil fuel combustion should contribute at the most to a 0.3‰ inter-hemispheric gradient. Francey and Tans thus concluded that the large CO_2 fluxes responsible for the North-South gradient of $\delta^{18}O$ in atmospheric CO_2 must be on land.

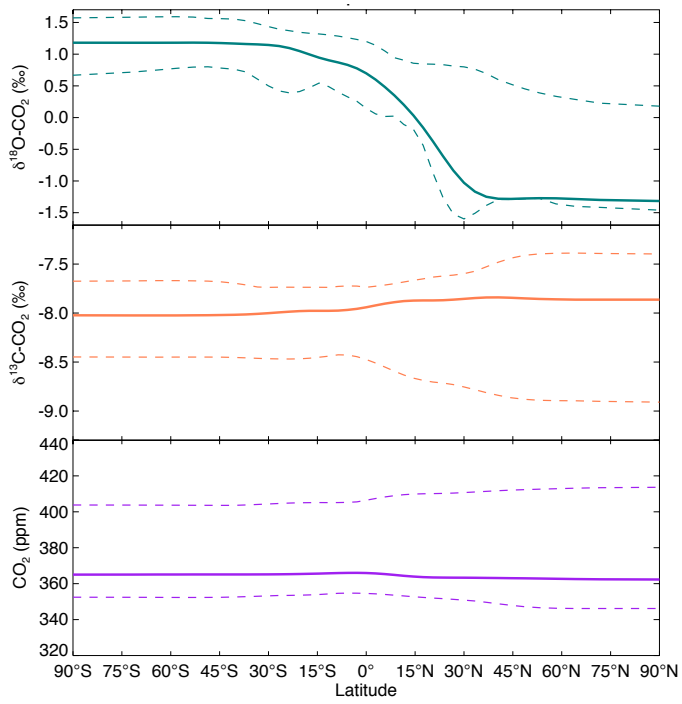

Figure 1.4 | Mean North-South gradient of dry-air atmospheric CO_2 and its isotopic abundance in September 1998 (strongest El Niño on record). Dotted lines show minimum and maximum values over the period 1991-2017. Data from the NOAA ESRL Carbon Cycle Cooperative Global Air Sampling Network (www.esrl.noaa.gov/gmd/ccgg/).

Based on the observations that the ratio of CO_2 concentration in the intercellular air space of leaves (C_i) to the outer air (C_a) is rather constant during photosynthesis, around 0.67 (Wong *et al.*, 1979), they estimated that "one third of the CO_2 entering the leaves is fixed during photosynthesis while two-thirds diffuses back out". Leaves were already known to contain large amounts of carbonic anhydrase (CA, see review by Badger & Price, 1994), an enzyme that was known to catalyse very efficiently CO_2 hydration and thus CO_2-H_2O isotopic exchange rates (Silverman, 1973; 1982). This led Francey and Tans to conclude that a flux about twice the size of net photosynthesis was going back to the atmosphere,

[2] The mass balance equations for the two-box model of the Northern hemisphere proposed by Francey and Tans can be formalised as:

$$\begin{cases} \left(\delta_{s1}-\delta_{a1}\right)F_1+\left(\delta_{a2}-\delta_{a1}\right)F_{mix}=0 \\ \left(\delta_{s2}-\delta_{a2}\right)F_2+\left(\delta_{a2}-\delta_{a1}\right)F_{mix}=0 \end{cases} \quad \text{(Eq. 1.1)}$$

where δ_{a1}, δ_{a2} are the $\delta^{18}O$ in CO_2 at Mauna Loa and Barrow ($\delta_{a2} = \delta_{a1} - 1.2‰$), δ_{s1}, δ_{s2} are the $\delta^{18}O$ in CO_2 in equilibrium with the water pools ($\delta_{s2} = \delta_{s1} - 10‰$), F_{mix} is the exchange flux between the two boxes ($F_{mix} = 175/0.25 = 2\times M_a$ GtC yr^{-1}, where $M_a = 350$ GtC is the *total* CO_2 content of the Northern hemisphere) and F_1 and F_2 are the CO_2 exchange fluxes in each box between the surface (ocean, land, cloud droplets) and the atmosphere (exchange with the Southern hemisphere is neglected). Assuming further that $F_1 \approx F_2$, and subtracting the two mass balances Eq. 1.1 leads to: $F \approx 4\times1.2/(10\text{-}1.2)\times M_a \approx 0.55\times M_a \approx 193$ GtC yr^{-1}.

carrying an isotopic signal of the leaf water pool. However they also recognised that, if this large "one-way" flux could explain the inter-hemispheric gradient, it would also generate an atmospheric signal with a stronger seasonality and values about 1-2‰ too enriched compared to the observations. This is because water pools in a transpiring leaf is more enriched in ^{18}O compared to source (soil) water, as described by Dongmann *et al*. (1974). They finally concluded that CO_2 exchange with soil water pools, catalysed "either by the presence of carbonic anhydrase in soils or by inorganic catalytic sites such as metal oxides", must also contribute to the $\delta^{18}O$ signal in atmospheric CO_2. Similar conclusions were made simultaneously by Friedli *et al*. (1987) based on measurements of vertical gradients of CO_2 mixing ratio and $\delta^{18}O$ over Switzerland.

Farquhar *et al*. (1993) proposed a formalism enabling a more precise quantification of the $C^{18}OO$ flux coming from photosynthesis. They recognised that the C_i/C_a ratio, rather than being constant at 0.67, can vary with environmental conditions (notably air relative humidity, temperature or CO_2 mixing ratio C_a). They also acknowledged that carbonic anhydrase (CA) is located inside the mesophyll cells so that the CO_2 back diffusing from the intercellular air space has not yet equilibrated with leaf water. Using optimum stomatal conductance theory (Cowan & Farquhar, 1977) and a CO_2 concentration difference between the intercellular air space and the CA site inside the mesophyll cells of $0.1C_a$ (i.e. $C_i - C_{CA} = 0.1C_a$) they estimated a global mean C_{CA}/C_a ratio of 0.57. With this number, they calculated that, on average, it takes 2.2 years for the entire atmospheric CO_2 to interact with leaf water pools, compared to 8.3 years with surface ocean water[3].

Farquhar *et al*. (1993) also estimated the average oxygen isotope composition of CO_2 in equilibrium with leaf water using measurements of the $\delta^{18}O$ in precipitation (Rozanski *et al*., 1992) and estimates of the ^{18}O disequilibrium between precipitation and water vapour over continents from a climate model (Jouzel *et al*., 1991). Using a simplified (pre-industrial) atmospheric mass balance, they concluded that oxygen isotope exchange with leaf and soil water pools was the main cause of the large north-south gradient in the $\delta^{18}O$ of atmospheric CO_2. They also acknowledged that different biomes having markedly different $C^{18}OO$ fluxes, the $\delta^{18}O$ of atmospheric CO_2 could "allow the identification of components of the terrestrial biota currently acting as net C sinks."

At the same time similar efforts were being made to refine estimates of $C^{18}OO$ fluxes from soil surfaces (Hesterberg & Siegenthaler, 1991; Tans, 1998). As for leaves, these fluxes included the effect of the one-way fluxes in and out of the soil carrying different isotopic signals as CO_2 interacted with soil water. This can be formally written as:

$$F = F_{in} - F_{out} \tag{1.2a}$$

$$0.5^{18}F = \alpha_d F_{in} R_a - \alpha_d F_{out} R_{eq} = \alpha_d F R_{eq} - \alpha_d F_{in}\left(R_{eq} - R_a\right) \tag{1.2b}$$

[3] For these estimates, Farquhar *et al*. used an atmospheric CO_2 content of M_a = 62.5 Pmol (750 GtC), a gross ocean-to-air flux of 7.5 Pmol (90 GtC) and a (back-of-the-envelope) net land photosynthetic flux of 12.5 Pmol (150 GtC). With a global mean C_{CA}/C_a ratio of 0.57, the one-way flux of CO_2 inside leaves (see p. 19) is $F_{in} = 12.5C_a/(C_a - C_{CA}) \approx 29$ Pmol. Then it takes $62.5/12.5 \approx 5$ yr for a CO_2 molecule to be carboxylated, $62.5/7.5 \approx 8.3$ yr for a CO_2 molecule to see surface ocean water and $62.5/F_{in} \approx 2.2$ yr for a CO_2 molecule to enter a leaf. However, to truly estimate the time it takes to be hydrated, we should use the one-way flux out $F_{out} = 12.5C_{CA}/(C_a - C_{CA}) \approx 16.6$ Pmol, leading to $62.5/F_{out} \approx 3.8$ yr for a CO_2 molecule to be hydrated inside a leaf.

F and ^{18}F denote the net CO_2 and $C^{18}OO$ fluxes from the soil (soil respiration) or the leaf (net leaf assimilation), α_d is the fractionation factor during diffusion from the outside air to the site of equilibration (in the soil or the leaf) and R_a and R_{eq} are the $^{18}O/^{16}O$ ratio of CO_2 in the air and in equilibrium with the (soil or leaf) water pool. The factor 0.5 accounts for the fact that there is only one ^{18}O atom per $C^{18}OO$ molecule.

For photosynthesis, the one-way flux F_{in} is usually expressed as the product of the CO_2 mixing ratio in the air (C_a) and the total conductance for CO_2 (through the leaf boundary layer, stomatal pores and inside the leaf to the point where CA-catalysed CO_2 hydration takes place): $F_{in} = g_{tc}C_a$. Similarly, $F_{out} = g_{tc}C_{CA}$. Because the ratio C_{CA}/C_a is rather conservative, F_{out} is often written as $\kappa_c F$ where $\kappa_c = C_{CA}/(C_a - C_{CA})$ is around 1.33 globally (Farquhar *et al.*, 1993). Then $F_{in} = (1 + \kappa_c)F$ so that the net leaf $C^{18}OO$ flux is (roughly) proportional to net photosynthesis F (Eq. 1.2b).

For soils, g_{tc} is replaced by the "piston velocity", defined as the effective $C^{18}OO$ diffusivity through the soil matrix divided by the depth (z_1) where "isotope equilibration with soil water and diffusive escape to the atmosphere are equally important, and above which isotope equilibration is incomplete" (Hesterberg & Siegenthaler, 1991). Although CA activity from soils had been acknowledged as a possible important mechanism affecting the $\delta^{18}O$ of atmospheric CO_2 (Francey & Tans, 1987), most studies at the time considered that CO_2 hydration in soils operated at the uncatalysed rate, so that z_1 was large and the piston velocity was negligible (Hesterberg & Siegenthaler, 1991). In this situation $F_{in} \approx 0$ and the net soil $C^{18}OO$ flux is simply proportional to soil respiration F (Eq. 1.2b).

These theories of $C^{18}OO$ fluxes over land were incorporated in the land surface model SiB2 and transported using a 3D atmospheric transport model (Ciais *et al.*, 1997a; 1997b; Peylin *et al.*, 1999). After adjustments of the fractionation factor during CO_2 diffusion in soils (α_d) to close the atmospheric $C^{18}OO$ budget, a first study concluded that, at the global scale, the land biota dominates the ^{18}O budget in CO_2 and "exchange with the canopy produces an isotopic enrichment of CO_2, whereas exchange with soils has the opposite effect" {(Ciais *et al.*, 1997a; 1997b). By looking at the contribution of each process to the inter-hemispheric and seasonal variations in the $\delta^{18}O$ of atmospheric CO_2, it was also concluded that the inter-hemispheric gradient was determined primarily by respiration over land (Ciais *et al.*, 1997b), and particularly over continental Siberia (Peylin *et al.*, 1999).

These "bottom-up" approaches clearly demonstrated the potential of the $\delta^{18}O$ of atmospheric CO_2 as a tracer for CO_2 gross fluxes over land. They also showed that our understanding of the processes regulating the $C^{18}OO$ atmospheric budget was almost complete. Yet, estimates of land photosynthesis and respiration by the different LSMs were not questioned nor corrected using the tracer but used as an input to identify the drivers of the seasonal cycle and inter-hemispheric gradient in atmospheric $C^{18}OO$.

2000s: inter-annual variability in the C sinks and first coupled C-climate models

At the beginning of the new millennium, atmospheric CO_2 transport inversion techniques had reached maturity and were now able to retrieve not only land and ocean CO_2 sinks but also their inter-annual variability (Bousquet *et al.*, 2000; Le Quéré *et al.*, 2003). It was found that the land C sink had an inter-annual variability larger than the ocean (Bousquet *et al.*, 2000; Le Quéré *et al.*, 2003) and this variability was dominated by tropical or extra-tropical ecosystems depending on the time window (Bousquet *et al.*, 2000). Also both ocean and land C sinks were shown to increase steadily with time and their sensitivity to ENSO cycles was in line with previous findings at the global scale (e.g. Keeling *et al.*, 1995).

These atmospheric inversions results were in broad agreement with a network of ocean C fluxes estimated from measurements of the CO_2 partial pressure gradient at the surface of the ocean (Bousquet *et al.*, 2000; Le Quéré *et al.*, 2003). Increasingly refined land and ocean C models also agreed with the idea that the C fluxes from the terrestrial biosphere were more variable on a year-to-year basis than those over the ocean. However the large inter-annual variability predicted by land C models differed in "where an how they attributed the shifts to underlying processes (photosynthesis and respiration)" (Bousquet *et al.*, 2000).

Around the same time, these land and ocean C models were starting to be fully coupled to climate models. Until then, climate models included the C cycle and its effects on climate (CO_2, albedo…) but it was assumed to be insensitive to climate change. With this new generation of coupled climate-carbon cycle models we were able to study the feedbacks on the climate caused by the interactive response of the land and ocean C fluxes to warming, increasing CO_2 and climate variability. The first coupled climate-carbon cycle simulations suggested an extra increase in atmospheric CO_2 of +200ppm by 2100 compared to a simulation without climate-carbon cycle feedbacks (Cox *et al.*, 2000). This 'positive' feedback (in the sense of an enhanced warming) was mainly driven by a runaway increase in soil respiration caused by CO_2-induced warming. Another study using a different model also found a positive but much weaker climate-C cycle feedback (Dufresne *et al.*, 2002) and this was later explained by differences in the sensitivity of the Southern ocean C sink to the increase in CO_2 (Friedlingstein *et al.*, 2003). These two studies revealed the importance of accounting for these feedbacks when projecting climate change, and initiated the launch of the Coupled-Carbon-Cycle-Climate Model Inter-comparison Project (C4MIP) that gathers now more than ten global models worldwide.

By the mid 2000s, the number of multiannual datasets of energy, water vapour and CO_2 fluxes had significantly increased and spread over a wide range of ecosystem types (Baldocchi *et al.*, 2001). These fluxes allowed testing the ability of land surface models in predicting the heat, water and CO_2 exchanges with the atmosphere from sub-hourly to annual timescales. A systematic assessment of the data quality was not available as it is now because the technique was still developing and each group adapted their eddy covariance systems to their specific needs and situations (frost, snow, pollution, slope, flux footprint, power supply…). With my background in micrometeorology acquired duing my PhD years, I selected a total of 87 years of half-hourly flux data, using criteria based on energy balance closure and atmospheric stability conditions. I then used this dataset to evaluate the land surface model ORCHIDEE over different biomes and from daily to seasonal time scales (Krinner *et al.*, 2005). Some biomes were clearly underrepresented, notably in tropical regions, but the strengths and weaknesses of the model in predicting key components of the energy, C and water cycles over land could still be identified. Sensible heat fluxes were almost systematically overestimated, and thought to be due to the use of a single energy balance for vegetation and soil. Discrepancies on the diurnal and/or seasonal variations of water and CO_2 fluxes emphasised weaknesses in the model in reproducing stomatal response to water deficits, notably in Mediterranean and C_3 grasslands (Krinner *et al.*, 2005; Friend *et al.*, 2007). Overall, these model-data comparisons mostly showed that the land surface models succeeded in capturing the main differences between plant functional types at both diurnal and seasonal time scales (Morales *et al.*, 2005; Friend *et al.*, 2007). However, it was also noted that a complete model validation over annual to decadal timescales required information on the balance between assimilation and respiration processes, information not readily available from net CO_2 flux measurements (Reichstein *et al.*, 2005; Friend *et al.*, 2007).

The heat wave that hit a large part of Europe in spring and summer 2003 was used as an opportunity to test our ability to predict changes in the land C sink and its component fluxes photosynthesis and respiration during such extreme climate anomaly. Using eddy covariance net CO_2 flux measurements, remotely-sensed NDVI data and country-level crop yields, we reported that the European 2003 heat wave resulted in a strong anomalous net C source of about 0.5 PgC yr^{-1} that reversed the effect of four years of carbon sequestration (Ciais *et al.*, 2005). The effect of this Europe-wide climate anomaly on ecosystem productivity was further assessed using the land surface model ORCHIDEE, validated against eddy covariance and remotely sensed data. Results from the model suggested that reduction in productivity had been caused by rainfall deficits in Eastern Europe and by extreme heat in the western part, and that ecosystem respiration decreased together with gross primary productivity under water limitations (Ciais *et al.*, 2005; Reichstein *et al.*, 2007).

Empirical evidence for large-scale C-cycle–climate interactions such as the European heat wave are scarce and of limited temporal projection. The assessment of these interactions over longer time scales (decades to centuries) could be attempted only by means of coupled carbon-cycle-climate models. A comparison of different model simulations over the period 1850-2100 using the same CO_2 emission scenario revealed a large variety of response amongst models. While almost all the models predicted a land C sink during the 19th and 20th centuries, a strong divergence between the models started to emerge during the 21st century (Friedlingstein *et al.*, 2006). In some models, the land C 'sink' turned into a substantial C source, strongly amplifying global warming. The widespread of results from the different model simulations demonstrated the very poor understanding of processes such as photosynthesis and respiration in determining the net land C uptake, as "no consensus emerged among the models" (Friedlingstein *et al.*, 2006).

2000s: searching for data constraints on photosynthesis and respiration over land

The uncertainty around the inter-annual and long-term trend of land photosynthesis and respiration stimulated research to find observational constraints on these gross CO_2 fluxes. Algorithms using net ecosystem CO_2 exchange measurements and ancillary climate data were being developed and refined (Reichstein *et al.*, 2005). Several groups also explored further the possibility to use measurements of CO_2 isotopologues ($^{13}CO_2$, $C^{18}OO$) as additional constraints on these gross CO_2 fluxes.

Carbon isotope discrimination during photosynthesis depletes the assimilated sugars in ^{13}C. This discrimination fluctuates with environmental conditions and these fluctuations are smoothed over time in the $^{13}C/^{12}C$ ratio of the pool of carbohydrates used for growth and respiration. This creates carbon isotope disequilibrium between photosynthesis and respiration at a sub-daily to seasonal time scale. It had been suggested that this isotopic disequilibrium, although small, might carry enough information to partition photosynthesis and respiration (Yakir & Wang, 1996; Bowling *et al.*, 2001). We evaluated this proposition using atmospheric $^{13}CO_2$ measurements performed in a temperate forest (Ogée *et al.*, 2003). We found that the partitioning worked best in mid-afternoon when isotopic disequilibrium was the strongest. The partitioning method had an uncertainty on mean gross CO_2 fluxes around 15-20% over a 22-day period. However, the method seemed limited because too sensitive to some poorly constrained parameters such as the isotopic fractionation during respiration or the mesophyll conductance to CO_2 (Ogée *et al.*, 2003). A full error propagation analysis also showed that the uncertainty on the *instantaneous* (hourly) gross CO_2 fluxes retrieved using atmospheric $^{13}CO_2$ data remained very large. This led us to the conclusion that the ^{13}C disequilibrium between photosynthesis and respiration was too small to make the atmospheric ^{13}C signal a useful tracer of these gross CO_2 fluxes (Ogée *et al.*, 2004). We

also suggested that the ^{18}O in CO_2 had greater potential ought to the much stronger ^{18}O disequilibrium that was expected between photosynthesis and respiration.

However, studies on the $\delta^{18}O$ in CO_2 were starting to show more evidence that the CO_2 escaping the leaf interior was not always in full isotopic equilibration with leaf water (Gillon & Yakir, 2000a; 2000b; 2001). Large differences in leaf CA activity were reported among major plant types (Gillon & Yakir, 2001) leading to an estimated extent of ^{18}O equilibration ($0 \leq \theta_{eq} \leq 1$) as low as 0.1 in some species, with a clear distinction between C_3 trees and shrubs (high θ_{eq}) and C_4 grasses (low θ_{eq}) and a global mean of 0.78. Although this made $C^{18}OO$ a potential indicator of changes in C_3 and C_4 productivity and distribution (Gillon & Yakir, 2001), it also complicated substantially the interpretation of this tracer in terms of gross CO_2 fluxes over land. Indeed, a reduction of the extent of ^{18}O equilibration in leaf water pools reduced the influence of photosynthesis (and strengthened that of respiration) on atmospheric $C^{18}OO$ (Cuntz *et al.*, 2003b). It was also found that the a strong reduction of θ_{eq} in C_4 grasses changed, but not improved, the seasonality of the $\delta^{18}O$ in CO_2 at various atmospheric stations (Cuntz *et al.*, 2003b).

At the same time, studies started to demonstrate also that the 'invasion' of atmospheric CO_2 (i.e. the diffusion of CO_2 into the soil followed by partial equilibration with soil water and retro-diffusion) may not be negligible (Miller *et al.*, 1999; Stern *et al.*, 2001). Using a modelling approach, and without evoking any biological (CA-driven) isotopic exchange with soil surfaces, it was shown that this "non-biological" $C^{18}OO$ flux was significant in many biomes and, at the global scale, larger than the annual fossil fuel combustion (Stern *et al.*, 2001). Laboratory experiments also showed that it was an essential component of the soil $C^{18}OO$ flux that influenced strongly the estimation of the depth of equilibration (Miller *et al.*, 1999). In one experiment, and evoking the possible "presence of CA or other catalytic processes", the CO_2 hydration rate had to be increased to 20 times the un-catalysed rate to reconcile the CO_2 and water isotope data (Miller *et al.*, 1999).

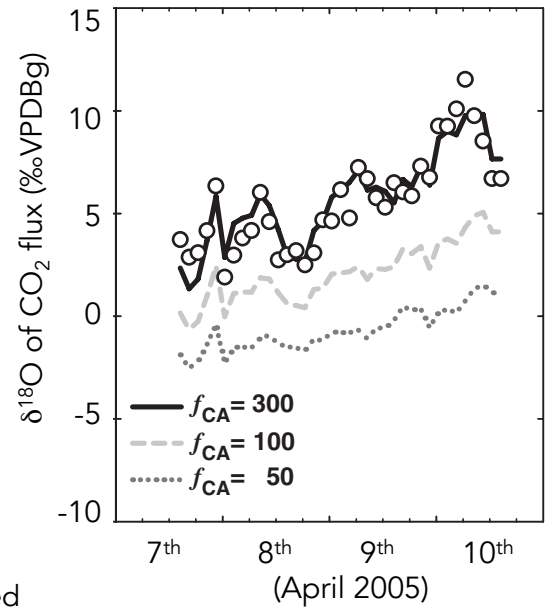

Figure 1.5 | Observed (circles) and simulated (lines) oxygen isotope signature of the soil CO_2 flux in a Mediterranean oak savannah woodland. Simulations were performed with an un-catalysed (f_{CA}=1) or enhanced (f_{CA}>1) CO_2 hydration rate in the soil. Redrawn from Wingate *et al.* (2008).

A few years later, a series of field studies demonstrated that soil CA activity had to be evoked to reproduce accurately the strong diurnal and seasonal variations of soil-air $C^{18}OO$ fluxes in natural settings (Seibt *et al.*, 2006; Wingate *et al.*, 2008; 2010) (Fig. 1.5). The exact role of CA on these isotope fluxes was not demonstrated but based on the literature data showing that CA was a widespread enzyme found in many soil dwelling organisms such as bacteria and fungi (Smith *et al.*, 1999; Wingate *et al.*, 2008). By compiling all the soil-air $C^{18}OO$ field data from different

studies, we later showed that an enhancement of the isotopic exchange with soil water pools compared to the uncatalysed rate had to be evoked in all datasets (Wingate *et al.*, 2009). This enhancement factor varied between 20 and 300 depending on biomes. Using the isotope-enabled global scale model MECBETH (Cuntz *et al.*, 2003a), we also showed that this enhanced CO_2 hydration rate in soils had large implications on the North-South gradient of the $\delta^{18}O$ in CO_2 (Fig. 1.6) and on its interpretation in terms of gross CO_2 fluxes (Wingate *et al.*, 2009).

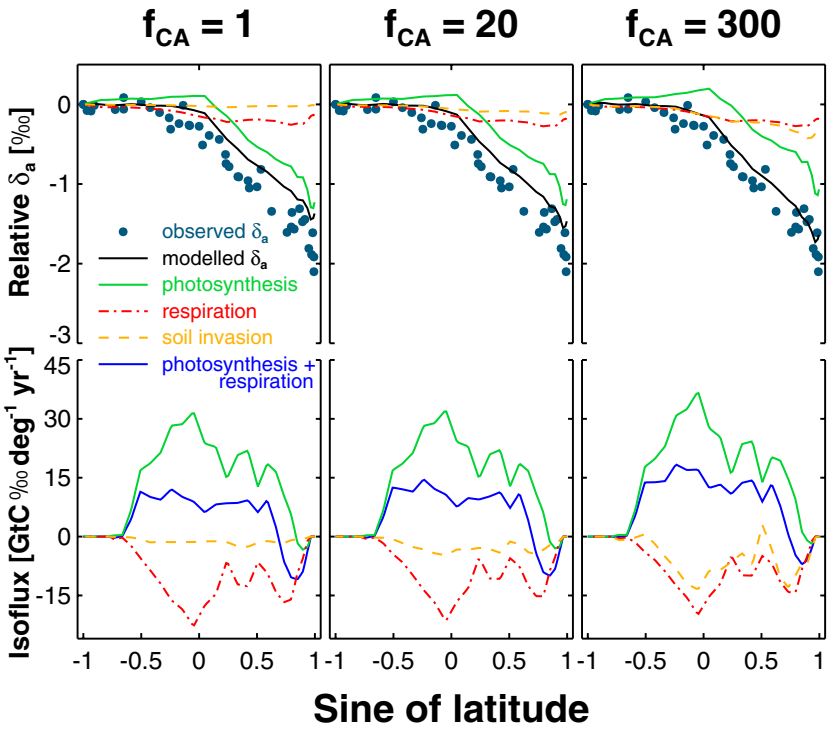

Figure 1.6 | Simulated contributions of different biospheric processes to the N-S gradient in the $\delta^{18}O$ of CO_2 (δ_a) for un-catalysed (f_{CA}=1) or enhanced (f_{CA}>1) CO_2 hydration rates in the soil, compared with measured δ_a. Enhanced hydration increases the corresponding isofluxes of soil invasion and photosynthesis + respiration, i.e., the isotopic imbalance required for gross flux partitioning. Note that δ_a values are always reported relative to the South Pole and thus do not show the absolute changes in δ_a. After Wingate *et al.* (2009).

The increasing need for independent estimates of photosynthesis and respiration over land led research groups to find alternative solutions besides atmospheric tracers. Refinements in CO_2 flux partitioning techniques (Reichstein *et al.*, 2005; Lasslop *et al.*, 2010), combined with machine-learning algorithms to upscale spatially the results, started to emerge. Using an artificial neural network trained on flux-derived gross photosynthesis and gridded climate data, a global distribution of terrestrial photosynthetic fluxes was produced for the period 1998-2005 (Beer *et al.*, 2010). The gridded product of terrestrial photosynthesis exhibited a clear latitudinal distribution, with a much smaller uncertainty in the tropics when compared to the between-model variations of an ensemble of land surface C cycle models. These LSMs also showed higher spatial correlations between photosynthesis and precipitation than suggested by the data-driven approach, suggesting "the existence of missing processes or feedback mechanisms in the models" (Beer *et al.*, 2010). The data-driven approach was then proposed as a benchmark for testing global land surface models.

At about the same time, another estimate of global land productivity was estimated using an impressive 30-year long record of $^{18}O/^{16}O$ ratio in CO_2 (Welp *et al.*, 2011). Noting that the inter-annual variability of the $\delta^{18}O$ in precipitation, but also in CO_2, were correlated with ENSO cycles, it was suggested that El Niño events were creating a pulse change in the isotopic records that faded out afterwards *via* the isotopic exchanges occurring in the ocean and on land (in soils and leaves). Based on a 2-box inter-hemispheric model and the isotopic record, the average decay rate of these pulses over the 30-yr long period was estimated and related to the average photosynthetic rate over the same period. Using estimates of the soil invasion flux (Wingate *et al.*, 2009) and the degree of equilibration in foliage (Gillon & Yakir, 2001), they arrived at a best guess of global productivity of 150-175 PgC yr^{-1}. This number was some 25-45% more than the one derived from eddy covariance data (Beer *et al.*, 2010) but was also quite sensitive to the values taken for the soil invasion flux and the degree of equilibration in leaves, two rather uncertain parameters (see above). Collectively, these results demonstrated that the interpretation of atmospheric $C^{18}OO$ signals was more complicated than previously thought, and that, to be able to use the $\delta^{18}O$ in CO_2 as a tracer of the C cycle, having a more accurate picture of the drivers of CA activity in soils and leaves was becoming a priority.

At about the same time, a few studies suggested that carbonyl sulphide (COS) could be another potential tracer of land photosynthesis (Montzka *et al.*, 2007; Campbell *et al.*, 2008). Until then, this trace gas had been studied mostly for its large contribution to the global sulphur cycle and its greenhouse potential as a stratospheric aerosol (Kettle *et al.*, 2002). A growing network of atmospheric stations was recording the seasonal and latitudinal variations of COS and CO_2 in the troposphere (Montzka *et al.*, 2007). The seasonal variations of COS in the northern hemisphere paralleled those of CO_2 but with nearly 5-fold larger amplitude. These variations in the northern hemisphere were recognised as being driven to a large part by photosynthetic activity over land (Montzka *et al.*, 2007; Campbell *et al.*, 2008). The link between COS uptake by vegetation and photosynthesis had been recognised for some time (Kesselmeier & Merk, 1993) but it was the first time that COS was proposed as a C cycle tracer.

Enzymatic and manipulation studies had demonstrated that the uptake of COS by plants, and also oxic soils, was driven by carbonic anhydrase activity (Protoschill-Krebs & Kesselmeier, 1992; Protoschill-Krebs *et al.*, 1996; Kesselmeier *et al.*, 1999). The parallel with the processes regulating atmospheric $C^{18}OO$ was evident and it was anticipated that any progress that we would make on the understanding of the drivers regulating one tracer would directly benefit the understanding and applicability of the other tracer. It seemed therefore logical to attempt using the two C cycle tracers in combination.

The work that I will develop in the next chapters was initiated in this general context. The challenges that we had to face were two fold. First, it required getting a deeper understanding of the biotic and abiotic drivers of CA activity in leaves and soils. Second, it required developing algorithms of these drivers that could be implemented in global C cycle models, using readily available state variables and parameters.

Before closing this chapter, I felt it was important to attempt clarifying what would be the added value of using these atmospheric tracers, in the context of the current state of understanding of the C cycle and the breadth of other approaches that are being developed to constraint photosynthesis and respiration over land. This is discussed in the following section.

1.2 Rationale

As briefly summarised, our understanding of the contemporary C cycle has greatly improved over the last decades. We are now certain that both land and ocean contribute to the mitigation of anthropogenic CO_2 emissions, in almost equal proportions but with different long-term trends and inter-annual variability (IAV). While both land and ocean C fluxes have IAVs that are related to ENSO cycles, the IAV of the land C sink is larger than that of the ocean and driven by climate anomalies affecting drought-sensitive ecosystems (Poulter *et al.*, 2014; Ahlström *et al.*, 2015; Bastos *et al.*, 2016; 2018). It has also been recognised that northern hemisphere ecosystems largely contribute to the global C carbon sink, and with an increasing trend (Ciais *et al.*, 2019).

This improved understanding has been made possible with the use of satellite products, land surface models and atmospheric transport inversions. These different approaches have now been reconciled within their own uncertainties, even over specific regions (e.g. Ciais *et al.*, 2010; Le Quéré *et al.*, 2015). However, model-ensemble (LSM) results are still too spread to help reduce the uncertainties on the land C sink obtained from atmospheric inversions (Le Quéré *et al.*, 2015). In addition, and contrary to LSMs, bottom-up observation-based approaches are still in strong disagreement with atmospheric inversions, highlighting "observational gaps and limitations of data-driven models in tropical lands, but also North America" (Zscheischler *et al.*, 2017). The trends of the Northern Hemisphere land C sink from LSMs and atmospheric inversions are also in disagreement, whereby atmospheric inversions typically predict a steeper trend of the land C sink compared to LSMs (Ciais *et al.*, 2019). Yet these models are the only tools available to project the future of the land C sink, and thus climate change.

Because of the almost two orders of magnitude difference between the net ecosystem CO_2 exchange and its component gross fluxes, photosynthesis and respiration, the future of the land C sink is still extremely uncertain (Friedlingstein & Prentice, 2010; Friedlingstein *et al.*, 2014). Small uncertainties in projected photosynthesis can translate into large uncertainties in the future land C sink and consequently climate change projections. To reduce the large model uncertainty and the associated climate change projections we need to find observational constraints of these two large CO_2 fluxes over climate sensitive regions, and at intra-annual to decadal time scales (Friedlingstein & Prentice, 2010; Wenzel *et al.*, 2016).

Recent reviews on global photosynthesis estimates from LSMs, eddy-covariance flux measurements and remote sensing products reported annual sum values ranging from 100 to 170 PgC yr^{-1} and trends[4] varying from 0.005 to 0.621 PgC yr^{-1} (Anav *et al.*, 2015; Ryu *et al.*, 2019). Also, while observation-based estimates of global photosynthesis from flux measurements and remote-sensing data show little IAV and trend, global photosynthesis from LSMs have a large IAV (Zscheischler *et al.*, 2014; Anav *et al.*, 2015) as well as significant trends (Anav *et al.*, 2015), in good 'coherence' with atmospheric CO_2 observations (Wenzel *et al.*, 2016).

Global photosynthesis estimates from both flux and remote-sensing data rely on rather crude models such as light-use efficiency (LUE) models. This is a major issue because it means that they are nothing more than simplified LSMs (i.e. LUE models), forced by remotely sensed data or trained on ecosystem flux measurements. They are informative in the sense that they can be used to evaluate the added value of using more elaborate LSMs that include other processes (temperature acclimation, nutrient and hydraulic constraints, ecosystem response to rain

[4] These figures exclude estimates from sun-induced fluorescence products from the GOME satellite that predict an unrealistic collapse of land photosynthesis because of sensor degradation (Ryu *et al.*, 2019).

pulses,…) but their result is also dictated by the structural relationships that is implied between GPP and climatic drivers. To address this issue, some groups are developing machine learning methods where the predictors (climate, remotely-sensed products…) are prescribed but the relationships between them and the CO_2 fluxes are only inferred from the data, allowing a larger flexibility (Anav *et al.*, 2015; Ryu *et al.*, 2019). Still, the success of the machine learning approach depends on the representativeness of the input datasets, both spatially and temporally, and flux data are lacking tremendously in some regions like the tropics (Schimel *et al.*, 2015). More critical, these photosynthetic estimates from eddy covariance data or remote sensing products are limited in their capacity to extrapolate to completely different environmental conditions, and are therefore not able to predict future C fluxes.

There would be a lot to gain in using observational constraints of global photosynthesis that could be directly related to LSMs output, without duplicating them (i.e. recalculating photosynthesis). This would open avenues to develop data assimilation techniques directly into the LSMs, although at some computational cost. More importantly, it would lift the confusion that revolves around the many meanings of what we call 'photosynthesis' (Wohlfahrt & Gu, 2015). During the day, mature leaves both take up CO_2 *via* 'true' photosynthesis and emit CO_2 *via* maintenance respiration and photorespiration, resulting in a net flux into the leaf that we call *net* photosynthesis. At night, only maintenance respiration takes place. Photosynthetic fluxes reported by LSMs are what we call 'apparent' photosynthesis, i.e. true photosynthesis minus photorespiration. This is because these two fluxes are both light-dependent processes that cannot be separated, except in low oxygen environments. Conceptually, flux-based and remote-sensing approaches are also targeting 'apparent' photosynthesis. However, in practice, flux-based estimates are probably closer to true photosynthesis (Wohlfahrt & Gu, 2015).

As we briefly presented above, the $C^{18}OO$ fluxes are mostly proportional to the one-way fluxes of CO_2 in and out of the leaves, which are related to *net* photosynthesis only when the ratio C_{CA}/C_a is maintained constant. Similarly, the COS fluxes are more directly linked to the one-way flux of CO_2 into the leaves and to stomatal conductance than to net or 'apparent' photosynthesis (Seibt *et al.*, 2010). In addition, at night, photosynthesis stops but leaves can continue to take up COS and exchange $C^{18}OO$ with the atmosphere as long as stomata remain open. Thus, in the same way as sun-induced fluorescence may help improve the representation in LSMs of light absorption and conversion within the canopy, i.e. the light-limited rates of photosynthesis, COS and $C^{18}OO$ may help better parameterise the diffusional and enzymatic limitations of photosynthesis, but also transpiration.

So far, measurements of COS mixing ratio or the $^{18}O/^{16}O$ ratio in CO_2 have contributed little to the overall understanding of the C cycle. It has mainly been shown that the inter-hemispheric gradient and seasonal cycle of $\delta^{18}O$ in CO_2 are in broad agreement with a global photosynthetic flux over land between 90-100 GtC yr^{-1} (e.g. Ciais *et al.*, 1997b; Peylin *et al.*, 1999; Cuntz *et al.*, 2003b) and 150-175 GtC/yr (e.g. Farquhar *et al.*, 1993; Welp *et al.*, 2011), while atmospheric COS budgets are coherent with a large photosynthetic C uptake by vegetation in the northern hemisphere (Montzka *et al.*, 2007), and a trend of about +30% for global-scale land photosynthesis over the last century (Campbell *et al.*, 2017). Only one study (Welp *et al.*, 2011) has attempted to produce estimates of the land photosynthesis from $^{18}O/^{16}O$ ratio in CO_2 but it was only a 30-yr mean, global estimate with a surprisingly high value (150-175 PgC yr^{-1}). Clearly these two tracers are still largely under-used. Their sensitivity to C fluxes in the northern hemisphere and the strong link of the $\delta^{18}O$ signal in CO_2 to ENSO cycles are key advantages that should be useful to refine our predictions of the future of the land C sink using LSMs. For this, we

need to develop parameterisations of the $C^{18}OO$ and COS fluxes that could be easily implemented in the different LSMs, either online or offline. This implementation should be done coherently, not only between the tracers, but also with the different C and water fluxes and pools simulated by the models. Only then we will be able to gain insight from these atmospheric tracers on the models' structural strengths and weaknesses. This requires a deeper physiological understanding of the biotic and abiotic drivers regulating CA activity and COS and $C^{18}OO$ fluxes in soils and plants. Progresses on this front are summarised in the next two chapters.

Chapter 2 – Soil-air $C^{18}OO$ and COS exchange

2.1 Introduction

The transport and fate of trace gases in porous media has multiple applications and theories and models on this topic can been found in many text books (e.g. Scanlon *et al.*, 2002). Transport processes are fairly well understood and similar between different trace gases. On the other hand the processes responsible for the emission or destruction of a gas are usually quite unique, i.e. specific to each gas species. The difficulty is thus two-fold: it requires understanding the drivers regulating these emission and destruction processes and then deriving physical and/or ecological up-scaling theories to describe these processes at large (continental or global) scales.

In the first chapter, we have seen that theories describing the $C^{18}OO$ exchange at the soil surface were quite well established. When confronted to experimental data, these theories suggested that the CO_2 hydration rate and the associated CO_2-H_2O isotope exchange rate were orders of magnitude higher than the un-catalysed rate (Seibt *et al.*, 2006; Wingate *et al.*, 2008; 2009; 2010). Because carbonic anhydrase (CA) is very efficient at catalysing this isotopic exchange (Silverman, 1973) and is widespread in diverse soil micro-organisms from the Archaea, Bacteria and Fungi domains (Smith *et al.*, 1999), it was identified as the main enzyme responsible for this enhanced hydration rate (Seibt *et al.*, 2006; Kapiluto *et al.*, 2007; Wingate *et al.*, 2008; 2009; 2010). However, it has never been proven, for example using CA-specific inhibitors, that carbonic anhydrase is the only soil enzyme (or group of enzymes[5]) responsible for the observed enhanced CO_2-H_2O isotope exchange. More importantly, major difficulties in predicting soil-air $C^{18}OO$ exchange in time and space still remain. One difficulty consists in **identifying the isotopic composition of the soil water pool that the CO_2 is equilibrating with** (Hsieh *et al.*, 1998; Miller *et al.*, 1999; Kapiluto *et al.*, 2007; Wingate *et al.*, 2008) and predicting its spatiotemporal variations. Another major difficulty is to **understand better the biotic and abiotic drivers regulating CA activity in soils** in order to describe how it varies in different biomes and seasons (Wingate *et al.*, 2009).

It has also been known for some time that soils generally act as COS sinks. This COS consumption by soils is mainly of biotic origin, because the uptake rate is strongly reduced when the soil is either autoclaved or mixed with water containing ethoxyzolamide, one of the most efficient CA inhibitors (e.g. Isik *et al.*, 2009; Syrjänen *et al.*, 2013). This later finding, together with empirical (Ogawa *et al.*, 2013) and theoretical (Schenk *et al.*, 2004) studies showing how CA can catalyse COS hydrolysis ($COS + H_2O \rightarrow CO_2 + H_2S$), strongly support the idea that COS uptake by soils is dominated by CA activity. Soils can also emit COS. For anoxic soils, this has been known for more than two decades (Mello & Hines, 1994; Devai & Delaune, 1995; Kettle *et al.*, 2002) but recent studies, mostly conducted on agricultural soils with litter, indicate that some oxic soils also emit COS when exposed to high temperature or high light conditions (Maseyk *et al.*, 2014; Whelan & Rhew, 2015). It is still **unclear however what mechanisms are responsible for such COS emissions** (Mello & Hines, 1994; Whelan & Rhew, 2015).

[5] Carbonic anhydrase is a generic term describing a group of widespread metallo-enzymes that catalyse CO_2 hydration: $CO_2 + H_2O \leftrightarrow H_2CO_3$. Because carbonic acid de-protonation ($H_2CO_3 \leftrightarrow HCO_3^- + H^+$) is a very rapid process (*ca.* 10^{-7} s) relative to CO_2 hydration, CAs are often said to catalyse the (reversible) inter-conversion of CO_2 into bicarbonate. Although with the same function, genetic studies have shown that CAs belong to at least six known classes (α, β, γ, δ, ζ, η) that are evolutionary unrelated (Smith *et al.*, 1999; So *et al.*, 2004; Rowlett, 2010; Del Prete *et al.*, 2014). These CA families are beautiful examples of convergent evolution of catalytic function.

At the global scale, COS consumption by soils seems to dominate over COS emission, leading to a net COS sink whose size is about a third that of vegetation but with a large uncertainty, with values of -130 GgS yr^{-1} (Kettle *et al.*, 2002), -355 GgS yr^{-1} (Berry *et al.*, 2013) or even -510 GgS yr^{-1} (Launois *et al.*, 2015). This large spread in the global COS uptake by soils is partly caused by the variety of approaches used to estimate this flux. Kettle *et al.* (2002) assumed soil COS fluxes responded to soil surface temperature and moisture only, and used a parameterisation derived by Kesselmeier *et al.* (1999) from incubation measurements performed on a single arable soil in Germany. More recent approaches have assumed that the COS flux from soils is proportional to other soil-air trace gas fluxes. Berry *et al.* (2013) related the COS uptake to heterotrophic (microbial) respiration, using a relationship from one study on **three** tropical soils (Yi *et al.*, 2007), while Launois *et al.* (2015) used a relationship with the H_2 deposition rate, also based on one study on one single soil (Belviso *et al.*, 2013). In summary, **all the approaches for estimating the contribution of anoxic soils in the COS atmospheric budget remain essentially empirical** and based on hypotheses that are largely non-validated.

Over the past 6 years, we have addressed these knowledge gaps by developing systems to perform gas exchange measurements in perfectly controlled conditions and retrieve, non destructively and simultaneously, the uptake and production rates of COS, or the CO_2 hydration and the isotopic composition of the soil water that the CO_2 equilibrates with. By using soils from different biomes and history, manipulating their environment and conditioning, and analysing their microbial abundance and diversity, we were able to develop physically- and ecologically-based models of COS and $C^{18}OO$ transport and fate in soils. These models, with some simplifications, are now being incorporated in global scale C cycle models. Quite surprisingly, our controlled experiments also evidenced that our current theories of the physical transport of water and CO_2 isotopes in soils may be over-simplified, notably concerning the dynamics of CO_2 isotope exchange between the gaseous and liquid phases or the distribution of soil water isotopes between soil micro- and macro-pores. The remaining of this chapter briefly summarises these different findings.

2.2 Recent advances on soil COS and $C^{18}OO$ fluxes

General modelling framework

The first description of $C^{18}OO$ transport in soils was proposed by Hesterberg and Siegenthaler (1991). In this model, diffusion through the soil matrix only occurred in the gas phase (with effective diffusivity D_{iso}) while CO_2-H_2O isotopic exchange was described by a first-order reaction rate (k_{iso}). Finally, $C^{18}OO$ production occurred *via* soil respiration that was assumed to decline exponentially with soil depth and produce CO_2 in isotopic equilibrium with bulk soil water at that depth. The soil was also assumed horizontally homogeneous so that the soil air CO_2 concentration (C, in mol m^{-3}) and its $^{18}O/^{16}O$ isotope ratio (R) are only functions of time (t, in s) and soil depth (z, in m). At natural abundance, $R << 1$ so that the $C^{18}OO$ concentration is well approximated by the product CR. The mass balance equation for $C^{18}OO$ in a soil layer was then written as:

$$\left[\phi + (B-1)\theta\right]\frac{\partial RC}{\partial t} = \frac{\partial}{\partial z}\left(D_{iso}\frac{\partial RC}{\partial z}\right) - B\theta k_{iso} C\left(R - R_{eq}\right) + PR_{eq}\,, \qquad (2.1)$$

where ϕ (m^3 m^{-3}) is soil porosity, θ (m^3 m^{-3}) is soil moisture content, B (m^3 m^{-3}) is the (dimensionless) CO_2 solubility in water (Sander, 2015), R_{eq} is the $^{18}O/^{16}O$ isotope ratio of CO_2 in equilibrium with soil water at depth z and P (mol m^{-3} s^{-1}) is the CO_2 production rate (i.e. respiration). The term in brackets on the left-hand side of Eq. 2.1 is called "total CO_2 porosity" and is the sum of the air-

filled volume fraction $\phi - \theta$ and the water-filled volume fraction θ, expressed on a gas-volume equivalent by means of the solubility B.

Equation (2.1) can be seen as the sum of two mass balance equations, one for gaseous CO_2 and one for dissolved CO_2. In the gaseous phase, only (vertical) diffusion and equilibration with the liquid phase are considered, while in the liquid phase, CO_2-H_2O isotope exchange, CO_2 production (respiration) and equilibration with the gas phase are considered:

$$\left(\phi - \theta\right)\frac{\partial RC}{\partial t} = \frac{\partial}{\partial z}\left(D_{\text{iso}}\frac{\partial RC}{\partial z}\right) - k_{g\to l}\left(RC - \frac{R_l C_l}{{}^{18}B}\right), \tag{2.2a}$$

$$\theta\frac{\partial R_l C_l}{\partial t} = -\theta k_{\text{iso}} C_l\left(R_l - R_{\text{eq}}\right) + PR_{\text{eq}} + k_{g\to l}\left(RC - \frac{R_l C_l}{{}^{18}B}\right), \tag{2.2b}$$

where C_l (mol m^{-3}) and R_l denote the concentration and $^{18}O/^{16}O$ ratio of CO_2 dissolved in water and $k_{g\to l}$ (m^3 s^{-1}) represents the transfer coefficient between the liquid and gas phase (expected to be proportional to the area of the gas-liquid interface) and ^{18}B is the solubility of C^{18}OO in water.

If we further assume that CO_2 in both phases stay in chemical ($C_l = BC$) and isotopic ($^{18}C_l = {}^{18}B\,{}^{18}C$, i.e., $R_l = {}^{18}BR/B \approx R$) equilibrium then the sum of the two mass balance equations (2.2a) and (2.2b) simplifies to Eq. (2.1). I will come back later on these different assumptions, and also on other assumptions that are implicit to Eq. (2.1) and often overlooked. Yet, Eq. (2.1) has been used in all the studies on C^{18}OO fluxes (including those I co-authored), with variations only[6] on the way to model diffusion (D_{iso}) or CO_2-H_2O isotopic exchange (k_{iso}). For example, in Eq. (2.2b) diffusion in the liquid phase was neglected because it is expected to be orders of magnitude lower than in the gas phase, at least in unsaturated conditions. However, it was considered in all the results presented here, for completeness and for saturated conditions when diffusion is only possible in the liquid phase.

The soil-to-air C^{18}OO flux is estimated by solving Eq. (2.1) and computing $^{18}F = D_{\text{iso}}\,\partial(RC)/\partial z$ at z = 0. At steady state Eq. (2.1) simplifies to:

$$0 = \frac{d}{dz}\left(D_{\text{iso}}\frac{dRC}{dz}\right) - B\theta k_{\text{iso}} C\left(R - R_{\text{eq}}\right) + PR_{\text{eq}}, \tag{2.3}$$

Equation (2.3) can be solved analytically when soil properties (porosity, soil water content and temperature, k_{iso} and R_{eq}) do not vary (rapidly) with depth (Hesterberg & Siegenthaler, 1991; Tans, 1998). With boundary conditions $C(z) = C_a$, $R(z) = R_a$ at $z = 0$ and $dC/dz = 0$ and $dR/dz = 0$ when $z \to \infty$ this gives (Tans, 1998):

$${}^{18}F = \alpha_D R_{\text{eq}} F\left[1 + \left(\frac{1}{\alpha_D} - 1\right)\frac{z_1}{z_1 + z_0}\right] + \frac{D_{\text{iso}}}{z_1} C_a\left(R_{\text{eq}} - R_a\right), \tag{2.4a}$$

where $\alpha_D = D_{\text{iso}}/D_{\text{eff}}$, D_{eff} represents the effective diffusivity of CO_2 through the soil matrix, z_0 is the e-folding depth of soil respiration, i.e., $P(z) = P_0 \exp(-z/z_0)$ and $z_1 = \sqrt{D_{\text{iso}}/(B\theta k_{\text{iso}})}$ corresponds to the depth where the diffusion of C^{18}OO out of the soil ($D_{\text{iso}}CR/z_1$) balances the hydration rate ($B\theta k_{\text{iso}}CRz_1$). Defining $R_F = {}^{18}F/F$ and using the delta notation (i.e., $\delta = R/R_{\text{std}} - 1$ where R_{std} is the $^{18}O/^{16}O$ ratio of the international standard VPDB$_g$), Eq. (2.4a) becomes:

[6] There is one exception from Stern *et al*. (1999) that briefly discusses the impact of CO_2 advection on C18OO fluxes (see also 2.3 below).

$$\delta_F = \delta_{eq} + \varepsilon_D \frac{z_0}{z_0 + z_1} + \frac{V_{inv} C_a}{F}\left(\delta_{eq} - \delta_a\right), \quad (2.4b)$$

where we defined $V_{inv} = \sqrt{B\theta k_{iso} D_{iso}}$ and $\varepsilon_D = \alpha_D - 1$ and noting that second-order terms in $\varepsilon_D\delta_{eq}$ have been discarded.

The effective diffusivity of any trace gas through the soil matrix D_{eff} is commonly expressed relative to the binary diffusivity D_0 (in m^3 air m^{-1} s^{-1}) of the same gas in air: $D_{eff}/D_0 = (\phi - \theta)\tau_a$ where τ_a is the so-called air tortuosity factor that accounts for the tortuosity[7] of the air-filled pores, as well as their constrictivity[8] and water-induced disconnectivity (e.g. Moldrup *et al.*, 2003). The air-filled porosity ($\phi - \theta$) appears in this equation to account for the reduced cross-sectional area of air space in the soil matrix relative to free air, although the effective porosity for diffusion could be smaller if the soil contains small pores that do not contribute to the overall transport such as dead end or blind pores. The binary diffusivity D_0 depends on pressure and temperature and can be approximated using the Chapman-Enskog theory for ideal gases (i.e. Bird *et al.*, 2002): $D_0(T,p) = D_0(T_0,p_0)(T/T_0)^{1.5\text{-}2}(p_0/p)$, where $D_0(T_0,p_0)$ is inversely proportional to the square root of the reduced molar mass of the gas mixture: $D_0 \propto 1/\sqrt{M_a M_g/(M_a + M_g)}$, where M_a and M_g are the molar masses of dry air and the trace gas, respectively[9]. From this formulation, we should expect $\alpha_D = D_{iso}/D_{eff} = D_{eff}(C^{18}OO)/D_{eff}(CO_2) = 0.9913$.

Equation (2.4a) has the form of Eq. (1.2b) with the correspondence: $\alpha_d \approx 1 + \varepsilon_D z_0/(z_0 + z_1)$ and $F_{in} \approx V_{in} C_a$. In other words, α_d is not a purely diffusive fractionation factor like α_D, but also depends on the e-folding of soil respiration with depth (z_0) and the competition between CO_2 diffusion and hydration (z_1). The fractionation factor $\varepsilon_d = \alpha_d - 1 \approx \varepsilon_D z_0/(z_0 + z_1)$ is then expected to be smaller than ε_D. Indeed, Miller *et al.* (1999), based on microcosm measurements on five different soil types, proposed a mean value for ε_d of -7.2‰, which is somewhat lower (in absolute value) than the theoretical maximum ε_D = -8.7‰. Some global scale studies used this value for the entire globe (Cuntz *et al.*, 2003a) while other studies (Farquhar *et al.*, 1993; Ciais *et al.*, 1997a; Peylin *et al.*, 1999) considered ε_d as a variable of adjustment to close the atmospheric $C^{18}OO$ budget.

The analytical solution Eq. (2.4b) is useful to identify the main, first-order drivers of soil-air $C^{18}OO$ fluxes. However the conditions of soil vertical homogeneity (in terms of porosity but also soil moisture and temperature, soil water $^{18}O/^{16}O$ ratio and hydration rate k_{iso}) are questionable in real conditions. Steady state conditions may also be questioned. For these reasons, solving Eq. (2.1) numerically with depth-resolved soil properties was sometimes preferred at the ecosystem scale (Riley *et al.*, 2003; Seibt *et al.*, 2006; Wingate *et al.*, 2008; 2010), and even at the global scale (Buenning *et al.*, 2014). Alternatively, recognising that δ_F was most sensitive to the depth-dependent variable δ_{eq} (Riley, 2005) because of potentially very large water isotope gradients at the soil surface (Allison *et al.*, 1983), Eq. (2.4b) was still used, taking porosity, moisture and temperature of the topsoil layer and only adjusting the value of δ_{eq} based on the expected

[7] Tortuosity is a quantitative measure of the reduction of diffusive flux caused by the sinuous path imposed by the obstacles compared to the straightest path in an unrestricted medium.

[8] Constrictivity is a dimensionless factor assessing the impact of the variation of pores cross section on the mass transport, which becomes important when the size of the diffusing molecules is comparable to the dimensions of the pores.

[9] The exponent for the temperature dependency is 1.5 for monoatomic gases but increases to about 2 for other gases because of the temperature-dependent collisional integral of each gas species (Bird *et al.*, 2002).

equilibration depth ($z_{eq} \approx 2.35 z_1$) and depth-resolved estimates of the $^{18}O/^{16}O$ ratio of soil water (Wingate *et al.*, 2009).

In climate-controlled microcosm experiments, the conditions of soil homogeneity can be better satisfied and steady state can be attained. If the soil column is well mixed, we also have $P(z) = P_0$, corresponding to $z_0 \to \infty$. In addition, the zero flux boundary conditions at the bottom of the soil column are still valid but only occur at a finite depth z_{max}, not at $z \to \infty$. Equation (2.4b) must then be modified (Jones *et al.*, 2017; Sauze *et al.*, 2017; 2018):

$$\delta_F = \delta_{eq} + \varepsilon_d + \frac{\tilde{V}_{inv} C_a}{F}\left(\delta_{eq} - \delta_a\right) \quad (2.4c)$$

with $\varepsilon_d = \varepsilon_D((1 - z_1 / z_{max} \tanh(z_{max} / z_1))$ and $\tilde{V}_{inv} = V_{inv} \tanh(z_{max} / z_1)$.

Inspection of Eq. (2.4c) shows that, from measurements of F, δ_F and C_a and δ_a, we do not get a unique value of V_{inv}, and thus k_{iso}, unless δ_{eq} is known. This is why field studies investigating how soil CA activity impacted the soil-air $C^{18}OO$ flux have been relying on depth-resolved soil water $^{18}O/^{16}O$ data (Wingate *et al.*, 2008; 2009). Alternatively, we can see from Eq. (2.4c) that δ_F and δ_a should be linearly related, with a slope independent of δ_{eq} and depending only on k_{iso} and other variables like F or C_a. Thus, in laboratory settings, where it is possible to perform measurements of δ_F for different values of δ_a while holding other variables constant (notably C_a and F), we should be able to estimate k_{iso} and δ_{eq} simultaneously from a linear regression between δ_F and δ_a.

To test this approach, we conducted laboratory incubations using air-dried soil samples, all coming from the same temperate evergreen forest but mixed with different waters that differed in terms of their $^{18}O/^{16}O$ ratio (Jones *et al.*, 2017). In all the incubations, δ_F and δ_a were strongly ($r^2 > 0.93$) and negatively correlated (Fig. 2.1). The slopes of the linear regressions were broadly similar among water treatments, with means of -1.83 ± 0.25, -1.32 ± 0.25 and -1.53 ± 0.15 for the more depleted, intermediate and more enriched water treatments, respectively. These values led to CO_2-H_2O isotopic exchange rates k_{iso} that were not significantly different between treatments (Table 2.1). Similarly, estimates of the apparent fractionation factor (ε_d) did not differ between irrigation water treatments, with rather small values around -5‰ (Table 2.1). In contrast, intercepts of the linear regressions between δ_F and δ_a differed amongst water treatments (Fig. 2.1), with treatment means of -30.17 ± 2.14 ‰VPDBg, -20.08±2.66‰ VPDBg and -14.29±1.21‰ VPDBg for the most depleted, intermediate and most enriched water treatment, respectively. This result was expected because the slope of the regression is linearly related to δ_{eq} (Eq. (2.4c)) and should thus differ between water treatments.

To allow for comparison with the $\delta^{18}O$ of bulk soil water determined following cryogenic extraction, estimates of δ_{eq} were converted to equivalent values of the $\delta^{18}O$ of soil water in equilibrium with CO_2 ($\delta_{sw,eq}$), based on the temperature-dependent equilibration fractionation between water and CO_2 and the difference between the VPDBg and VSMOW scales (Brenninkmeijer *et al.*, 1983). As expected, estimates of $\delta_{sw,eq}$ were found significantly different between treatments. More surprisingly they were always significantly more depleted than the isotopic composition of irrigation water (Table 2.1), but also of bulk soil water at all depths (Jones *et al.*, 2017). This was surprising given the great care that had been taken to dry the soil samples, mix and homogenise them with irrigation water and avoid any isotopic contamination during soil preparation and incubation (Jones *et al.*, 2017). This result can have large repercussions for studies that applied Eq. (2.4b) at the large scale. For example, if soil CO_2 interacts with more depleted water pools than bulk soil water, then the contribution of soil CO_2 fluxes to the North-South gradient of the $^{18}O/^{16}O$ ratio in atmospheric CO_2 (see chapter 1) must have been

underestimated. We will come back on this point in section 2.3, with some possible explanations for this isotopic offset between $\delta_{sw,eq}$ and bulk soil water.

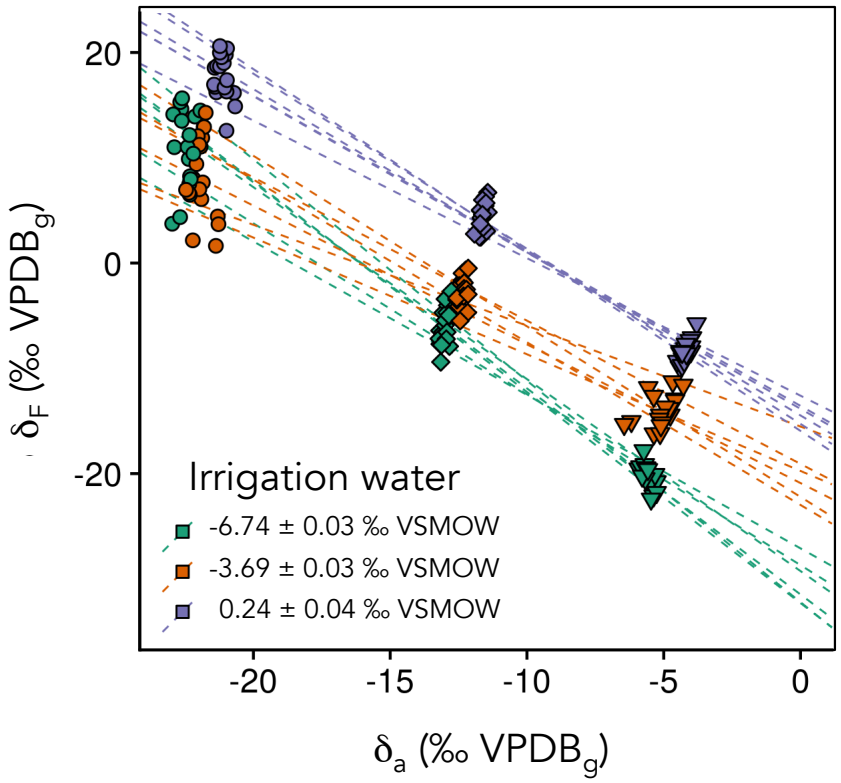

Figure 2.1 | Relationships between the $\delta^{18}O$ of soil-air CO_2 exchange (δ_F) and the $\delta^{18}O$ of CO_2 of the air above the soil surface (δ_a) for different irrigation water treatments. Dashed lines indicate linear regressions for individual incubations. After Jones *et al.* (2017).

Table 2.1 | Model solutions by irrigation water treatments. Means (n = 6) and standard deviations (in parenthesis) for the apparent rate of isotopic exchange between CO_2 and soil water (k_{iso}), the effective fractionation factor (ε_d), and the $\delta^{18}O$ of soil water in equilibrium with CO_2 as determined from gas flux measurements ($\delta_{sw,eq}$). Superscript letters following each mean and deviation indicate significant differences (one-way analysis of variance and Tukey's HSD, $p < 0.01$) among water treatments. After Jones *et al.* (2017).

Irrigation water (‰VSMOW)	k_{iso} (s^{-1})	ε_d (‰)	$\delta_{sw,eq}$ (‰VSMOW)
-6.74 (0.03)^a	0.080 (0.009)^a	-5.36 (0.16)^a	-9.31 (0.20)^a
-3.69 (0.03)^b	0.063 (0.015)^a	-4.88 (0.43)^a	-7.04 (0.52)^b
0.24 (0.03)^c	0.071 (0.012)^a	-5.14 (0.29)^a	-4.16 (0.18)^c

The theory of soil-air $C^{18}OO$ exchange briefly developed above can easily be transposed to study soil COS fluxes. A mass balance equation similar to Eq. (2.1) can be derived for COS (Sun *et al.*, 2015; Ogée *et al.*, 2016):

$$\left[\phi+(B-1)\theta\right]\frac{\partial C}{\partial t}=\frac{\partial}{\partial z}\left(D_{\text{eff}}\frac{\partial C}{\partial z}\right)-B\theta k_{\text{h}}C+P\,, \tag{2.5}$$

where D_{eff} now represents the effective diffusivity of COS through the soil matrix and k_{h} is the first-order COS hydrolysis rate. The soil-to-air COS flux is then estimated by solving Eq. (2.5) and computing $F=D_{\text{eff}}\,\partial C/\partial z$ at z = 0. Assuming again steady state and uniform conditions, and zero flux boundary condition at the bottom of the soil column ($z = z_{max}$), an analytical solution can be found (Ogée *et al.*, 2016; Kaisermann *et al.*, 2018b):

$$F=\left\{Pz_1-\frac{D_{\text{eff}}}{z_1}C_{\text{a}}\right\}\tanh\left(\frac{z_{\max}}{z_1}\right), \tag{2.6a}$$

where z_1 is now defined as $z_1=\sqrt{D_{\text{eff}}/(B\theta k_{\text{h}})}$. For field applications, the condition at the lower boundary must be modified to $dC/dz(z\to\infty)=0$ and the production rate P can only be positive (and assumed uniform) above a certain depth z_P (and zero elswhere). In this case the steady-state solution becomes (Ogée *et al.*, 2016):

$$F=Pz_1\cdot\left(1-\exp(-z_{\text{P}}/z_1)\right)-\frac{D_{\text{eff}}}{z_1}C_{\text{a}}\,, \tag{2.6b}$$

We can verify that both equations (2.6a) and (2.6b) give the same results if $z_{max}\to\infty$ and $z_P\to\infty$, and also that Eq. (2.6b) leads to $F\to Pz_P$ when $k_h\to 0$.

As explained in the introduction of this chapter, it is only recently that investigators have started to interpret and model soil-air COS fluxes using a physically based approach such as Eq. (2.5) (Sun *et al.*, 2015; Ogée *et al.*, 2016). This approach is suitable to describe how the COS flux responds to instantaneous changes in temperature and moisture. It is also useful to retrieve key parameters such as the COS hydrolysis or production rate, in order to identify their physical and ecological drivers. In Ogée *et al.* (2016) we proposed a relationship between the hydrolysis rate k_h and microbial biomass and CA kinetics parameters. Acknowledging the fact that both COS hydrolysis and CO_2 hydration are related to soil CA activity, we also proposed constraints on the relationship between k_h (for COS) and k_{iso} (for $C^{18}OO$). These theoretical propositions were further tested in subsequent studies (Sauze *et al.*, 2017; 2018; Kaisermann *et al.*, 2018a; 2018b; Meredith *et al.*, 2019) and briefly summarised in the following sections.

Understanding the response of soil COS fluxes to soil moisture and temperature

Kesselmeier *et al.* (1999) first proposed a model that describes the response of soil-air COS exchange to changes in soil moisture and temperature. Soil samples from a temperate, arable soil in Germany were sieved and incubated at a set gravimetric water content of 13.5% and a set temperature (between 0 and 30°C, depending on the incubation). The COS gas exchange (F) was subsequently measured over a range of COS mixing ratios (C_a, from 100 to 2000 ppt). They also performed incubation measurements at 15°C and different gravimetric soil water contents (between 5 and 43%). They found that the soil COS flux had optima for both temperature (around 18.5°C) and gravimetric water content (around 15%). These different gas exchange measurements were used to derive empirical relationships between the net soil-air COS flux F and soil

gravimetric water content (W)[10] and temperature (T): $F = F_{opt} f_W(W) f_T(T)$, where F_{opt} represents the COS flux at optimum soil moisture and temperature. These empirical relationships were subsequently applied at the global scale with a single value for F_{opt} of -10 pmol m^{-2} s^{-1} leading to a global COS sink from oxic soils of -130 GgS yr^{-1} (Kettle *et al.*, 2002).

The generality of these empirical responses for global scale applications can be questioned, not only because they assume that soil moisture and temperature act on the COS flux independently, but also because they are mixing time scales. Variations in incubation temperatures are useful to study seasonal changes, but are less representative of rapid (hourly to daily) changes in temperature. On the other hand, changes in soil moisture at a set temperature are more representative of what happens at daily to synoptic time scales, during soil surface evaporation and drying. The physically-based approach described above explicitly accounts for sub-daily changes in soil moisture and temperature, while seasonal changes are only taken care of implicitly, through changes in nominal (or potential) rates (i.e. rates at, for example, 25°C) of COS hydrolysis and production (Ogée *et al.*, 2016). It can therefore be used to disentangle the responses at different time scales.

Assuming (for the moment) $P = 0$, Eq. (2.6a) simplifies to:

$$F = -C_a \sqrt{B\theta k_h D_0 \left(\phi - \theta\right) \tau_a} \tanh\left(\sqrt{\frac{B\theta k_h z_{max}}{D_0 \left(\phi - \theta\right) \tau_a}} \right), \tag{2.7}$$

Expressions for τ_a differ depending on whether the soil is repacked or undisturbed (see Table 1 in Ogée *et al.*, 2016). The expression proposed by Moldrup *et al.* (2003) for repacked soils, $\tau_a = (\phi - \theta)^{3/2}/\phi$, is suitable to interpret data from Kesselmeier *et al.* (1999). With this expression for τ_a and assuming that the soil column is deep enough (typically $z_{max} > 2z_1$), Eq. (2.7) displays an optimum soil moisture that only depends on soil porosity: $\theta_{opt} \approx 0.286\phi$ (Ogée *et al.*, 2016). When the soil column is less than a few centimetres deep (it is 1-2 cm in the study by Kesselmeier *et al.*), this optimum will be lower (Ogée *et al.*, 2016) and become sensitive to COS hydrolysis (i.e. it will decrease with higher k_h). When expressions for τ_a applicable to undisturbed soils are used (Deepagoda *et al.*, 2011), which is more suitable for field applications, the optimum soil water content is also reduced, around 0.25ϕ for z_{max} = 1m. On the other hand, when COS production is non zero, the optimum soil moisture increases (Ogée *et al.*, 2016). All these optima have been estimated assuming that the COS hydrolysis and production rates did not respond to instantaneous changes in soil moisture. On the other hand, they may change over the season. In field conditions or deep soil microcosms, our model predicts that θ_{opt} should be insensitive to seasonal changes in k_h but not in P. It also suggests that, given the very shallow soils studied by Kesselmeier *et al.*, the reported θ_{opt} is not independent of k_h and may thus vary with incubation temperatures. Indeed, in a follow up study by vanDiest and Kesselmeier (2008), similar measurements over a drying cycle were reported on the same arable soil, but at three temperatures (15°C, 20°C and 25°C), and showed smaller optimum moisture θ_{opt} at higher temperature. This is coherent with the idea that k_h responds positively to temperature.

From the slope and intercept of the linear regressions between F and C_a, Kesselmeier *et al.* (1999) were also able to retrieve the COS production and consumption rates at different incubation temperatures. They found that COS consumption (that they defined as the slope of the linear

[10] Gravimetric water content W (g g^{-1}) can be derived from volumetric water content θ and soil bulk density ρ_b (g cm^{-3}): $W = \theta\rho_w/\rho_b$, where ρ_w = 1 g cm^{-3} is the density of water.

regression) had an optimum temperature, around 20°C, i.e., higher than the optimum temperature for the net flux (around 18.5°C). Eq. (2.6a) also predicts a lower temperature optimum for F than for k_h, especially at large production rates P (Ogée *et al.*, 2016). However, the optimum temperature reported in Kesselmeier *et al.* (1999) is relative to *incubation* temperature, not *instantaneous* temperature, and is likely dominated by changes in the microbial community size and composition in response to incubation temperature that will lead to changes in nominal rates of k_h and/or P. For example, they reported a temperature optimum for COS production around 25°C, although with a large uncertainty (Kesselmeier *et al.*, 1999). In contrast, all recent studies are now reporting a rapid, but monotonic increase of P with *instantaneous* temperature (Maseyk *et al.*, 2014; Whelan *et al.*, 2016; Kitz *et al.*, 2017; Meredith *et al.*, 2018; Kaisermann *et al.*, 2018b). Most likely, the optimum for COS production reported by Kesselmeier *et al.*[11] reflects the fact that the nominal rate of P may change with incubation temperature, leading to a larger pool of COS precursors when incubated at 25°C than at other temperatures.

To summarise, the empirical response of the soil COS flux to soil moisture and temperature proposed by Kesselmeier *et al.* (1999) on shallow, repacked soil samples are difficult to extrapolate to field conditions and to apply at the global scale. This is because the temperature and moisture optima will depend on the depth of the soil sample used during incubation and will also differ between repacked and undisturbed soils. They will also differ whether they are relative to instantaneous or seasonal changes in temperature and moisture. Instead, a physically based approach such as Eq. (2.6a) should be preferred because it provides a framework to shape these response curves to instantaneous changes in temperature and moisture, while disentangling other factors such as soil porosity and nominal COS hydrolysis and production rates, that can be extrapolated to field conditions using Eq. (2.6b).

We tested this proposition by evaluating Eq. (2.7) on incubation data by vanDiest and Kesselmeier (2008) from five soils spanning a range of climates (tropical, temperate and boreal) and land use types (crops, forests). We used this dataset because it reported soil COS fluxes over a full drying cycle (from saturation to complete dryness) at a set incubation temperature. It was therefore perfectly designed to test the soil moisture response of our model.

For each drying curve, we fitted the data with our model by adjusting one model parameter, f_{CA}, defined as the enhancement of the hydrolysis rate above the un-catalysed rate: $k_h = f_{CA} k_{h,uncat}$ (see also Eq. 2.9 below). This was enough to broadly reproduce the soil moisture response of the measured COS flux (Fig. 2.2). However, for a given soil, different f_{CA} values were obtained at different incubation temperatures. The f_{CA} values followed very closely the maximum COS flux measured for each drying cycle (Fig. 2.2 far right bottom panel). We justified adjusting different f_{CA} values for a given soil by the way measurements were performed. For each drying cycle, a soil sample was saturated with water and acclimated to a given and fixed temperature. The COS exchange was then measured at regular intervals during the full drying cycle (lasting usually 1-2 days). The same soil sample, or a different one from the same geographical location, was used for each drying cycle. Sometimes several months separated measurements at two different temperatures. This means that, for a given soil origin, the microbial community was experiencing different environmental conditions and history between each drying curve. Thus, the size and

[11] Note that COS production, as defined in Kesselmeier *et al.*, does not correspond to P but rather to the intercept of the linear regression of F *vs.* C_a. According to Eq. (2.6a) this intercept equals $Pz_1\tanh(z_{max}/z_1)$, which corresponds to Pz_{max} only when $z_{max} \geq 2z_1$. Because Kesselmeier *et al.* used very shallow soils, the COS production that they estimated incorporates (via z_1) the temperature dependency of other factors, such as COS solubility B, diffusivity D or hydrolysis rate k_h.

diversity of the microbial population were likely different for each incubation temperature, justifying the use of different enhancement factors (and thus nominal hydrolysis rates) at each temperature. Although these f_{CA} (and k_h) values seemed compatible with typical microbial population sizes and our understanding of CA activity for COS (Ogée *et al.*, 2016), we could not test further whether k_h was related (and if so, how) to microbial population size or diversity, because no microbial data had been collected. This information is however critical to apply Eq. (2.6b) to the large scale, because this requires a description of how k_h (and P) vary across the landscape.

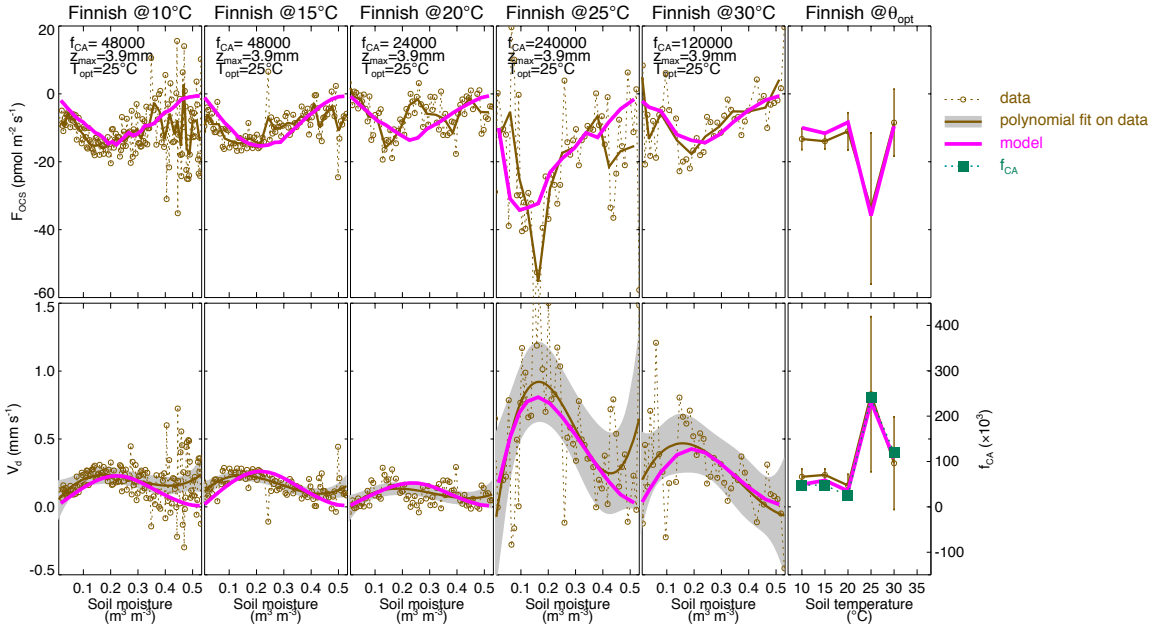

Figure 2.2 | Observed and modelled soil–air COS flux (F_{OCS}) and deposition velocity (V_d) during a drying cycle at different incubation temperatures (indicated above each panel), and their value at a soil moisture content $\theta_{opt} \approx 0.12$ m^3 m^{-3} (far right panels). The soil moisture and temperature response curves shown here were recalculated from data by Van Diest and Kesselmeier (2008) (open circles and brown line) or computed with Eq. (2.7) (thick pink line). For each drying cycle and incubation temperature, a different value of f_{CA} was obtained, as indicated in each panel. The data shown here are representative of an agricultural soil near Hyytiälä, Finland. Redrawn from Ogée *et al.* (2016).

COS production by anoxic soils

By performing similar incubation measurements as in Kesselmeier *et al.* (1999) or vanDiest and Kesselmeier (2008) but for a variety of soils from the US (Meredith *et al.*, 2019) and Europe (Kaisermann *et al.*, 2018a; 2018b) and complemented, this time, by detailed analysis of the physical-chemical and microbial properties of each soil, we investigated the biotic and abiotic drivers of the COS production rate P, and COS hydrolysis rate k_h, across these two continental regions. The soil texture, pH and microbial biomass of the different soils that we studied are shown in Fig. 2.3, along with the expected distribution of the same variables across the entire globe. Our soil samples seem representative of the global soils in terms of pH and microbial biomass. On the other hand their soil texture seems to contain too much silt compared to the global distribution. This could be a result of the sieving process that removed the coarse sand (> 4mm) but also probably finer sand (*ca.* 1-2mm) aggregates. Increasing the sand fraction would decrease the silt (and clay) fractions, moving the individual points in the soil texture triangular

diagram closer to the maxima in the global distribution (i.e. anti-clockwise rotation and contraction towards the bottom left corner of the triangle).

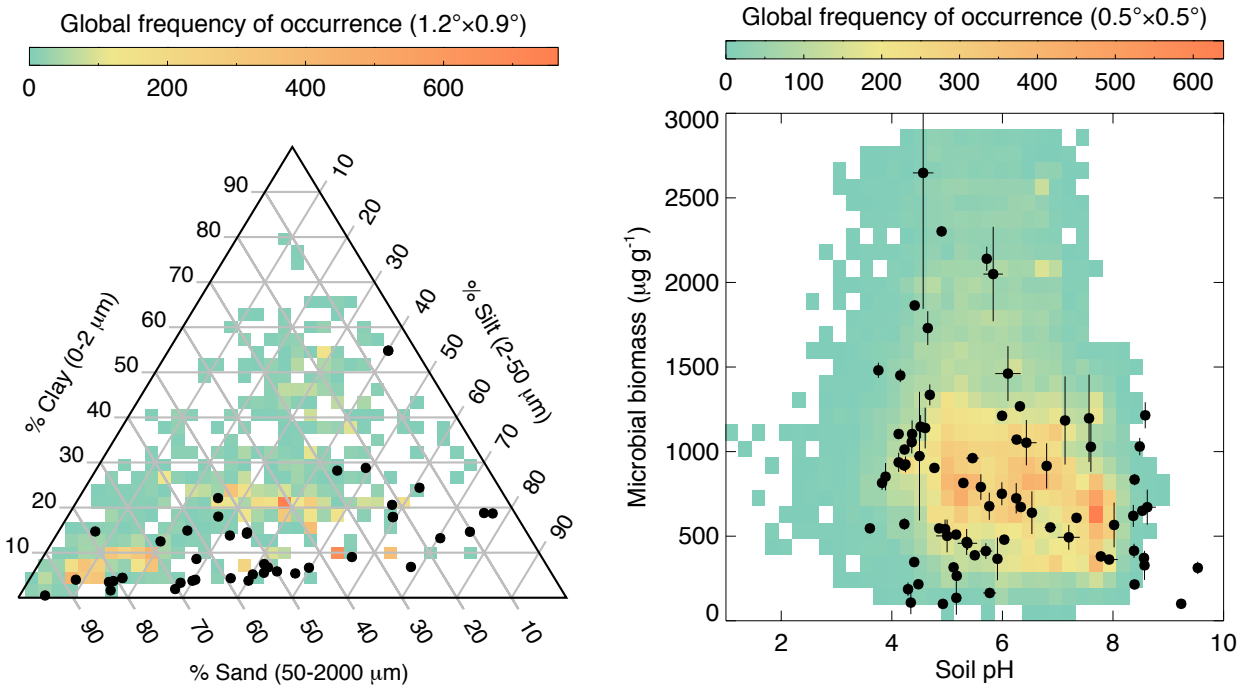

Figure 2.3 | Left panel: texture distribution of the studied soils. Right panel: microbial biomass (carbon) and pH distribution of the studied soils. Also shown is the the global distribution, based on the gridded datasets of Serna-Chavez *et al.* (2013) (microbial biomass) and the Harmonized World Soil Database, v1.2 (soil pH and texture).

Soil COS production was deduced from soil-air COS flux measurements performed either on dry soils (to suppress hydrolysis) (Meredith *et al.*, 2018; 2019) or on moist soils (at various COS concentrations) (Kaisermann *et al.*, 2018a) or both (Kaisermann *et al.*, 2018b). According to Eq. (2.6a), when $\theta \rightarrow 0$, $F \rightarrow Pz_{max}$ and when $\theta > 0$, the production rate can be estimated from the intercept of the linear regression between F and C_a (Lehmann & Conrad, 1996; Kesselmeier *et al.*, 1999; Kaisermann *et al.*, 2018b).

We found that 'dry' and 'moist' estimates of P were well correlated (Kaisermann *et al.*, 2018b), suggesting that soil moisture is not a major driver of COS production. This was quite surprising given that the gas exchange measurements on moist soils were performed several weeks after those on dry soils (but after some re-acclimation time after re-wetting). This result is however coherent with the recent study from Bunk *et al.* (2018) that shows that the net COS flux under very low COS concentration (10 times lower than ambient, to minimise COS uptake) remains constant (and positive) over an entire drying cycle (from field capacity to complete dryness). Bunk *et al.* (2018) also performed fully-resolved soil moisture response of COS production (defined as in Kesselmeier *et al.* (1999) by the intercept of the linear regression of F vs. C_a) and found very little variations with soil moisture, confirming that P is not sensitive to changes in soil moisture.

In contrast, and in agreement with previous studies (Maseyk *et al.*, 2014; Whelan & Rhew, 2015; Whelan *et al.*, 2016), we found that COS production was strongly sensitive to temperature, with median Q_{10} values typically around 3 (Meredith *et al.*, 2018; Kaisermann *et al.*, 2018b), i.e. much larger than the temperature sensitivity of the COS uptake (usually around 1.5-2, see above).

Finally we found that COS production increased with total soil nitrogen (N) (Meredith *et al.*, 2018; Kaisermann *et al.*, 2018b) or inorganic N (Kaisermann *et al.*, 2018a) (Fig. 2.4). It is still not clear what is the exact mechanism linking COS production and soil N content. However, using metatranscriptomic data, we found that COS production at 25°C (P_{25}) and its temperature sensitivity (Q_{10}) were both positively correlated with the number of cystine and methionine biosynthesis genes present in soils (Meredith *et al.*, 2018). These sulfur-containing amino acids are all potential precursors of COS formation when degraded biotically or abiotically (for example in the presence of ozone or light) (Kaisermann *et al.*, 2018a and references therein). It is therefore plausible that soils exposed to higher nitrogen inputs may be associated with an increase in the biosynthesis of S-containing amino acids, thereby increasing the pool of COS precursors, and *in fine* soil COS production.

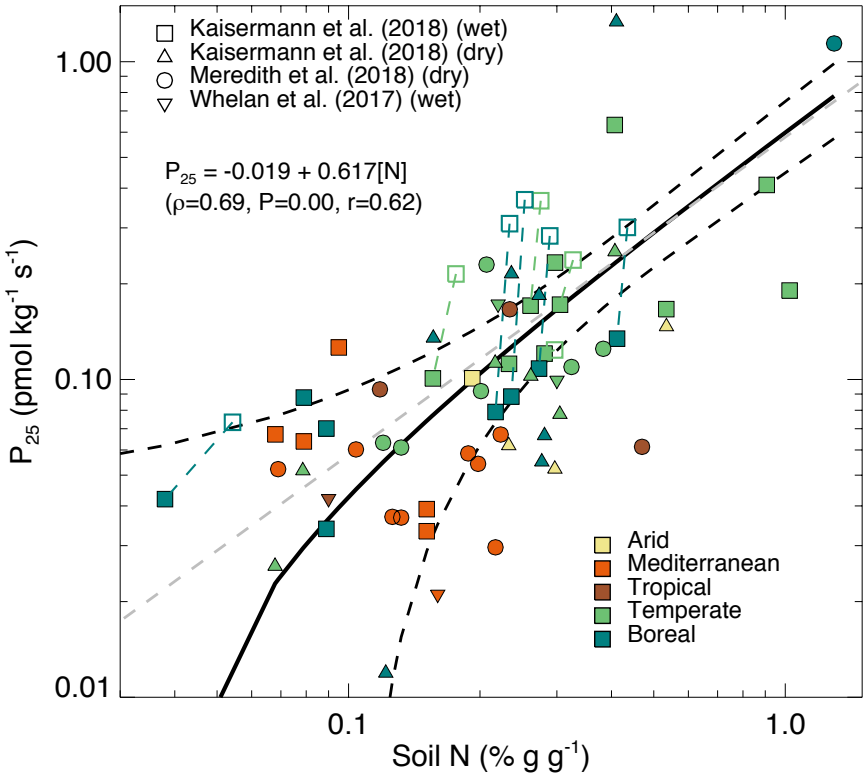

Figure 2.4 | Relationship between the COS production rate at 25°C and soil N content (% g g^{-1}) from three different studies. Nine soils (indicated by open symbols) were also incubated after inorganic N (NO_3NH_4) addition and the effect of this addition is indicated by a dotted line. A linear regression performed on soils without inorganic N addition (i.e. closed symbols) is shown (black solid line) with its confidence interval (± 2 SD, indicated by black dotted lines).

Collectively these results suggest a COS production term of the form:

$$P = P_{25}\left([N]\right)Q_{10}^{\frac{T-298.15}{10}}, \tag{2.8}$$

with $Q_{10} \approx 3$ (Whelan *et al.*, 2016; Meredith *et al.*, 2018; Kaisermann *et al.*, 2018b) and where P_{25} represents the N-dependent COS production rate at 25°C. By compiling all available datasets

where both COS production at 25°C and total N content were estimated, we found a linear relationship between the two variables (Fig. 2.4).

This relationship (P_{25} = -0.019 + 0.618 [N] ≈ 0.579 [N] where P_{25} is in units of pmol kg^{-1} s^{-1} and [N] is in %) may be used to upscale the COS production rate over continental areas. However, we must remain cautious when performing this upscaling. The relationship shown in Fig. 2.4 is mostly designed to describe broadly the spatial patterns of P_{25} across continental areas. On the other hand, it is probably less suited to capture seasonal changes of P_{25} at a given location, for example with seasonal changes in inorganic N (Kaisermann *et al.*, 2018a) or mean daily temperature (Kesselmeier *et al.*, 1999). Indeed, in all studies revisited in Fig. 2.4, the temperature range used to acclimate the soils prior to gas exchange measurements was rather narrow (all around 20°C). Regarding inorganic N, we showed that an artificial N fertilisation systematically increased P_{25}, bringing most individual points outside the confidence interval of the linear regression (Fig. 2.4). Further experiments would be needed to verify whether the relationship between P_{25} and total N is re-established once the inorganic N is leached from the soil. Experiments performed over a range of acclimation temperatures would also be required to test the validity of Eq. (2.8) over seasonal changes in temperature.

CA-catalysed COS hydrolysis in soils

The CO_2-H_2O isotope exchange rate (k_{iso}) and the COS hydrolysis rate (k_h) appearing in equations (2.1) and (2.5) are effective rates for a given soil layer. Nevertheless, they are primarily related to chemical and enzymatic activities so that their dependencies to biotic and abiotic drivers should be predictable. For example, COS is consumed through hydrolysis in the bulk soil water at an un-catalysed rate k_{uncat} (s^{-1}) that depends mostly on temperature (T) and *pH* (Elliott *et al.*, 1989):

$$k_{h,uncat(COS)} = 2.15\cdot10^{-5}\exp\left(-10450\left(\frac{1}{T}-\frac{1}{298}\right)\right)+12.7\cdot10^{-pK_w+pH}\exp\left(-6040\left(\frac{1}{T}-\frac{1}{298}\right)\right), \quad (2.9)$$

where pK_w is the dissociation constant of water (i.e. 10^{-14} at 25°C). The uncatalysed soil COS uptake rate is then computed as $S_{uncat} = k_{uncat}B\theta C$, where the volumetric soil water content θ is used to convert the hydration rate from mol m^{-3} water s^{-1} to mol m^{-3} soil s^{-1}.

This uncatalysed rate is rather small and cannot explain the large COS uptake rates observed in oxic soils, thought to be mainly enzymatic and governed by soil micro-organisms' CA activity (Kesselmeier *et al.*, 1999; Van Diest & Kesselmeier, 2008; Ogée *et al.*, 2016). The catalysed reaction by CA-containing organisms can be described by Michaelis-Menten kinetics (Sun *et al.*, 2015; Ogée *et al.*, 2016), as was observed for COS in several marine algae species (Protoschill-Krebs *et al.*, 1995; Blezinger *et al.*, 2000) and one flour beetle (Haritos & Dojchinov, 2005). Because of the low concentrations of COS in ambient air and the comparatively high values of the Michaelis-Menten coefficient of CA for COS (Km, see Protoschill-Krebs *et al.*, 1995; 1996; Ogawa *et al.*, 2013), we proposed to approxiamte the catalysed uptake rate (S_{cat}, mol m^{-3} s^{-1}) as (Ogée *et al.*, 2016):

$$S_{cat} = \theta k_{max}[CA]\frac{BC}{K_m + BC} \approx \frac{k_{max}}{K_m}[CA]B\theta C\,, \quad (2.10)$$

where k_{max} (s^{-1}) and K_m (mol m^{-3}) are the maximum (non substrate-limited) turnover rate and the Michaelis-Menten constant of the enzymatic reaction, respectively and [*CA*] (mol m^{-3}) is the total CA concentration in soil water.

The ratio k_{max}/K_m is also expected to vary with temperature and *pH* (see below), so that the total COS hydrolysis rate k_h appearing in Eq. (2.5) can be written as:

$$k_h = k_{h,uncat}(T,pH) + \frac{k_{max}}{K_m}(T,pH)[CA] \approx \frac{k_{max}}{K_m}(T,pH)[CA]\,. \quad (2.11)$$

In the following we will assume that the ratio k_{max}/K_m has a temperature dependency that can be approximated as:

$$\frac{k_{max}}{K_m} \propto x_{CA}(T) = \frac{\exp(-\Delta H_a/RT)}{1+\exp(-\Delta H_d/RT + \Delta S_d/R)}\,, \quad (2.12)$$

where ΔH_a, ΔH_d and ΔS_d are *apparent* thermodynamic parameters. Other formulations for the temperature response of enzyme kinetics exist that are more theoretical than Eq. (2.12), either from the 'equilibrium model' that explains enzyme thermal behaviour under reaction conditions "by introducing an inactive (but not denatured) intermediate in rapid equilibrium with the active form" (Daniel *et al.*, 2010) or from the macromolecular rate theory (MMRT), that extends the classical transition state theory (TST) by accounting for the temperature dependence of the enthalpy and entropy of reactions catalysed by large macromolecules such as enzymes (Liang *et al.*, 2017). These theories give a temperature response that can always be well approximated by Eq. (2.12).

The dominant CA class expected in soils is β-CA (Smith *et al.*, 1999; Meredith *et al.*, 2019 see below). Very few studies report the temperature response of this class of CA (or even any other CA). I could only find two studies where such a temperature response was characterised for the cytosolic β-CA from *Zea mays* leaf extracts (Burnell & Hatch, 1988; Boyd *et al.*, 2015). While Burnell and Hatch (1988) found a monotonic increase over the temperature range 0-17°C with a Q_{10} of 1.9, Boyd *et al.* (2015) explored a wider temperature range and found an optimum temperature around 35°C. Taking ΔH_a = 40 kJ mol^{-1}, ΔH_d = 200 kJ mol^{-1} and ΔS_d = 660 J mol^{-1} K^{-1} as in Ogée *et al.* (2016) leads to a temperature optima $T_{opt,CA}$ = 25°C and reproduces well the temperature response of β-CA reported by Burnell and Hatch (1988) in the range 0-17°C (Fig. 2.5). On the other hand, it fails at capturing the data from Boyd *et al.* (2015) for temperatures greater than 25°C (Fig. 2.5). A fit to their data, while keeping ΔH_a = 40 kJ mol^{-1} and setting $T_{opt,CA}$ = 35°C, leads to ΔH_d = 100 kJ mol^{-1} and ΔS_d = 321 J mol^{-1} K^{-1}. All parameterisations lead to almost similar results in the range 0-25°C, with a Q_{10} around 1.7-1.9 (Fig. 2.5). This is significantly larger than the Q_{10} that we reported for the COS hydrolysis k_h in the range 17-23°C, with a median value (± s.d.) of 1.23 ± 0.29 (Kaisermann *et al.*, 2018b). Such a low Q_{10} is more typical of physical (diffusion) processes (Fig. 2.5), rather than biological activities. This is interesting as it suggests that k_h and k_{max}/K_m may not be related as directly as would suggest Eq. (2.11). I will come back on this point later, but for the moment we will keep Eq. (2.11) as a working hypothesis.

In addition to the temperature response, plant β-CA activity has also been shown to exhibit a reduced activity when *pH* drops below 7, for both COS hydrolysis (Protoschill-Krebs *et al.*, 1996) and CO_2 hydration (Rowlett *et al.*, 2002). This is because the excess of protons in acidic solutions slows down the regeneration of the active site that requires the deprotonation of a EZn^{2+}-OH_2 complex (Rowlett *et al.*, 2002; Schenk *et al.*, 2004). In soils, because CA is most often located inside the cytoplasm of micro-organisms, cytoplasmic *pH* rather than soil *pH* should be considered. The two are related but variations of cytoplasmic *pH* are much smaller (i.e. buffered towards more neutral values) compared to those of soil *pH*. Using data reviewed by Krülwich *et al.* (2011) we could derive an empirical relationship between soil *pH* and internal *pH* (pH_{in}) whereby

pH_{in} varies between 6 and 9 when soil *pH* increases from 1 to 11.5 (i.e. more than 10 pH units) (see also Fig. 2.11c below). The pH dependence of k_{max}/K_m to variations in cytoplasmic pH_{in} can then be described as (Rowlett *et al.*, 2002):

$$\frac{k_{max}}{K_m} \propto y_{CA}(pH_{in}) = \frac{1}{1+10^{-pH_{in}+pK_{CA}}} . \quad (2.13)$$

A value of $pK_{CA} \approx 7.2$ was found for the cytosolic CA response of the wild-type *Arabidopsis thaliana* for CO_2 hydration (Rowlett *et al.*, 2002).

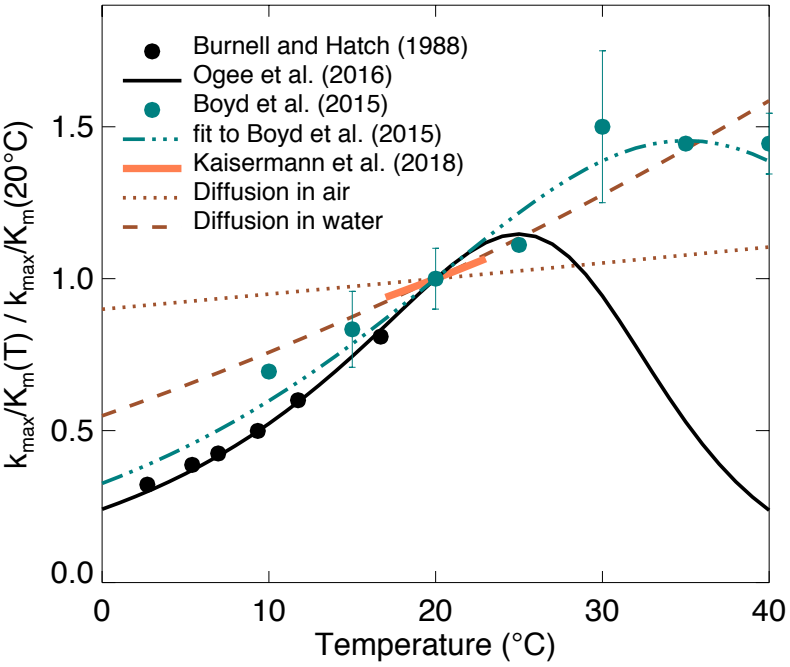

Figure 2.5 | Measured and modelled temperature response of CA activity, normalised at 20°C. Activity measurements (for CO_2 hydration) were performed on *Zea mays* leaf extracts by Burnell and Hatch (1988) and Boyd *et al.* (2015). Fits of Eq. (2.12) to these datasets are also shown together with the median Q_{10} response for COS hydrolysis reported by Kaisermann *et al.* (2018) over the range 17-23°C, and the temperature sensitivities of COS diffusion in air and water (as proposed in Ogée *et al.*, 2016). The fit to the data of Hatch and Burnell was used in Ogée *et al.* (2016).

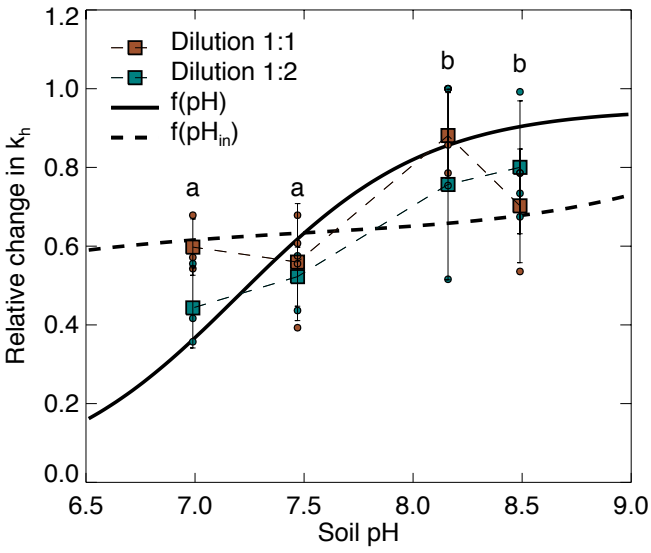

Figure 2.6 | Relative change in COS hydrolysis rate in response to soil pH. The hydrolysis rates were estimated from measurements of soil COS uptake by dry pure sand, irrigated with buffer solution containing various concentration of βCA. Four different buffer solutions were used, covering a range of pH between 6.5 and 9. Between 1.5g (dilution 1:2) and 3g (1:1) of microbial slurry of *Mycobacteria Tuberculosis* triggered to over-express βCA genes were added to 30mL of buffer solution and used to moist the sand, that had been previously autoclaved. The final pH range found in the sandy soil was narrower than the range covered by the different buffers, as a result of mixing with the microbial slurry and the soil particles (J. Sauze and L. Wingate, unpublished data).

As far as I know, no pK_a value has been estimated yet regarding COS hydrolysis. Only a quantitative description of the pH response can be found in Protoschill-Krebs *et al*. (1996). Preliminary results based on measurements of soil COS uptake by dry pure sand irrigated with buffer solutions containing various concentrations of βCA, seem coherent with a pK_a around 7.2 as for CO_2 (Fig. 2.6). However, the pH range covered by the various buffer solutions was too narrow to determine precisely the pK_a. Also, because the CA-containing microbial slurry that was added to the buffer solution had been concentrated by several washing and spinning, it was not clear if the activity had to be related to internal or external pH.

Revisiting data on β-CA from pea (*Pisum sativum*) by Protoschill-Krebs *et al*. (1996), we estimated a typical value of k_{max}/K_m at 20°C and pH 8.2 of 2.39 s^{-1} μM^{-1} (Ogée *et al.*, 2016). Equation (2.11) was thus approximated as:

$$k_h \approx k_{uncat}(T,pH) + \frac{x_{CA}(T)}{x_{CA}(20°C)} \frac{y_{CA}(pH_{in})}{y_{CA}(8.2)} 2390[CA], \quad (2.14)$$

where [CA] is expressed in mM.

Equation (2.11) (and its approximation Eq. (2.14)) are, in many ways, an over-simplification of the reality. First, the competition of COS with other possible substrates for CA, notably CO_2 or bicarbonate, is neglected. Accounting for competition with CO_2 would translate into multiplying K_m in Eq. (2.11) by a factor $1 + [CO_2]/K_{m(CO2)}$ where $K_{m(CO2)}$ represents the Michaelis-Menten constant of CA for CO_2. Because the later is of the order of 3mM (at 25°C and *pH* 8-9) or even higher depending on the type of CA (see a review of values by Bunk *et al.*, 2017), and given the range of CO_2 mixing ratios encountered in soil surfaces (300-5000 ppm or 0.01-0.15 mM at 25°C and 1atm), we had concluded that the competition with CO_2 must be negligible (i.e. less than 5%) (Ogée *et al.*, 2016). The CO_2 concentration inside microbial cells (i.e. at the CA site) must be somewhat larger than in the surrounding soil water but certainly not to an extent that would justify accounting for competition between the two substrates.

Recent results by Bunk *et al*. (2017) on soil COS fluxes under different CO_2 fumigation levels seem to contradict this conclusion. They found that COS uptake was reduced when soils were acclimated to CO_2 concentration as low as 2000 ppm (Bunk *et al.*, 2017). At these CO_2 levels, the competition between COS and CO_2 for CA should still be neglibible (see above). A possible explanation is that the results reported by Bunk *et al*. are not caused by the inhibition of COS hydrolysis by CO_2 but rather by changes in nominal rates of COS hydrolysis and production caused by community changes in response to their CO_2 environment. Unfortunately, the net COS flux was not separated into uptake and production to test this hypothesis.

Equation (2.11) also implicitely assumes that CA concentration is the same everywhere within soil water, while remaining in the cytoplasm of micro-organisms. In other words, it assumes that microbes act as 'generalised enzymes' floating in soil water (Tang & Riley, 2019). In this situation, bulk soil CA concentration [CA] can be related to the average cytoplasmic CA concentration ($[CA]_{in}$):

$$[CA]\theta = [CA]_{in}\rho_{mic}, \quad (2.15)$$

where ρ_{mic} (m^3 microbes m^{-3} soil) denotes the volumetric microbial content of the soil. This simple dilution of microbial cells into soil water is very crude, but it was found compatible with estimates of soil CA activity (Ogée *et al.*, 2016). The CA requirements in leaf mitochondria or in unicellular algae is of the order of 100 µM (Tholen & Zhu, 2011). Assuming this CA concentration value is also applicable to microbial cells, and using a typical microbial population size of $3\,10^9$ cm^{-3} and

an average cell size of 1 μm^3 (Wingate *et al.*, 2009), we obtained a microbial content of ρ_{mic} = 0.003 $m^3\ m^{-3}$ leading to [CA] = 1 µM at θ = 0.3. Using this value of [CA] and the k_{max}/K_m value for COS of 2.39 $s^{-1}\ \mu M^{-1}$ leads to a COS hydrolysis rate about 127 000 greater than the uncatalysed rate (at 20°C and pH 4.5). This enhancement factor is in the same order of magnitude as those estimated when revisiting the data of vanDiest and Kesselmeier (2008) over a range of soils (between 21 600 and 336 000, with a median value at 66 000) (Ogée *et al.*, 2016).

However, if this simple dilution of microbial cells into soil water is valid (Eq. 2.15), and if the CA requirements in microbial cells do not vary with water stress (i.e constant $[CA]_{in}$), then the COS hydrolysis rate k_h should vary linearly with ρ_{mic}/θ (Eq. 2.11) while the catalysed uptake rate (S_{cat}) should be proportional to ρ_{mic} (Eq. (2.10)). This seems to contradict the fact that one single f_{CA} value could be fitted on an entire drying curve (e.g. Fig. 2.2), so that $k_h = f_{CA}k_{h,uncat}$ does not change as soil dries. It also contradicts results shown in Fig. 2.7 that compares our model (Eq. 2.6a) against temperature response measurements of the soil-air COS exchange performed at different soil water content. A single set of the two 'free' parameters of the model ([CA] and P_{25}) was optimised in order to minimise the discrepancy with the entire dataset (see insert). The fact that one single value of [CA] was enough to fit the data supports the idea that [CA] (and thus k_h) does not vary with soil moisture. In other words, the simple dilution of microbial cells presented above should be revised.

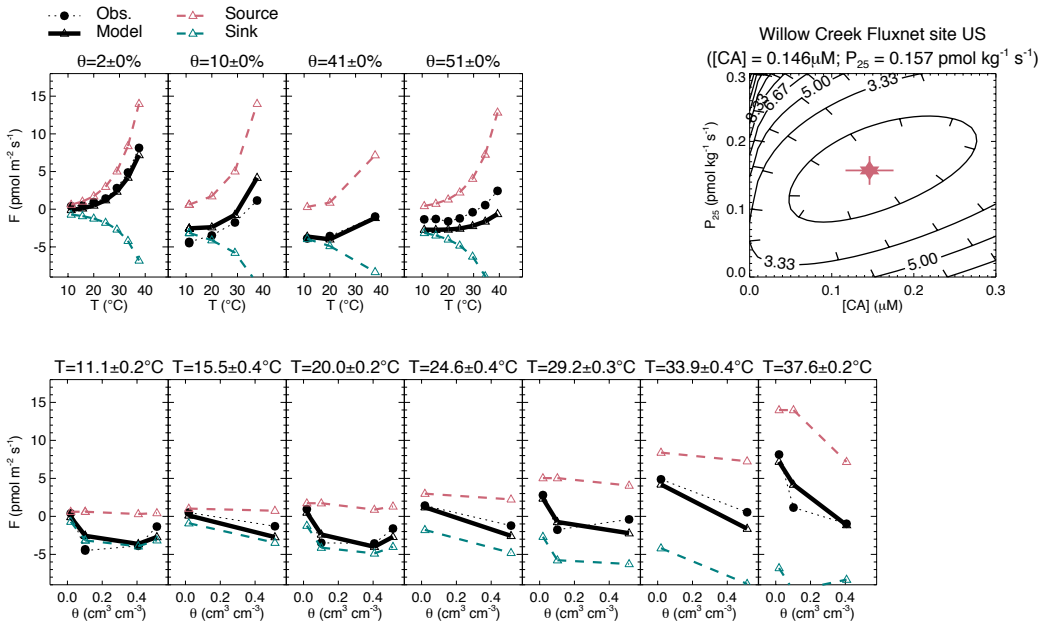

Figure 2.7 | Measured and modelled (Eq. 2.6a) COS fluxes as a function of soil temperature and moisture. Soil was sampled from Willow Creek (US). Data and model have been binned by soil moisture or temperature to show the individual responses. Model parameters (P_{25} and [CA]) have been optimised to minimise a cost function defined as the square root of the differences between data and model over the entire dataset. The insert in the top right corner shows contours of this cost function. Data is from Whelan *et al.* (2016).

First, there is no reason to believe that microbes do not secrete CA outside their cells. However, even if this is the case, the total CA content in soil water ([CA]θ) should still be somehow proportionnal to microbial biomass ρ_{mic}. Alternatively, it could be that the average CA activity per

organism also changes upon drying. The breaking of the water film continuity that occurs at low soil water content leads to a reduction in microbial activity, owing to the spatial separation of the microbes and their different metabolic substrates (Manzoni & Katul, 2014). When the substrate is a (dissolved) gas, like COS, soil water discontinuity should only affect marginally the supply of the enzyme's active site (i.e. dissolved COS should be almost equally available in all soil pores). On the other hand, internal CA requirements may vary during drought stress, although it is not clear in which direction. During water limitations, microbial activity (e.g. respiration) and growth is usually reduced, but slow growth rates and heat stress have been shown to cause an up-regulation of CA gene expression in *Escherichia coli* (Merlin *et al.*, 2003), probably to supply the need of inorganic carbon for lipid biosynthesis. If $[CA]_{in}$ was upregulated during drought, then k_h would increase even more rapidly than ρ_{mic}/θ[illegible], i.e., the opposite of what is found. Thus, our results would rather support the idea that CA gene expression (per unit of microbial biomass) is down regulated during drought. This is something that would need to be tested using metatranscriptomics data and analysis.

Another aspect that has been completely neglected so far is the co-limitation of the uptake by diffusional constraints, i.e., the fact that the COS concentration at the CA site inside microbial cells may be somewhat lower than at the air-water interface because of the finite transfer conductance across water films and microbial cell walls. Using typical values of transfer conductance across cell walls and plasma membranes (Evans *et al.*, 2009), we had estimated that the limitation of COS uptake by diffusion into the microbial cells alone was negligible for COS uptake by CA-catalysed hydrolysis (see Appendix A in Ogée *et al.*, 2016). We had however noted that this may not be true for CO_2 hydration. More importantly, these calculations only considered the transfer resistance across the microbial cell walls and plasma membranes, which occurs over very short distances (typically < 0.1 µm). However, if microbial cells are located closer to the soil particles, then the diffusion of COS across the water film, from the air-water interface to the microbial cell walls, could become an important limiting factor for COS uptake. In this situation, Eq. (2.10) needs to be re-written:

$$S_{cat} = \rho_{mic} k_{max} [CA]_{in} \frac{BC_{in}}{K_m + BC_{in}} \approx \rho_{mic} \frac{k_{max}}{K_m} [CA]_{in} BC_{in}, \quad (2.16a)$$

where C_{in} represents the (gas-equivalent) COS concentration at the CA site inside microbial cells. The COS uptake can also be written in terms of transport across the water film from the air-water interface to the cell wall:

$$S_{cat} = g_{film} S_{wall} B\left(C - C_{in}\right), \quad (2.16b)$$

where g_{film} (m s^{-1}) represents the transfer conductance to COS diffusion from the air-water interface to the microbial cell walls and S_{wall} (m^2 wall m^{-3} soil) is the microbial surface density in the soil. Equations (2.16a) and (2.16b) can be combined:

$$S_{cat} \approx \frac{B\rho_{mic} k_{max} [CA]_{in} / K_m}{1 + \dfrac{\rho_{mic} k_{max} [CA]_{in} / K_m}{g_{film} S_{wall}}} C. \quad (2.17)$$

Note that Eq. (2.17) above is formally equivalent to the substrate kinetics model within microbial microsites recently proposed by Tang and Riley (2019) (their equation 8) with the correspondances between notations $k_{1w} \rightarrow k_{max}/K_m[CA]_{in}$, $\kappa_m \rightarrow g_{film}S_{wall}$ and $B_m/\nu_m \rightarrow \rho_{mic}$ and with

the main difference that we do not distinguish substrate transporters and active sites (i.e. K_0 = 1 in their notations).

The ratio ρ_{mic}/S_{wall} represents the average volume-to-surface-ratio of microbial cells. If we assume that microbes are spherical, this ratio can be approximated by $d_{mic}/6$ where d_{mic} is the average microbial diameter. The expression for g_{film} is more complicated but it should decrease with water content (thicker water film) and increase with soil specific surface area (SSA) (thinner water film for higher SSA). In the extreme case where diffusion through the water is the only limiting factor (i.e. $k_{max}[CA]_{in}/K_m \rightarrow \infty$) we have $S_{cat} \rightarrow g_{film}S_{wall}BC = g_{film}(6\rho_{mic}/d_{mic})BC$ that will also decrease with soil water content and increase with SSA and ρ_{mic}. In this situation k_h, now defined as $S_{cat}/BC\theta$, will be proportionnal to $g_{film}\rho_{mic}/\theta$ and would again increase more rapidly than ρ_{mic}/θ[illegible], contradicting our mesocosm results. On the other hand k_h would respond to temperature as g_{film}, and would thus follow the temperature response of COS diffusion in water, which would be coherent with the Q_{10} values for k_h that we have reported (Kaisermann *et al.*, 2018b) (see Fig. 2.5). It would be instructive to perform similar experiments as those in Kaisermann *et al.* (2018b) but exploring a wider temperature range, to better understand the exact signficance of the retrieved hydrolysis rate k_h using our model (Eq. (2.6a)).

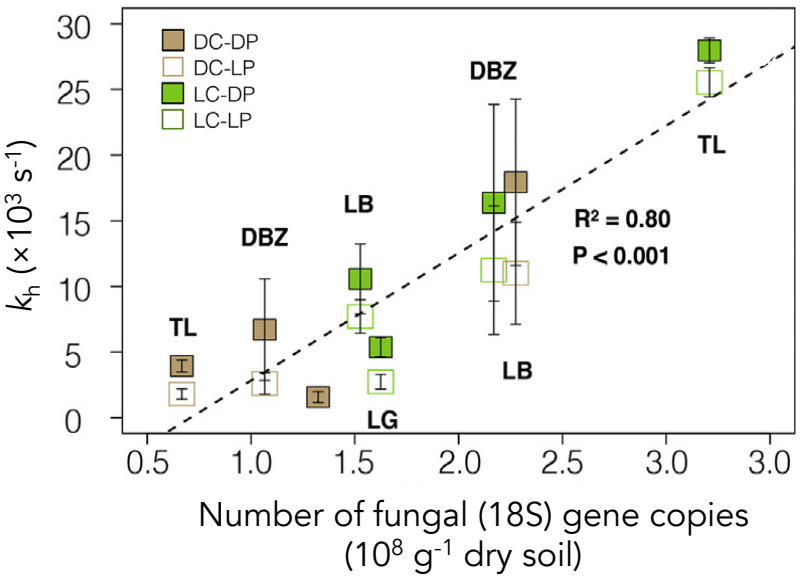

Figure 2.8 | Relationship between the COS hydrolysis rate and the number of fungal gene copies per gram of dry soil for four different soils (LB, LG, DBZ, TL) measured in the light (open symbols; LP) and the dark (close symbols; DP) after ~40 days of incubation in the dark (brown symbols; DC) or the light (green symbols; LC). After Sauze *et al.* (2017).

Most probably, the lack of response of k_h to soil moisture results from the fact that k_{max} and K_m are not true kinetic parameters but rather volume-averaged parameters for the entire soil microbial community (Ogée *et al.*, 2016). Different organisms may have different k_{max}/K_m values so that the spatially-averaged k_{max}/K_m could vary with changes in microbial diversity. Rapid changes in microbial diversity have been reported during wetting-drying cycles (Placella *et al.*, 2012). Our current knowledge of how k_{max}/K_m for COS varies amongst different life forms is too scarce to know if its community-average value should increase or decrease during such changes. We thus adopted the 'null' hypothesis that microbial diversity does not affect k_{max}/K_m. We also tested this

hypothesis by incubating four soils of different pH in the dark or with a diurnal cycle for forty days to vary the abundance of native phototrophs (micro-algae, but also cyanobacteria), and measuring soil-air COS, CO_2 and $C^{18}OO$ fluxes to estimate CA activity alongside the abundance of bacteria, fungi and phototrophs (Sauze *et al.*, 2017). The abundance of soil phototrophs increased in the light (as expected), but mostly at high soil pH, and this was accompanied by an increase in CO_2 uptake and CO_2-H_2O isotopic exchange (k_{iso}). In contrast, COS fluxes and hydrolysis rates (k_h) were primarily attributed to fungal gene copies (Fig. 2.8) whose abundance was positively enhanced in alkaline soils but only in the presence of increased phototrophs (Sauze *et al.*, 2017).

Our findings demonstrated that soil-atmosphere CO_2, COS and $CO^{18}O$ fluxes were impacted by the microbial community structure in response to changes in soil pH and light availability. This result was surprising because the relative number of fungal gene copies to the total number of gene copies g^{-1} of soil was very small. However it was indirectly confirmed by a later study reporting a reduction of COS uptake in soils exposed to fungicides (Bunk *et al.*, 2017).

As mentionned already, little is know about the specific activity (k_{max}/K_m) of different CA classes for COS hydrolysis. However, it has been reported that some β-CAs have an affinity to COS up to 1000 times larger than α-CAs (Haritos & Dojchinov, 2005; Ogawa *et al.*, 2016; Ogée *et al.*, 2016). Unpublished results by our group, based on COS exchange measurements performed on soil columns irrigated with water containing large amounts of α-CA from bovine erythrocytes, confirmed that this type of CA does not take up COS very efficiently. In Sauze *et al.* (2017) we thus explained the observed relationship between k_h and fungal gene copies by concluding that fungal populations must express high quantities of these COS-specific β-CAs.

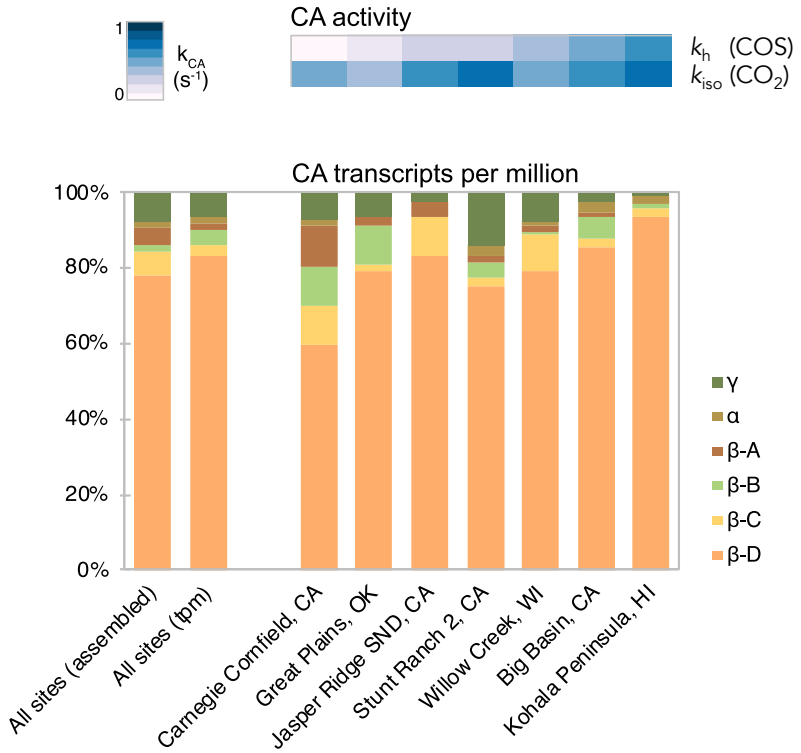

Figure 2.9 | Patterns in measured CA activity in soils in relation to the diversity of expressed CA. Top: enzyme-catalyzed reaction rates for COS (k_h) and CO_2 (k_{iso}). Bottom: relative abundance of α-, β- and γ-CAs in the different soils, with β-CAs further classified in 4 clades (A, B, C and D). After Meredith *et al.* (2019).

In a follow up study we complemented the gas exchange measurements with metatranscriptomics data to better infer which specific CAs were related to higher COS uptake rates (Meredith *et al.*, 2019). We also caracterised the microbial diversity of those soils and found that k_h was positively correlated with the relative abundance of 19 operational taxonomic units (OTUs) from fungal lineages. These results are coherent with those reported in Sauze *et al.* (2017) (Fig. 2.8). More importantly, we found that β-CA, and more specifically β-CA clade D, was the most highly expressed CA in all studied soils (Fig. 2.9) and that the COS hydrolysis rate was correlated with CA expression levels of β-CA from clade D ($r = 0.83$, $p < 0.02$) and anti-correlated with those from clade A ($r = -0.94$, $p < 0.01$). Belonging to clade D is the sequence of carbonyl sulfide hydrolase (COSase), a β-CA previously described in *Thiobacillus thioparus* to have a high affinity for COS and low specificity to CO_2 (Ogawa *et al.*, 2013). Although *Thiobacillus* spp. were rare in the studied soils and characteristic COSase amino acid residues were not found, it is possible that other CAs belonging to the same clade also have a high affinity for COS. If these CAs are specific to fungal lineages, this would explain the correlation we found between k_h and fungal abundance.

Collectively, these results suggest that, for a given temperature, fungal abundance, more than total microbial biomass or pH, drives changes in COS hydrolysis rates. The pH response of individual CAs may all follow the one shown in Fig. 2.6 but this response may be masked by pH-driven changes in the diversitiy of microbes and their respective intrinsic CA activity. Indeed, when we look at the correlation between k_h and explanatory variables suggested by Eq. (2.14) (i.e. temperature, soil moisture, pH and microbial biomass), only the relationship with microbial biomass (ρ_{mic}) seems to hold while the relationships with θ and *pH* do not seem to follow the expected patterns (Fig. 2.10).

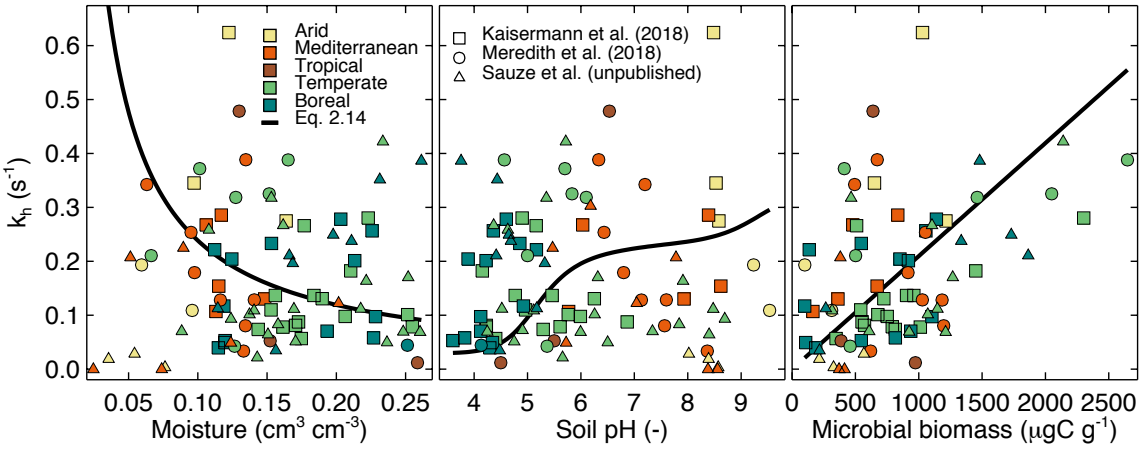

Fig. 2.10 | COS hydrolysis rates from different studies (identified by different symbols) measured on soils from a variety of biomes (identified by different colors), as a function of soil moisture, pH and microbial biomass. Predictions of each relationship using Eq. (2.14) and holding other factors constant and equal to the median value of all the soils are also shown. Variations in soil temperature are not shown but ranged between 17°C and 23°C.

By applying linear mixed models to try identifying the variables that explained best the variations in the COS hydrolysis rate, we found that the best model included microbial biomass, nitrate content and pH (Kaisermann *et al.*, 2018a). Results showed that, within a pH and NO_3^- range, the COS hydrolysis rate (at 18°C and 30% water holding capacity) increased linearly with microbial biomass but its sensitivity to microbial biomass was dependent on the soil NO_3^- content and pH. The strongest response of k_h to an increase in microbial biomass were in alkaline soils with high

nitrate content, while in acidic soils with high nitrate content, the response to an increase in microbial biomass was weak and the absolute k_h values were also lower. Lower NO_3^- content were usually associated with higher k_h.

To date, such linear mixed model seems to be the only way forward to describe with relatively good accuracy (r2 = 0.68, see Kaisermann *et al.*, 2018a) the observed variability of k_h across biomes and land use (at a given temperature and moisture). However, because soil NO_3^- content is very variable temporally and spatially, it cannot be direcly used to predict COS fluxes over continental areas. Other linear mixed models using microbial or total N contents performed also reasonably well (Kaisermann *et al.*, 2018a; 2018b; Meredith *et al.*, 2019). Combined with the N-dependent parameterisation of the COS production rate (Eq. (2.8)) it can be used to upscale soil-air COS fluxes across continents and provide new estimates of the contribution of oxic soils to the global COS budget.

CA-catalysed CO_2 hydration in soils

The model of CA-catalysed COS hydrolysis described above can be extended to the CA-catalysed CO_2-H_2O isotope exchange in soils. A major difference between COS and CO_2 is that the activity for CO_2 of the different CA classes are more similar, with α-CAs typically having only slightly higher k_{max}/K_m (of the order of 30-150 s^{-1} μM^{-1}) than β- or γ-CAs (of the order of 20-100 s^{-1} μM^{-1}). This means that microbial diversity should play a minor role in determining k_{iso}, and stronger correlations between k_{iso} and total microbial biomass shiould be expected.

However, an extra complication should be anticipated regarding the pH response of k_{iso} because, in alkalyne solutions, the ratio of dissolved CO_2 to bicarbonate is very small, so that the *uncatalysed* oxygen isotope exchange between CO_2 and water is dramatically slower than in more acidic soils (Mills & Urey, 1940). To a very good approximation, the $^{18}O/^{16}O$ ratio in CO_2 once in contact with water will follow an exponatial decay towards its equilibrium value with a time constant τ whose inverse ($\tau^{-1} = k_{iso}$) equals (Uchikawa & Zeebe, 2012):

$$k_{iso} = 0.5k_h\left\{1+\frac{C}{S}-\sqrt{1+\frac{2}{3}\frac{C}{S}+\left(\frac{C}{S}\right)^2}\right\}, \quad (2.18)$$

where k_h (s^{-1}) denotes here the CO_2 hydration (and hydroxylation) rate, C (mol m^{-3}) is the concentration of dissolved CO_2 and $S = [H_2CO_3] + [HCO_3^-] + [CO_3^{2-}]$. Assuming that the ratio C/S is close to its equilibrium value (this assumption is actually required to derive Eq. 2.18), the ratio k_{iso}/k_h is only a function of temperature and pH (Uchikawa & Zeebe, 2012). In acidic solutions ($pH < 5.5$), k_{iso}/k_h is close to one third independently of pH or temperature but this ratio rapidly drops in more alkaline pH, with a value at pH 7.4 (and 20°C) about 10 times lower (i.e. 0.028). At pH > 8, CO_2 hydroxylation ($CO_2 + OH^- \leftrightarrow HCO_3^-$) increases rapidly, leading to an increase of (uncatalysed) k_h and a slower decrease of (uncatalysed) k_{iso} despite the continuous drop in the ratio k_{iso}/k_h. This is illustrated in Fig. 2.11 below (see curves [CA] = 0 in panels a and b).

In the original study from Hesterberg and Siegenthaler (1991) and others (Ciais *et al.*, 1997a; Tans, 1998), k_{iso} was (mistakenly) taken equal to the (un-catalysed) CO_2 hydration rate ($k_{iso} = k_{h,uncat}$) and CO_2 hydroxylation was not considered, i.e., $k_{h,uncat} \approx 0.03$ s^{-1} irrespective of pH. In subsequent studies (e.g. Miller *et al.*, 1999; Riley *et al.*, 2002; Cuntz *et al.*, 2003a) k_{iso} was set to $k_{h,uncat}/3 \approx 0.01$ s^{-1}, irrespective of soil pH. Several authors noted however that k_{iso} may be higher than the uncatalysed rate (i.e. $k_{iso} > k_{h,uncat}/3$) if carbonic anhydrase, (Stern *et al.*, 1999) or roots (Riley *et al.*, 2002), was present in the soil (Ciais *et al.*, 1997a; Tans, 1998; Miller *et al.*, 1999; Riley

et al., 2002; Cuntz *et al.*, 2003a; Seibt *et al.*, 2006). However, with no theory at hand to describe this enzymatic activity, the isotopic exchange rate k_{iso} was simply set as a multiple of $k_{h,uncat}/3$: $k_{iso} \approx f_{CA} \times (0.01\ s^{-1})$ where f_{CA} was considered as a parameter of adjustment for sensitivity analysis (Amundson *et al.*, 1998; Miller *et al.*, 1999; Riley *et al.*, 2002). Based on a compilation of field data of soil-air $C^{18}OO$ exchange, we previously suggested f_{CA} values between 20 in extra tropical regions (above 20° latitude) and 300 in tropical regions (20°S-20°N) as a good proxy for large scale applications (Wingate *et al.*, 2009). This is substantially higher than in initial global scale applications where f_{CA} was set to either 1 (Cuntz *et al.*, 2003a) or 3 (Ciais *et al.*, 1997a). These enhanced isotopic exchange rates are also shown in Fig. 2.11 with color bars indicating the frequency distribution of each soil pH range for the entire globe (Ciais *et al.*, 1997a) or each latitudinal bands (Wingate *et al.*, 2009).

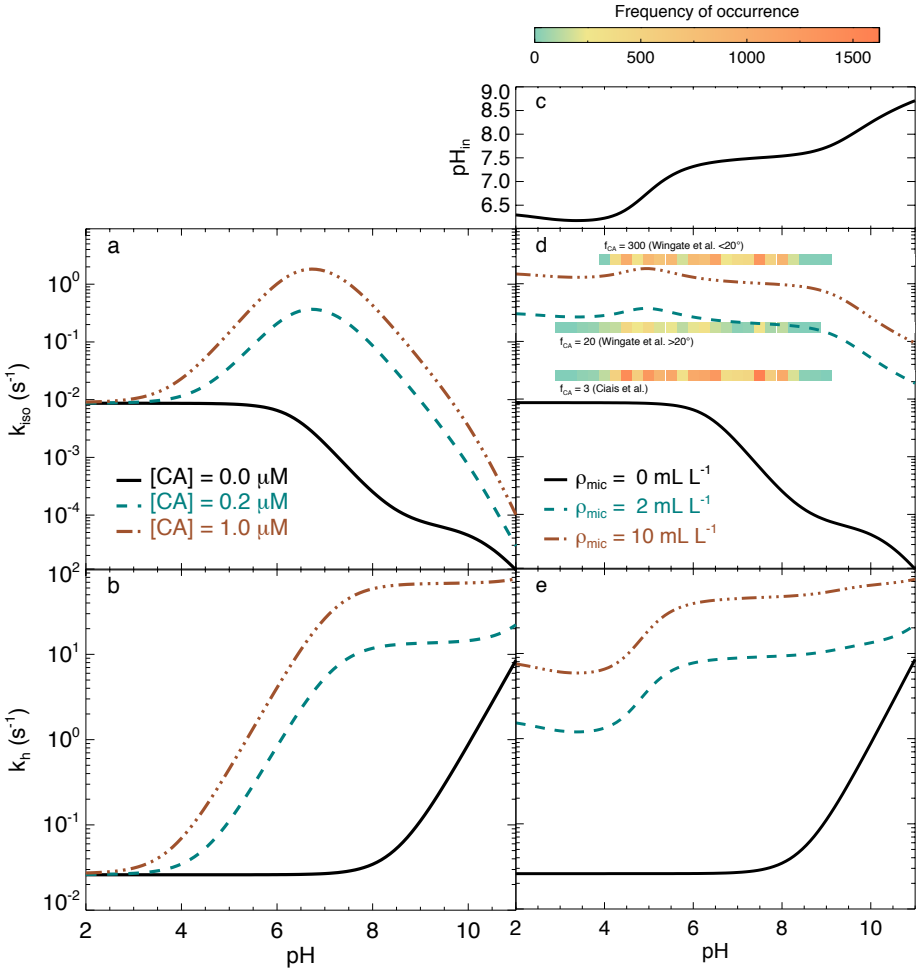

Figure 2.11 | Theoretical rates of CO_2 hydration (k_h) and CO_2-H_2O oxygen isotope exchange (k_{iso}) as a function of soil *pH*, for three concentrations of CA in soil water solution ([CA], left panels) or inside icrobial biomass (ρ_{mic}, right panels). In the latter case, CA is supposed to respond to internal *pH* (pH_{in}) and its concentration is estimated as $[CA] = [CA]_{in}\rho_{mic}/\theta$, with $[CA]_{in}$ = 30 µM and θ = 0.3 $cm^3\ cm^{-3}$. These theoretical curves have been obtained using the uncatalysed rate formula compiled in Uchikawa and Zeebe (2012) and Eq. (2.11) with enzymatic parameters for β-CA (k_{max}/K_m = 68 $s^{-1}\ \mu M^{-1}$ and pK_a = 7.2) from Rowlett et al. (2002). Values of $k_{iso} = f_{CA} \times (0.01\ s^{-1})$ with f_{CA} = 3 (Ciais et al. 1995) or f_{CA} = 20-300 depending on latitude (Wingate et al. 2009) are also represented by color bars indicating the global distribution of soil *pH* in each latitudinal band (see text).

A second effect of pH comes from the pH response of CA activity itself, with much higher turnover rates in alkalyne conditions (see Eq. (2.13) and Fig. 2.6). This means that for a given amount of CA, the enhancement above the uncatalysed rate should be stronger at high pH. This is illustrated in Fig. 2.11 that shows how the uncatalysed ($\rho_{mic} = 0$ or $[CA] = 0$) hydration and isotopic exchange rates vary with pH and how these rates become enhanced in presence of microbial biomass ($\rho_{mic} > 0$ or $[CA] > 0$). We distinguished two different cases depending on whether CA was freely available in soil water and thus responded to soil pH directly (panels a and b) or was inside microbial cells and thus responded to internal (cytoplasmic) pH (panels d and e). In the latter case, we see that, within the range of microbial biomass encountered in natural soils (1-2 mgC g^{-1}, corresponding to about 2-4 mL L^{-1}), we get k_{iso} values equivalent to $f_{CA} > 20$ over almost the entire pH range. On the other hand, a f_{CA} value of 300 corresponds to microbial biomass values greater than 10 mL L^{-1}, which is already an upper limit, even for boreal soils. However these remain theoretical curves and we would have predicted higher k_{iso} values with different values of $[CA]_{in}$ or k_{max}/K_m.

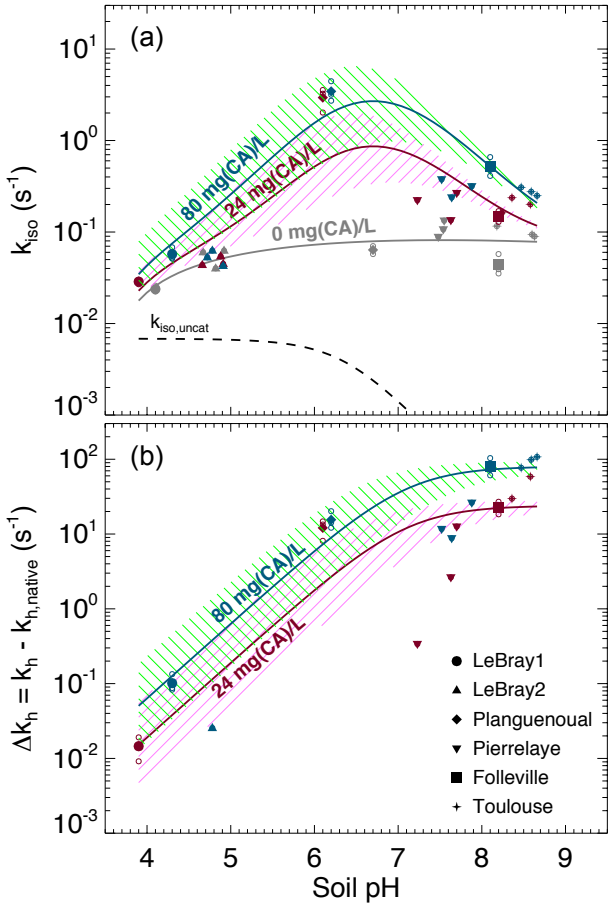

Figure 2.12 | Measured CO_2–H_2O isotopic exchange rates (k_{iso}) in the different soils for different levels of α-CA addition and associated enhancement (k_h - $k_{h,native}$) caused by the α-CA addition. The pH dependence of the native isotope exchange rates (grey points in a) is interpolated using a third-order polynomial fit (grey curve in a). Theoretical rates above this native rate that we would expect from α-CA addition of 24 mg L^{-1} (purple curve and hatched area) and 80 mg L^{-1} (green curve and hatched area) are also shown and have been obtained using k_{max}/K_m = 30 ± 5 s^{-1} μM^{-1} and pK_a = 7.1 ± 0.5. After Sauze *et al.* (2018).

We first tested the theoretical curves shown in Fig. 2.11a and b using lyophilised α-CA powder from bovine erythrocytes that we diluted into soil water (Sauze *et al.*, 2018). We used four different soils covering a pH range between 4 and 8.5. Using a similar setup as described previously (Jones *et al.*, 2017), we then characterised how k_{iso} responded in each soil to an increase in CA concentration (Fig. 2.12).

The results were complicated by the fact that each soil had a native CA activity and also differed in their chemical composition. Several studies have shown that some anions commonly found in soils could act as CA inhibitors or activators, depending on their ability to exchange protons. For

example, phosphate or sulfate ions were reported to be activators or inhibitors of different isoforms of bovine or human α-CA for CO_2 hydration (Rowlett *et al.*, 1991; Rusconi *et al.*, 2004). The presence of these ions also modifies, sometimes dramatically, the pH response of CA activity *in vitro* (Rowlett *et al.*, 1991).

Despite all these possible caveats, we found that the theoretical curves above the native rates predicted reasonably well our measurements (Fig. 2.12). These curves were obtained using a range of values for the kinetic parameters that were expected typical for bovine α-CA, with k_{max}/K_m and pK_a values of 30 ± 5 s^{-1} μM^{-1} (Uchikawa & Zeebe, 2012) and 7.1 ± 0.5 (Rowlett *et al.*, 1991), respectively. Phosphate concentrations did not explain the reported discrepancies between our measurements and the theoretical curves, but the strongest discrepancies occurred also on the two soils (Pierrelaye and LeBray2) that had the highest phosphate contents. Overall we concluded from these experiments that our theoretical understanding of how soil pH affects k_{iso} after exogenous CA addition was confirmed and that complications from the chemical composition of the soil solution (i.e. phosphate content) played only a secondary role.

These findings were very encouraging and could provide insights on how k_{iso} may vary in different soils. However, although α-CAs may be present in certain soil microbial communities with a high abundance of phototrophs such as cyanobacteria and micro- algae, the majority of microbial CAs in soils are β-CAs (Meredith *et al.*, 2019) and β-CAs are seldom active externally like α-CAs and are rather found in the internal cell components of the microbe, in particular the cytoplasm (Smith *et al.*, 1999; Merlin *et al.*, 2003). Thus, although β-CAs also exhibit a strong dependence of CA activity with pH (Rowlett *et al.*, 2002), it remained to be investigated whether the location and relative abundance of different CAs in soil communities modified the expected relationship with pH (Fig. 2.11).

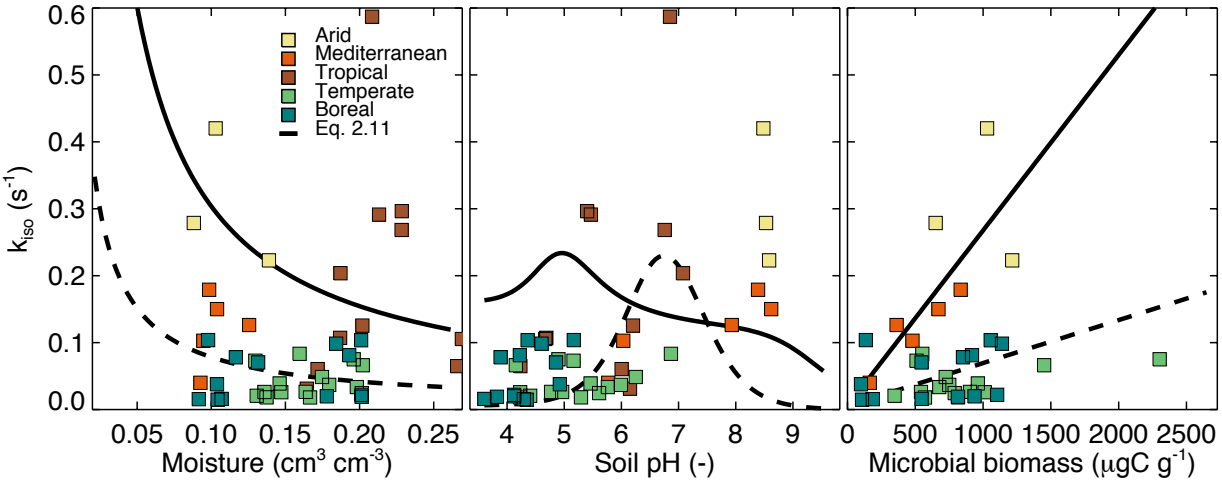

Fig. 2.13 | CO_2-H_2O isotopic exchange rates measured at 21-24°C and 30% water holding capacity (i.e. 13-35% water filled pore space) on soils from a variety of biomes (identified by different colors), as a function of soil moisture, pH and microbial biomass (Jones *et al.*, unpublished). Predictions of each relationship using Eq. (2.11) and holding other factors constant and equal to the median values of all the soils are also shown, with a distinction whether external (dotted line) or internal (solid lines) pH is used. Other parameter values are: $[CA]_{in}$ = 30 μM, k_{max}/K_m = 68 s^{-1} μM^{-1}, pK_a = 7.2.

We addressed this obvious next step by measuring the $C^{18}OO$ flux on a range of natural soils across Europe, and also Australia and Brazil. The preparation of the soils was similar to what is described in Kaisermann *et al.* (2018a) and the measurements were performed as in Jones *et al.*

(2017). The preliminary results of these experiments are shown in Fig. 2.13. The k_{iso} rates varied across these different soils mostly in response to soil pH, with highest values in alkaline soils that were not explained simply by changes in soil microbial biomass. Instead, our results suggest that the CA requirements per organism increase with the basicity of the soil. This result was not necessarily expected. Several studies have shown that CA requirements are usually lower when CO_2 increases, both in plants (Protoschill-Krebs *et al.*, 1996) and soil microbes (Merlin *et al.*, 2003). However, in the different microcosms here, the CO_2 levels were all near ambient, so that the alkalinity of the soil only plays on the capacity of the soil to store other DIC species (e.g. bicarbonate). The respiration rates per unit of microbial biomass were also broadly the same. We could not find any obvious reason why the CA requirements would need to be higher at high pH.

As we did for COS, we tested linear mixed models to help explaining k_{iso} variations amongst our soil types. We found that k_{iso} was mostly correlated with *pH* (r = 0.6) followed by NO_3^- (r = -0.3) and microbial biomass (r = 0.2). A model including additive effects of soil *pH*, NO_3^- and microbial biomass as well as the interaction between soil *pH* and NO_3^- was a very good predictor of k_{iso} (r^2 = 0.7) (Jones et al. (unpublished).

To summarise, both COS hydrolysis rate ($k_{h,S}$) and the $C^{18}OO$ isotope exchange rate (k_{iso}) were best described by linear mixed models including effects of soil *pH*, NO_3^- and microbial biomass and their interaction. These rates were all measured at temperatures around 20-23°C and at 30% water holding capacity, which created some variability in the volumetric soil moisture content. However, soil moisture was not a good predictor when all the soils were treated altogether. On a given soil, we could not find evidence for changes of $k_{h,S}$ with soil moisture during a drying cycle. It still remains to be tested whether changes in k_{iso} would be found as soil dries (preliminary results indicate that it does, see below). Finally, soil pH was a strong predictor but not in the direction that was implied by Eq. (2.11), probably because changes in community-scale k_{max}/K_m dominated the pH response. This is coherent with the idea that different CA classes present in different microbial communities have different affinities to CO_2 and COS, and that CA requirements will change with environmental conditions such as soil pH.

2.3 Remaining questions and future directions

Questions regarding the soil water isotopic composition

In Jones *et al.* (2017) we estimated an isotopic composition of the soil water pool relevant for $C^{18}OO$ fluxes ($\delta_{sw,eq}$) that was systematically more depleted than cryogenically-extracted bulk soil water (δ_{sw}) between 0 and 5 cm. Mean offsets ranged between -2.56 ± 0.11, -2.87 ± 0.56 and -3.61 ± 0.23‰ for the most depleted, intermediate and most enriched water treatments, respectively. We took great care during the preparation of the soil microcosms to ensure homogeneity in the water isotope composition. Isotope analysis of soil water at different depths confirmed that soil water was isotopically very homogeneous, with only a very small isotopic enrichment in the top 1 cm (Fig. 2.14). This means that CO_2 diffusing in and out of the soil should interact with an isotopically homogeneous water pool. Yet, our estimates of the isotopic composition 'seen' by CO_2 molecules based on the two steady state (2SS) approach presented in Jones *et al.* (2017) was systematically more depleted. To try explaining this surprising offset between $\delta_{sw,eq}$ and δ_{sw} we estimated the equilibrium depth (z_{eq}) that the CO_2 molecules are interacting with. Conceptually, z_{eq} corresponds to the shallowest depth at which respired or atmospheric CO_2 has sufficient time to fully equilibrate with soil water (Miller *et al.*, 1999; Wingate *et al.*, 2009). By solving numerically the depth-resolved transport model Eq. (2.1) under natural (i.e. field) conditions, Wingate *et al.* (2009) estimated z_{eq} as the soil depth below which CO_2

molecules would take more than 4 times longer to diffuse out of the soil than it would take them to re-equilibrate with soil water. This can be approximated to: $z_{eq} \approx 2.35 z_1$. Naturally, some degree of exchange still occurs above this depth, but this approximation is convenient when we want to compare with soil water data (Wingate *et al.*, 2009).

Interestingly, in the soil microcosms studied by Jones *et al.* (2017) this equilibration depth falls mostly at the bottom or even outside the microcosm (Fig. 2.14). This means essentially that CO_2 molecules from the headspace of the microcosm have a non-zero probability to diffuse to the bottom of the soil column and back out without equilibrating with soil water. When we do the same exercise with the soil microcosm experiments presented in Sauze *et al.* (2018), we get similar results for the two organic and most acidic sandy soils, including the soil used in Jones *et al.* (LeBray2), and despite the extra addition of exogenous CA in the soil solution and less care in preventing soil evaporation (Fig. 2.15). On the other hand, for all the other soils, the equilibration depth z_{eq} remains within the soil microcosm and the isotopic offset between $\delta_{sw,eq}$ and δ_{sw} is much smaller or non-existent.

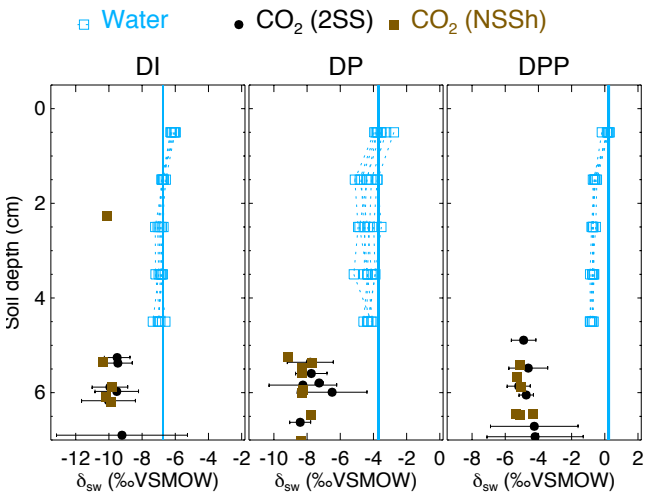

Figure 2.14 | Depth-resolved, soil water $\delta^{18}O$ in the microcosms studied in Jones *et al.* (2017). DI, DP and DPP stand for different irrigation waters (blue line) and blue symbols indicate individual microcosms (*n*=6, see also Fig. 2.1 and Table 2.1). Also shown, and placed at depth $z_{eq} \approx 2.35 z_1$, are the $\delta^{18}O$ of the soil water 'seen' by CO_2 molecules, computed either from the two steady state (2SS) approach of Sauze *et al.* (2018) or from a non-steady state, heterogeneous approach (NSSh, see text).

In Jones *et al.* (2017) we report results from extra microcosm experiments using the same organic sandy soil as the one used in Fig. 2.14 but at various soil water content, from 15% to 65% water-filled pore space, and found that the offset between $\delta_{sw,eq}$ and δ_{sw} decreases at higher water contents (Fig. 2.16). We interpreted these results as follows. Evidence from the recent literature indicated that hygroscopic water was isotopically depleted (up to 4‰) compared to bulk soil water (Chen *et al.*, 2016; Lin *et al.*, 2018) and we assumed it was the case in our soil and that CO_2 equilibrated primarily near the hygroscopic water, where microbial communities and most of the isotopic exchange should take place. By increasing the water-filled pore space, we were increasing the probability for CO_2 molecules to exchange with bulk water, thus decreasing the offset. This reasoning seemed to make sense and was coherent with the results that k_{iso} was also decreasing with increasing soil water content (Fig. 2.16), approaching the un-catalysed rate near saturation. Indeed, at these large soil water content, anoxic conditions reduced soil respiration by 50% and more bulk soil water had to be crossed by CO_2 molecules to escape the soil. If true, then this would mean that what we estimate as k_{iso} is not simply related to CA activity but would include also a diffusional part in the liquid phase, similar to Eq. (2.17).

We also performed extra experiments where soil depth was varied at a given soil moisture content (around 0.1 $cm^3\ cm^{-3}$). The results reassuringly showed that neither k_{iso} nor $\delta_{sw,eq}$ changed

significantly with soil depth (Fig. 2.16). However in all cases, the equilibration depth was below the soil depth. Clearly more experiments are needed to fully understand the exact meaning of what we call k_{iso} and its sensitivity to soil water content (see also below).

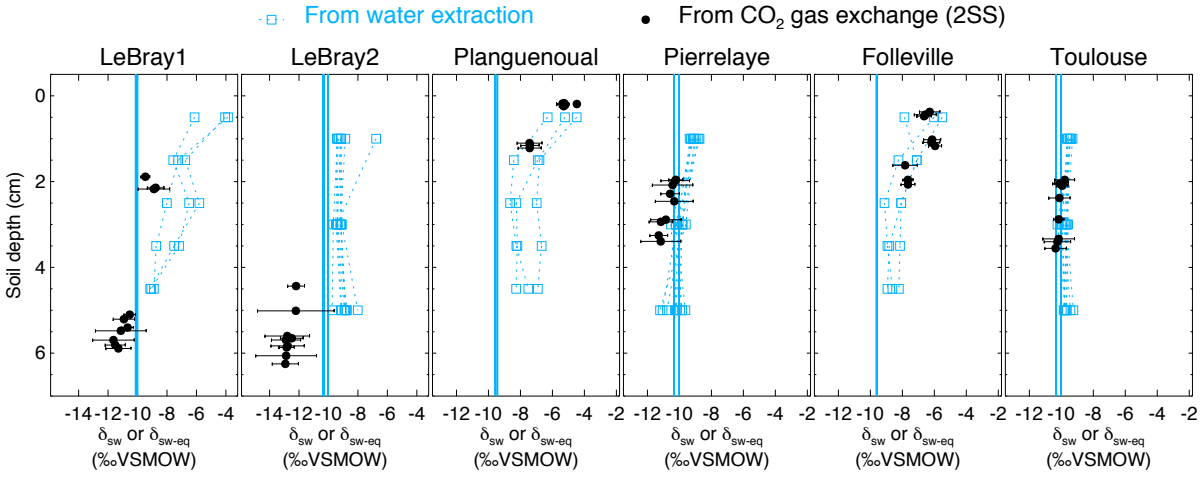

Figure 2.15 | Same as Figure 2.14 but for the soil microcosm experiments presented in Sauze *et al.* (2018). Replicated microcosms (*n*=3) were measured for gas exchange 3 times in a row, resulting in 9 estimates of $\delta_{sw,eq}$. Note that the 2SS estimates are slightly different from those presented in Sauze *et al.* (2018) because they have been post-corrected for a small isotopic offset between VPDBg scales from MPI-Jena (to which our calibration gases were referred) and NOAA (to which our labeled inlet was referred). We did this because the NOAA scale seems more compatible with the VSMOW scale (to which water samples are referred).

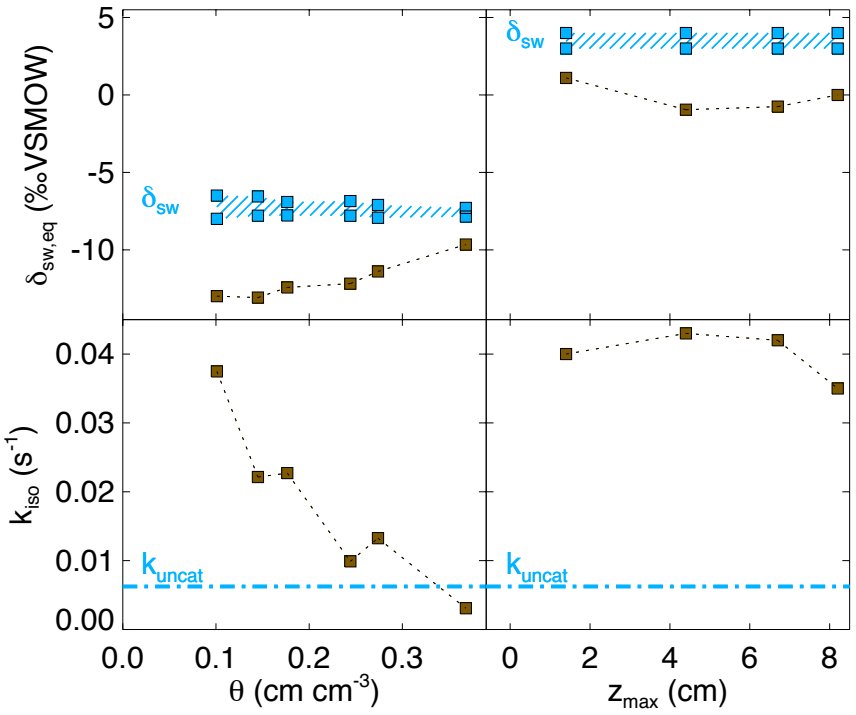

Figure 2.16 | Retrieved $\delta_{sw,eq}$ and k_{iso} as described in Jones et al. (2017) where either soil moisture (left) or soil depth (right) is varied, keeping all the other parameters as constant as possible. After Jones et al. (2017).

Questions regarding the $C^{18}OO$ mass balance

So far we only presented results from our $C^{18}OO$ microcosm experiments with the assumption that chemical and isotopic steady state was reached during gas exchange measurements. We attempted to check this assumption by solving the time-dependent mass balance equation (Eq. 2.1) numerically, using depth-resolved measurements of soil moisture content and $\delta^{18}O$, not only during steady state gas exchange but also during the transitions when the microcosm was installed on the gas exchange system (thus being suddenly flushed with air containing usually much less CO_2 than room air), and also during the transitions where the air inlet was switched between CO_2-in-air mixtures containing the same CO_2 mixing ratio but differing in isotopic composition (Jones *et al.*, 2017).

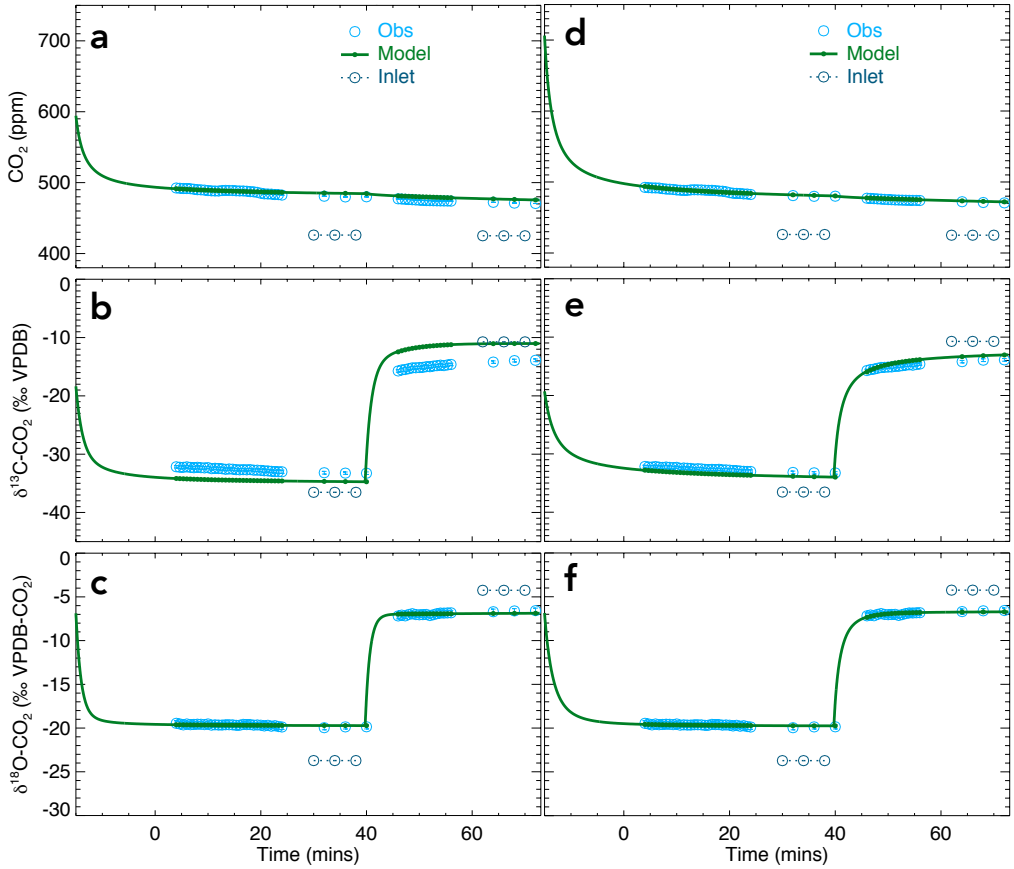

Figure 2.17 | Measured and modelled CO_2 mixing ratio and $^{13}C/^{12}C$ and $^{18}O/^{16}O$ ratios in the headspace of the soil microcosm during a step change in the isotope composition of the inlet air. The soil is an arable, alkalyne soil (pH 8). The model solves the mass balance equations for the three tracers in the non steady state, excluding (a, b, c) or including (d, e, f) exchange with other DIC species (see text). The impact on the retrieved k_{iso} and δ_{eq} is marginal (Sauze *et al.* 2018). Times when steady state conditions are assumed coincide with the times when we were also measuring the air on the inlet of the microcosm (open blue-green symbols).

When doing so, we had to optimise 3 parameters: k_{iso}, δ_{offset}, the offset between bulk soil water δ_{sw} and $\delta_{sw,eq}$ (assuming the offset was the same throughout the soil column) and $[CO_2]_{init}$, the CO_2 mixing ratio of the headspace prior to the experiment. We assumed that the $\delta^{13}C$ and $\delta^{18}O$ of this

initial CO_2 was equal to the isotope ratio of soil respiration measured during steady state (δ_F) because the microcosms, while being connected to the gas exchange system, were covered with a lid. For $\delta^{18}O$, using δ_{eq} instead of δ_F would be more correct ($\delta_F \neq \delta_{eq}$, see Eq. 2.3c) but this had no impact on the final results because the isotopic composition of the initial air was rapidly flushed away once the measurements started. The optimisation was performed on CO_2 concentration, $\delta^{13}C$ and $\delta^{18}O$ measured in the microcosm headspace during the entire measuring sequence. An example of the results is shown in Fig. 2.17 below (panels a-c), for the arable, alkaline (pH 8) soil labelled "Toulouse" in Fig. 2.15.

We can see that the transient model (Eq. 2.1) can capture the entire time series of CO_2 concentration and $\delta^{18}O$ in the chamber headspace very well, while accounting for the heterogeneity in soil water content and $\delta^{18}O$ through the soil column. On the other hand, there is a clear mismatch on the $\delta^{13}C$. This mismatch on the $\delta^{13}C$ was very reproducible and occurred systematically on alkaline soils, while it was much smaller or even within the measurement uncertainties on acidic soils. This is something that had been reported previously by Gamnitzer *et al*. (2011) and can be explained by the fact that the CO_2 also exchange chemically and isotopically with the bicarbonate (and carbonate) pool. Because the size of this bicarbonate pool is much larger under alkaline conditions, this creates a much slower response time after a step change in CO_2 concentration or isotopic composition in the headspace than in more acidic soils.

Formally, this exchange with the bicarbonate pool can be taken into account by including a third mass balance in Eq. (2.1) for all the non-CO_2 DIC species, on top of the mass balance equations for gaseous CO_2 and for dissolved CO_2. This third mass balance should be included for all the CO_2 isotopologues, and thus also for total CO_2 (Gamnitzer *et al.*, 2011). In fact for $C^{18}OO$, the way the isotopic exchange term is written in Eq. (2.1) or (2.2b) implicitly includes exchange with the bicarbonate pool. This is explained in Appendix B of Ogée *et al*. (2018) where we perform separate mass balances for CO_2 and bicarbonate. We showed that the isotopic exchange term that should appear in the liquid CO_2 mass balance (Eq. 2.2.b) should be written as $k_h C_l(R_l - \alpha_{cb} R_b)$ where k_h denotes the CO_2 hydration rate, R_b is the isotope ratio of the bicarbonate and α_{cb} the equilibrium isotope fractionation between CO_2 and bicarbonate. This is quite different from $k_{iso} C_l(R_l - R_{eq})$. The latter expression includes the bicarbonate mass balance, which at steady state and neglecting diffusion would write (Ogée *et al.*, 2018) (see Eq. 2.19c below): $2R_l + R_{eq} - 3\alpha_{cb} R_b = 0$. When we insert this equality into $k_h C_l(R_l - \alpha_{cb} R_b)$, this leads to $k_{iso} C_l(R_l - R_{eq})$ with $k_{iso} = k_h/3$. This translates the fact that the oxygen exchange does not occur directly between CO_2 and water but requires the formation of bicarbonate. In other words, the mass balance equations (Eq. 2.2) should be revised as follows [see Eq.B5 in Ogée *et al*. (2018)]:

$$\left(\phi - \theta\right)\frac{\partial RC}{\partial t} = \frac{\partial}{\partial z}\left(D_{iso}\frac{\partial RC}{\partial z}\right) - k_{g\to l}\left(RC - \frac{R_l C_l}{^{18}B}\right), \tag{2.19a}$$

$$\theta\frac{\partial R_l C_l}{\partial t} = -\theta k_h C_l\left(R_l - \alpha_{cb} R_b\right) + P R_{eq} + k_{g\to l}\left(RC - \frac{R_l C_l}{^{18}B}\right), \tag{2.19b}$$

$$\theta\frac{\partial R_b C_b}{\partial t} = -\theta\frac{k_h}{3} C_l\left(2R_l + R_{eq} - 3\alpha_{cb} R_b\right), \tag{2.19c}$$

where C_b (mol m^{-3}) denotes the concentration of bicarbonate in soil water, but also carbonate ions and carbonic acid because the ^{18}O composition of these different species are inseparable (Uchikawa & Zeebe, 2012; Ogée *et al.*, 2018): $C_b = [H_2CO_3] + [HCO_3^-] + [CO_3^{2-}]$ (it was denoted S earlier in Eq. 2.18).

In practice, we assume that chemical equilibration is reached between gaseous and dissolved CO_2 ($C_l = BC$) and between dissolved CO_2 and the other DIC species (Uchikawa & Zeebe, 2012):

$$C_b = C_l\left(K' + \frac{K'K_{H_2CO_3}}{[H^+]} + \frac{K'K_{H_2CO_3}K''}{[H^+]^2}\right) = K_bBC\,, \tag{2.20}$$

where we used the exact same notations as in Uckikawa and Zeebe (2012, see their Eq. 7).

The sum of the three mass balance equations (2.19) leads to Eq. (2.1) but with an extra storage term on the right-hand side (K_bB) and with the identity $k_{iso} = k_h/3$:

$$\left[\phi + (B(1+K_b) - 1)\theta\right]\frac{\partial RC}{\partial t} = \frac{\partial}{\partial z}\left(D_{iso}\frac{\partial RC}{\partial z}\right) - B\theta k_{iso}C\left(R - R_{eq}\right) + PR_{eq}\,, \tag{2.21}$$

Inclusion of this extra storage term in the mass balance equations for $C^{18}OO$ but also CO_2 and $^{13}CO_2$ improves the fit to the observed time series, especially the $\delta^{13}C$ data and particularly on alkaline soils (Fig. 2.17, panels d-f). For $\delta^{13}C$, this was already reported by Gamnitzer *et al*. (2011). Here we show it also for $\delta^{18}O$.

An important consequence of Eq. (2.21) is that, when steady state is reached, the isotopic exchange rate that we observe should be $k_{iso} = k_h/3$, not that given by Eq. (2.18). In other words, the pH dependency of k_{iso} at steady state should resemble that of k_h (shown in Fig. 2.11b or 2.11e) and should increase monotonously with increasing pH, even at high pH. The fact that in the microcosm experiments on exogenous CA we estimated an isotopic exchange rate that declined at higher pH (Fig. 2.12) may indicate that steady state was never reached completely in these alkaline soils (and despite the fact that the measurements in the head space indicated some sort of steadiness, see Fig. 2.17). We had to find a compromise between reaching steady state gas exchange while maintaining a constant soil water content and $\delta^{18}O$. It is likely that, in alkaline soils, reaching such steady state is impossible because it takes longer for the gaseous CO_2 to equilibrate with the entire bicarbonate pool than for soil evaporation to modify substantially the soil water content and isotopic composition. In these situations, the isotopic exchange rate may be approximated by the first-order decay rate constant of Eq. (2.21):

$$\tau^{-1} \approx \frac{k_h}{3}\frac{B\theta}{\phi + (B(1+K_b) - 1)\theta} = \frac{k_h}{3}\frac{1}{1 + K_b + \frac{\phi - \theta}{B\theta}}\,, \tag{2.22}$$

This is the equation derived by Gerster *et al*. (1971) to describe the isotopic dynamics of ^{18}O in gaseous CO_2 in a closed volume while in contact with a water pool, except that the exchange coefficient between the gas and liquid phase has been neglected here ($k_{g\to l} = 0$). As explained in Ogée *et al*., this expression (without the gas phase contribution) is a very good approximation of Eq. (2.18). It is possible that the results shown in Fig. 2.12 traduce the pH dependency of this decay rate. However, when used Eq. 2.21 and retrieved k_{iso} and δ_{eq} by fitting the entire time series (as shown in Fig. 2.16d-f for one particular microcosm) we obtained almost identical values of k_{iso} and δ_{eq} as those found using only steady state conditions (Fig. 2.14, see also Fig. S1 in Sauze *et al*., 2018). The reason for this is not completely clear. A possibility is that chemical equilibrium was not reached in our experiments, i.e., Eq. 2.20 does not hold. In this case, we would need to solve Eqs. 2.19a-c simultaneously. This would require knowledge of the exchange coefficient $k_{g\to l}$, a parameter that should increase with finer soil texture. This is something to be explored.

The idea that k_{iso} may be slower than the chemical rate was already proposed by Stern *et al.* (1999). They suggested that k_{iso} should be slower than the rate in pure water (i.e. $k_{iso} < k_{h,uncat}/3$) because the rate of exchange was "most probably" not controlled by chemical processes but by physical ones, namely by diffusion "across the soil air/soil water interface into the films of liquid water coating mineral grains". This argument was based on observations by Hsieh *et al.* (1998) that CO_2 takes longer to reach isotopic equilibrium with soil water in a finer and drier soil (sometimes > 24h at very low water contents and sterilised soils). These authors concluded that "isotopic exchange between CO_2 and water may be impeded by smaller pores and surface tension" because "low water content and fine pore sizes decrease the amount of water in which CO_2 may dissolve" and "increase the amount of mineral surface area on which water may adsorb and thus, reduce CO_2 dissolution into this tightly held adsorbed water" (Hsieh *et al.*, 1998). A higher air-liquid interface should however enhance $k_{g\to l}$ and thus favour chemical and isotope equilibrium between the two phases (i.e. $C_l = BC$ and $R_l = R$), unless the high air-liquid interface is also accompanied by the presence of many micro-pores where gas diffusion is restricted or slowed down. The pH values were not reported but, possibly, the fine grain soils studied by Hsieh *et al.* were also alkaline, so that the time to equilibration was dramatically increased (term K_b in Eq. 2.22). More importantly, we estimated that, in the experiment of Hsieh *et al.*, the last term in the denominator of Eq. 2.22 was around 250-300, thus explaining why the equilibration time was much slower than the one predicted from the chemical CO_2 hydration rate.

Another assumption of Eq. 2.1 or Eq. 2.21, and a possible complication to be explored, is that advection of CO_2 (and $C^{18}OO$) caused by air or water movement is negligible. Advection of gases can occur in both liquid and gas phases when the carrier fluid (water or air) moves relative to the soil matrix. Advective fluxes of CO_2 can be simply estimated as:

$$F_{adv,l} = q_l C_l = q_l BC, \tag{2.22a}$$

$$F_{adv,a} = q_a C, \tag{2.22b}$$

where q_l (m s^{-1}) and q_a (m s^{-1}) are the velocity fields for liquid water and air respectively. If the flow in the porous soil is laminar, these velocity fields are given by Darcy's law (Massman *et al.*, 1997; Scanlon *et al.*, 2002):

$$q_l = -\frac{k_l}{\mu_l}\frac{\partial \Psi_l}{\partial z} = -K_l\left(\frac{\partial h_l}{\partial z} + 1\right), \tag{2.23a}$$

$$q_a = -\frac{k_a}{\mu_a}\left(\frac{\partial p_a}{\partial z} + \rho_a g\right), \tag{2.23b}$$

where k_l and k_a (m^2) denote soil permeabilities for liquid water and air respectively, μ_l and μ_a (kg m^{-1} s^{-1}) are water and air dynamic viscosities, $\Psi_l = \rho_l g(h_l + z)$ is total soil water potential (Pa), ρ_l is water density (1000 kg m^{-3}), h_l (m) is matric potential height, g is gravitational acceleration (9.81 m s^{-2}), ρ_a is air density (*ca.* 1.2 kg m^{-3}) and p_a (Pa) is air pressure. We also defined the soil hydraulic conductivity K_l (m s^{-1}): $K_l = k_l\rho_l g/\mu_l$. In practice p_a can be expressed as the sum of the hydrostatic pressure ($-\rho_a gz$) and a fluctuating (non-hydrostatic) part: $p_a = -\rho_a gz + p_a'$ so that Eq. (2.23b) can be replaced by:

$$q_a = -\frac{k_a}{\mu_a}\frac{\partial p_a'}{\partial z}, \tag{2.23c}$$

Air pressure fluctuations can occur at different time scales, for example after venting the soil surface (according to Bernouilli's equation) or simply by atmospheric turbulence. Both can happen

in experimental setups and in the field. Typical air pressure fluctuations in field conditions are of the order of 10 Pa (Massman *et al.*, 1997; Maier *et al.*, 2012).

Stern and colleagues explored the influence of CO_2 advection by air movements on the $^{18}O/^{16}O$ ratio of soil CO_2. They numerically simulated advection resulting from a sinusoidally oscillating pressure variation at the soil surface with period of 1 minute and amplitudes of between 1 and 50 Pa (corresponding to extreme wind conditions) and soil permeabilities of between 10^{-5} and 10^{-6} cm^2. In most situations, advection modified the $\delta^{18}O$ of soil CO_2 only marginally (< 0.1‰). In the most extreme situations, the effect was small but measurable (up to 0.9‰). They concluded that "only in extreme cases of high permeability soils combined with high frequency surface pressure variations resulting from vigorous winds, will advection be a significant process affecting the $\delta^{18}O$ value of soil CO_2" (Stern *et al.*, 1999). In addition, because we are dealing with fluctuations, advective fluxes would start to become negligible compared to diffusive ones when averaged over a long enough timescale (typically >1h, see Massman *et al.*, 1997). Integration timescales of a few minutes were already assumed to allow gas-liquid chemical equilibration in Eqs. (2.1). This is the reason why advective fluxes are often neglected, although such an assumption may not be valid for time scales of less than 1h and rainy or windy conditions.

But even when advective fluxes are negligible, advection through porous media generates a diffusive-like flux called mechanical dispersion that reflects the fact that not everything in the porous medium travels at the average water or gas flow speed. Some paths are faster, some slower, some longer and some shorter, leading to a net spreading of the gas or solute plume that looks very much like diffusive behaviour. Since mechanical dispersion depends on the flow, it is expected to increase with increasing flow speed and is usually expressed as:

$$F_{\text{disp,l}} = -D_{\text{disp,l}} \frac{\partial C_{\text{l}}}{\partial z} = -\alpha_{\text{l}} \left| q_{\text{l}} \right| \frac{\partial BC}{\partial z}, \tag{2.24a}$$

$$F_{\text{disp,a}} = -D_{\text{disp,a}} \frac{\partial C}{\partial z} = -\alpha_{\text{a}} \left| q_{\text{a}} \right| \frac{\partial C}{\partial z}, \tag{2.24b}$$

where α_l (m) and α_a (m) are the longitudinal dynamic dispersivity of liquid water and air flow respectively and $D_{disp,l}$ (m^2 s^{-1}) and $D_{disp,a}$ (m^2 s^{-1}) are the corresponding dispersive diffusivities. Transverse dispersion (i.e. in a plane perpendicular to the flow) can also occur but will be neglected here.

In practice, because of these dispersive fluxes, we must know the liquid water and air velocity fields q_l and q_a in order to solve the mass balance equation (Eq. 2.1). This requires solving the total mass balance equations for liquid water and air separately. However, except during rain infiltration and immediate redistribution, q_l rarely exceeds a few mm per day while the drift velocity, defined as the ratio $F_{diff,a}/C$, is typically of the order of a few mm per minute. For this reason, dispersive fluxes in the liquid phase are generally neglected in soil gas transport models. Dispersive fluxes can still be accounted for as a correction factor to true diffusion, provided we have parameterisations of the dispersion diffusivities that are independent of the advective flux (e.g., expressions for $D_{disp,a}$ independent of q_a). For example Maier *et al.* (2012) proposed expressions of $D_{disp,a}/D_{0,a}$ that rely on the air-filled porosity ($\phi - \theta$) and permeability (μ_a) of the soil and the degree of turbulence above the soil surface (characterised by the friction velocity u_*).

In our microcosm experiments, we tried to minimise any pressure variation, notably when switching from one microcosm to another, or when changing the isotopic composition of the inlet air stream. In this case, we expect advection or dispersion fluxes to be small. On the other hand, neglecting these fluxes in field applications may not be valid. This means that the applicability of

Eq. 2.1 (or its extension Eq. 2.21) to natural soils would need to be tested under various wind and rainfall regimes.

Chapter 3 – Leaf-air $C^{18}OO$ and COS exchange

3.1 Introduction

The exchange of COS and $C^{18}OO$ between foliage and the surrounding air is controlled by diffusional and enzymatic processes. It is generally accepted that carbonic anhydrase (CA) is the principal enzyme involved in these exchanges, although some studies suggested that other photosynthetic enzymes may also play some role in the exchange of COS (Lorimer & Pierce, 1989; Protoschill-Krebs & Kesselmeier, 1992; Yonemura *et al.*, 2005) or $C^{18}OO$ (Stimler *et al.*, 2011). Despite the high CA activity inside foliage, it has also been reported that CO_2 coming out of foliage may not be fully equilibrated with leaf water, especially in C_4 plants (Gillon & Yakir, 2001) or that COS could be emitted by foliage, at least from (sulphur-rich) crops such as *Brassica napus* L. (oil seed rape) (Kesselmeier & Merk, 1993), and particularly during fungal infection (Bloem *et al.*, 2012). These observations complicate considerably our understanding of $C^{18}OO$ and COS fluxes from foliage and are thus ignored most of the time in large-scale applications, both for $C^{18}OO$ (Farquhar *et al.*, 1993; Riley *et al.*, 2002; Buenning *et al.*, 2014) and COS (Kettle *et al.*, 2002; Campbell *et al.*, 2008; Berry *et al.*, 2013).

Gillon and Yakir attempted to produce a global picture of the degree of CO_2-H_2O equilibration in foliage (θ_{eq}) from CA activity measurements performed on leaf extracts from different plant functional groups (Gillon & Yakir, 2001). This static map of θ_{eq} was subsequently used in a global scale model to estimate its impact on the atmospheric $C^{18}OO$ budget (Cuntz *et al.*, 2003b). A global scale average of the degree of equilibration θ_{eq} was also used in a two-box atmospheric budget model to retrieve global land photosynthesis from $C^{18}OO$ (Welp *et al.*, 2011). Results from this study (the only one so far that predicted a global estimate of photosynthesis using $C^{18}OO$) were shown to be highly sensitive to the exact value of θ_{eq} that was used (Cuntz, 2011). From this analysis, it was clear that a **better understanding of how the degree of equilibration between leaf water and CO_2 varies across plant functional types and with seasonal changes in stomatal conductance and photosynthetic rates** was a necessary step to use atmospheric $C^{18}OO$ as a tracer of the land C sink.

Besides CA activity, stomatal conductance is known to play a key role in regulating the leaf gas exchange of COS (Sandoval-Soto *et al.*, 2005; Yonemura *et al.*, 2005; Stimler *et al.*, 2010; Sandoval-Soto *et al.*, 2012; Stimler *et al.*, 2012; Kooijmans *et al.*, 2017; 2019) and $C^{18}OO$ (Barbour *et al.*, 2005; Seibt *et al.*, 2007). Other diffusional limitations, located inside the leaf to the CA reaction site, are also considered important, both for COS (Yonemura *et al.*, 2005; Kooijmans *et al.*, 2019) and $C^{18}OO$ (Farquhar & Lloyd, 1993; Gillon & Yakir, 2000a; Cousins *et al.*, 2006a; Barbour *et al.*, 2016; Ogée *et al.*, 2018). These diffusional limitations inside the leaf create a drawdown of CO_2 and COS partial pressures[12] between the intercellular air-liquid interface inside the leaf mesophyll (p_i) and the CA site inside the mesophyll cells (p_{CA}), and are characterised by a finite 'mesophyll' conductance (g_m, in mol air m^{-2} leaf s^{-1}). It is still unclear however how this mesophyll conductance responds to environmental conditions (temperature, CO_2…) and how it varies across nutritional gradients and plant functional types. As a consequence, most $C^{18}OO$ modelling studies so far have considered that mesophyll conductance for CO_2 was non-limiting ($g_m \rightarrow \infty$) (Riley *et al.*, 2002; Cuntz *et al.*, 2003a; Still *et al.*, 2009; Buenning *et al.*, 2014).

Other studies (Farquhar & Lloyd, 1993; Cuntz *et al.*, 2003b) attempted to consider g_m as a limiting factor by assuming it was co-varying with a proxy of photosynthetic capacity, defined as the ratio

[12] Following common practice, we express dissolved gas concentration in the liquid phase inside mesophyll cells in equivalent atmospheric partial pressures (p_x, in Pa). The two quantities are related *via* the gas solubility constant (in units of mol m^{-3} Pa^{-1}).

of net photosynthesis (A) to the atmospheric CO_2 mixing ratio: $g_m \approx (5\text{-}10)AP/p_a$, where P is total atmospheric pressure, p_a is the CO_2 partial pressure in the atmosphere and p_a/P its mixing ratio. This definition of g_m leads to a CO_2 partial pressure drawdown proportional to p_a: $p_i - p_{CA} \approx (0.1\text{-}0.2)p_a$. Because the interpretation of $C^{18}OO$ photosynthetic discrimination data was always complicated by the possible deviation from full equilibration ($\theta_{eq} < 1$), the exact value of the ratio $(p_i - p_{CA})/p_a$ was deduced instead from $^{13}CO_2$ photosynthetic discrimination on a few tree species (Lloyd *et al.*, 1992), and based on the idea that photosynthetic enzymes CA and RuBisCO[13] are co-located in C_3 plants[14] (Farquhar *et al.*, 1993). However it is now recognised that CA is present and relatively abundant in many parts of the mesophyll cells of C_3 plants, including the plasma membrane and the cytosol (Fabre *et al.*, 2007). Also this approach for estimating CA-based g_m from $^{13}CO_2$ photosynthetic discrimination cannot be used in C_4 species where CA and RuBisCO are physically separated between mesophyll and bundle sheath cells (Hatch & Burnell, 1990). Yet, a small error on g_m leads to a larger error on the predicted leaf $C^{18}OO$ flux because the retro-flux of CO_2 escaping the leaf interior is $F_{out} = \kappa_c A = Ap_{CA}/(p_a - p_{CA})$ (see chapter 1). Clearly **a better description of mesophyll conductance limitations in different plant functional types is required to improve our predictions of the $C^{18}OO$ flux from foliage and its contribution to the atmospheric $C^{18}OO$ budget**.

In some recent studies mesophyll conductance for COS was 'lumped' with the enzymatic CA activity into a total 'internal' conductance g_i and the latter was assumed to co-vary with either stomatal conductance for water vapour (g_{sw}) (Seibt *et al.*, 2010) or photosynthetic (RuBisCO-limited) capacity (V_{cmax}) (Berry *et al.*, 2013). A g_{sw}/g_i ratio of 0.05 was required to reproduce diurnal variations of leaf COS gas exchange measurements performed on *Fagus sylvatica* and *Quercus agrifolia* branches (Seibt *et al.*, 2010) and a g_i/V_{cmax} ratio of 1200 (C_3 species) and 13,000 (C_4 species) was found suitable to reproduce leaf gas exchange data from Stimler *et al.* (2012) (Berry *et al.*, 2013). These approaches are an improvement compared to other COS studies (Sandoval-Soto *et al.*, 2005; Campbell *et al.*, 2008; Asaf *et al.*, 2013; Berkelhammer *et al.*, 2014; Launois *et al.*, 2015; Campbell *et al.*, 2017) that simply assume that the leaf-air COS and CO_2 fluxes, normalised by their respective atmospheric partial pressures (i.e., $F_{COS}/p_{a,COS}$ and A/p_a) are proportional: $(F_{COS}/p_{a,COS})/(A/p_a)$ = constant. This ratio, called 'leaf relative uptake' (LRU), is however not constant. A recent review of the literature estimated its range between 0.7 to 6.2 with a median value around 1.68 (Whelan *et al.*, 2018). A constant LRU would mean not only that the ratio g_{sw}/g_i is constant and the same across all species, but also that the ratio of p_i/p_a is constant and the same between C_3 and C_4 species (Seibt *et al.*, 2010). This LRU approach also fails at explaining that COS uptake also occurs in the dark when photosynthesis is zero (Gimeno *et al.*, 2017; Kooijmans *et al.*, 2017). **Clearly an approach separating diffusional and enzymatic limitations of COS uptake by foliage is preferred.** Not only this would help account for differences between C_3 and C_4 species in terms of CA location and activity (Protoschill-Krebs & Kesselmeier, 1992) but it would also help capture the divergence between COS and CO_2 fluxes in the dark. Given the parallel between the diffusional and enzymatic processes governing COS and $C^{18}OO$ exchange by foliage It would also **help linking leaf COS and $C^{18}OO$ fluxes across biomes**.

[13] RuBisCO stands for ribulose-1,5-bisphosphate carboxylase oxygenase.

[14] The value for $(p_i - p_{CA})/p_a$ of 0.1 used by Farquhar *et al.* (1993) is supposedly based on data from Lloyd *et al.* (1992) However, while writing this chapter, I noticed that the original data suggest a ratio [of $(p_i - p_{RUBISCO})/p_a$] around 0.2. The lower value used by Farquhar *et al.* implicitly assumes that CA is located upstream of RuBisCO so that the mesophyll conductance for $^{13}CO_2$ is half that for $C^{18}OO$, thus contradicting this idea of co-location of the enzymes proposed by the same authors. It is however coherent with the more recent findings by Fabre *et al.* (2007).

Over the past few years, we have addressed these knowledge gaps by developing a model of $C^{18}OO$ gas exchange in C_3 and C_4 species that explicitly accounts for the location of CA and other photosynthetic enzymes and their potential competition (Ogée *et al.*, 2018). We then applied this new model to revisit published datasets and estimate the degree of equilibration (θ_{eq}) and the associated mesophyll conductance (g_m) in a range of C_3 and C_4 species. We found that the degree of equilibration was usually larger than previously thought, especially in C_4 grasses, and that the p_i - p_{CA} drawdown varied between species but also with light and leaf temperature. In contrast, for a given species, g_m responded mostly to temperature and leaf age. We also tested simplifications and derived parameterisations of the new model that could be suitable for global scale applications. Based on our knowledge of CO_2 and COS diffusivity in water and their different affinity to plant β-CA, we transposed our leaf $C^{18}OO$ model to describe COS transport and fate into foliage. Incorporating these parameterisations of leaf-air $C^{18}OO$ and COS fluxes into a global scale model, we found that the approach was coherent with global scale estimates of photosynthetic COS uptake by Berry *et al.* (2013), while linking for the first time this large COS flux to the even larger one-way $C^{18}OO$ flux from foliage. The remaining of this chapter briefly summarises these different findings.

3.2 Recent advances on foliar COS and $C^{18}OO$ fluxes

Diffusion across stomata and how it is influenced by transpiration

All gases (CO_2, $C^{18}OO$, COS and the like) enter or escape the leaf interior mainly through the stomatal pores. Leaf gas exchange measurements performed on leaves of *Vitis vinifera* L., where the abaxial (with stomata) side was sealed while the adaxial (stomata-free) was left intact, showed that leaf cuticules are very effective barriers for CO_2 transport while water vapour could escape more easily (Boyer *et al.*, 1997). This can be (partly) explained by the fact that CO_2 molecules have to move through the entire epidermal layer (because epidermal cells tend to have much less chloroplasts than mesophyll cells) while escaping water vapour molecules most likely originate in the epidermis itself with a much shorter path (Boyer *et al.*, 1997). For water vapour, cuticular conductance can represent *ca.* 5% of the total maximum conductance through the leaf surface, while for CO_2 it represents less than 1% (Boyer *et al.*, 1997; Boyer, 2015). At low irradiance, this percentage is higher because stomata close, but the transport of CO_2 through leaf cuticules still remains very small (less than 3%) (Boyer *et al.*, 1997). When soil water becomes limiting and leaves lose turgor, the cuticular conductance for both water vapour and CO_2 is even lower, by about half its maximum at leaf water potential of -1.5 MPa (corresponding to a leaf turgor pressure of 0.8 MPa) (Boyer, 2015). On the other hand, an increase in leaf temperature can induce a phase transition in cuticular waxes leading to drastic losses of water, corresponding to a 10-fold increase in cuticular transpiration (Riederer & Schreiber, 2001). This phase change usually occurs above 35-40°C depending on the species (Riederer & Schreiber, 2001). The effect of such phase transition on the permeability of leaf cuticules to other gases (CO_2 or COS) is not known. In the following, we will assume that CO_2 or COS diffusion through leaf cuticules remains much smaller than through stomata, at least below the transition phase temperature of the cuticle.

It is also generally assumed that CO_2, COS or $C^{18}OO$ gradients within the intercellular air space are small, although some studies report they can be sometimes significant, but "exactly how significant is open to interpretation" (Morison & Lawson, 2007). Measurements of CO_2 gradients on upper and lower sides of amphi- and hypo-stomatous leaves indicate that gradients of a few Pa (tens of ppm) are not uncommon (e.g. Parkhurst *et al.*, 1988). However, with regard to assimilation rates, several experimental and modelling studies indicate that diffusion limitations

within the intercellular air space are negligible (e.g. Genty *et al.*, 1998). For this reason, gas concentrations in the 'intercellular air space' and in the 'stomatal cavity air space' are often considered to correspond to the same thing and the two terms are used interchangeably (Fig. 3.1).

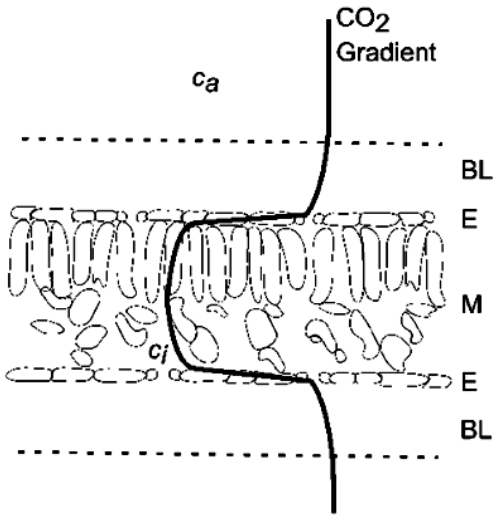

Figure 3.1 | schematic view of the CO_2 gradient across the boundary layer (BL), the epidermis (E) and the intercellular air space within the mesophyll (M) of a leaf. Adapted from Boyer and Kawanitsu (2011).

The uptake of trace gases such as CO_2 or COS through stomata is complicated by the fact that their flow is opposing the much larger flow of water vapour molecules escaping the leaf interior during transpiration. Jarman (1974) showed that the effect of transpiration rate on the diffusive flux of carbon dioxide through stomatal pores should be small but not negligible. These effects are now routinely taken into account in gas exchange measurements to estimate the CO_2 partial pressure in the intercellular air space (Caemmerer & Farquhar, 1981). Considering the air as a ternary mixture of dry air, CO_2 and water vapour leads to the following relationship between the CO_2 partial pressure drawdown ($p_a - p_i$), the net CO_2 assimilation rate A and the transpiration rate E (Caemmerer & Farquhar, 1981; Farquhar & Cernusak, 2012):

$$g_{ac}\left(p_a - p_i\right) \approx AP + 0.5\left(p_a + p_i\right)\frac{g_{ac}}{g_{wc}}E \tag{3.1}$$

where g_{ac} is the conductance to diffusion of air in CO_2 (and of CO_2 in air) through the leaf boundary layer and the stomatal pores and g_{wc} that of water vapour in CO_2 (and vice versa). Because the binary diffusivity of water vapour/CO_2 mixture at 20°C is 16.2 $mm^2\ s^{-1}$ while that of air/CO_2 mixture is 15.9 $mm^2\ s^{-1}$ (Marrero & Mason, 1972), we should expect $g_{wc} \approx g_{ac}$ and Eq. (3.1) simplifies to:

$$A \approx \frac{g_{ac}}{P}\left(p_a - p_i\right) - 0.5\frac{p_a + p_i}{P}E \tag{3.2}$$

In other words, leaf transpiration E breaks the linear relationship between net CO_2 assimilation (A) and CO_2 drawdown ($p_a - p_i$). Because g_{ac} is often of the order of 50-500 mmol $m^{-}\ s^{-1}$ while E is only 1-10 mmol $m^{-}\ s^{-1}$, the ratio E/g_{ac} is typically around 3%. Neglecting this correction factor leads to an overestimation of the p_i/p_a ratio by about 0.05. Although these 'ternary' corrections of leaf gas

exchange measurements have been applied routinely for decades now, it is only recently that we had experiments confirming their validity (Boyer & Kawamitsu, 2011).

When A is a measured quantity, the ternary corrections are mostly important for determining p_i. On the other hand, in land surface models, A has to be computed from estimates of p_i and stomatal conductance ($\approx g_{ac}$). If the ternary corrections are neglected, this could create a (positive) bias in the estimates of photosynthesis by these models, of the order of 5%. Yet, to my knowledge, most land surface models neglect these corrections, which is problematic especially when leaf gas exchange data have been used to parameterise these models. I will come back on this point later.

The corrections described above for CO_2 should also apply for COS. However, it is not clear whether the approximation we make for CO_2 ($g_{wc} \approx g_{ac}$) also applies for COS. To my knowledge, the binary diffusivities of water vapour/COS or COS/air mixtures have not been determined experimentally. Using tabulated pure gas properties and the kinetic theory of gases (Bird *et al.*, 2002), the binary diffusivity of COS/air mixtures was estimated to be about twice that for water vapour in air (Seibt *et al.*, 2010; Stimler *et al.*, 2010). This ratio of binary diffusivities is to be taken with caution because COS is a polar molecule (Svoronos & Bruno, 2002) so that the approximation used to compute the Lennard-Jones potential parameters of the mixture is not strictly valid (see Bird *et al.*, 2002, p. 525). Nevertheless the same theory predicted with good accuracy the binary diffusivity of water vapour in air (e.g. Seibt *et al.*, 2010) and H_2O is also a polar molecule with a stronger polar moment, which gives us confidence in using the approximation also for COS/air mixtures. However, using the same approximation for mixtures of two polar gas mixtures (COS and water vapour) is even more questionable. For these reasons, very few studies have attempted to estimate p_i for COS, and those that did it either ignored the ternary corrections (Seibt *et al.*, 2010), or used Eq. (3.2) assuming it was applicable for COS (Stimler *et al.*, 2010).

Ternary corrections were also ignored when interpreting $^{13}CO_2$ or $C^{18}OO$ leaf gas exchange data. It is only recently that we included them in the equations for carbon and oxygen isotope discrimination during photosynthesis (Farquhar & Cernusak, 2012). Because ternary corrections are mostly important when the ratio E/g_{ac} is large, which corresponds to large leaf-to-air vapour pressure deficits, it was shown that the ternary correction effect was greatest on parameters derived by difference, such as the mesophyll resistance to CO_2 assimilation (Evans *et al.*, 1986). This leads to an underestimation of this resistance (an overestimation of the mesophyll conductance) and a bias in the estimates of CO_2 in equilibrium with leaf water at low light (Farquhar & Cernusak, 2012). For these reasons, ternary corrections are now systematically applied in studies on leaf photosynthetic discrimination (Studer *et al.*, 2014; Barbour *et al.*, 2016; Ubierna *et al.*, 2017; Ogée *et al.*, 2018; Sonawane & Cousins, 2018).

If we denote by R_a and R_i the $^{18}O/^{16}O$ ratios of CO_2 in the atmosphere (canopy air) and the intercellular air space, an equation similar to Eq. (3.2) holds for the $C^{18}OO$ flux (^{18}A) but where p_a and p_i are replaced by p_aR_a and p_iR_i and g_{ac} is replaced by $g_{ac}/(1 + \bar{a}')$ where $\bar{a}'$ is the fractionation factor during CO_2 diffusion through the leaf boundary layer and the stomata. Dividing this new equation by Eq. (3.2) leads to (Farquhar & Cernusak, 2012):

$$R_A = \frac{p_aR_a - p_iR_i - t(p_aR_a + p_iR_i)}{(1+\bar{a}')(p_a - p_i) - t(p_a + p_i)}, \tag{3.3}$$

where R_A is the isotope ratio of net CO_2 assimilation ($R_A = 0.5\,^{18}A/A$) and $t = 0.5E/g_{ac}$.

The equations above are flux-gradient relationships that relate the partial pressure gradients (e.g., p_a - p_i) to the net flux (A). We cannot prescribe one without knowing the other. For this we need a second independent equation. For example, for net CO_2 assimilation, the biochemical model of photosynthesis proposed by Farquhar *et al*. (1980) relates A to p_i in terms of leaf carboxylation capacity and respiratory fluxes independently of Eq. (3.2). For $C^{18}OO$ and COS fluxes, we also need such biochemical descriptions to be able to implement those tracers in land surface models.

Biochemical models of $C^{18}OO$ discrimination during photosynthesis

Farquhar *et al*. (1993) first proposed a model of $C^{18}OO$ discrimination during photosynthesis. This model was based on the observation that, in C_3 plants, CA is most abundant in the chloroplast stroma of mesophyll cells (Badger & Price, 1994), so that the site of CA-catalysed hydration and equilibration must coincide roughly to the site of carboxylation by RuBisCO inside the chloroplasts. In this scheme, the CO_2 partial pressure at the site of CA activity (p_{CA}) equals that into the chloroplast (p_c), and can then be estimated from measurements of carbon isotope discrimination (Evans *et al*., 1986). Neglecting the ternary corrections introduced previously (we will come back on this assumption later), CO_2 and $C^{18}OO$ assimilation rates were simply written as a product of the partial pressure drawdown between the atmosphere (i.e. canopy air) and the chloroplast and the total conductance[15] (g_{tc}) for CO_2 diffusion between these two points[16]:

$$\begin{cases} A \approx g_{tc}\dfrac{p_a - p_c}{P} \\ {}^{18}A \approx \dfrac{2g_{tc}}{1+\bar{a}}\dfrac{p_a R_a - p_c R_c}{P} \end{cases} \tag{3.4}$$

where p_a and R_a are the CO_2 partial pressure and $^{18}O/^{16}O$ ratio in the atmosphere and $\bar{a}$ is the ^{18}O fractionation for CO_2 diffusion from the outside air to the site of carboxylation (see below).

The two flux-gradient relationships in Eq. (3.4) can be combined and re-arranged to:

$$\Delta_A = \frac{\bar{a} + \dfrac{p_c}{p_a - p_c}\Delta_{ca}}{1 - \dfrac{p_c}{p_a - p_c}\Delta_{ca}} \approx \bar{a} + \frac{p_c}{p_a - p_c}\Delta_{ca}, \tag{3.5}$$

where $\Delta_{ca} = R_c/R_a - 1$, $\Delta_A = R_a/R_A - 1$ and R_A represents the $^{18}O/^{16}O$ ratio of the net CO_2 flux (= $0.5\,{}^{18}A/A$). Δ_A refers to what we call $C^{18}OO$ photosynthetic discrimination (also noted $\Delta^{18}O$).

---

[15] The conductance g_{tc} is the inverse of the sum of all the resistances to CO_2 diffusion between the canopy air and the carboxylation site within the chloroplast, through the boundary layer, the stomata and the inter-cellular air space (Fig. 3.1) and through the wall, plasma membrane and cytosol of mesophyll cells and the envelope and stroma of chloroplasts (Fig. 3.2). We call g_{tc} 'total' conductance but it is a misnomer, as it is usually only slightly larger than the smallest conductance along this path and always much smaller than the usually large leaf boundary layer conductance.

[16] The flux gradient relationships in Eq. (3.4) parallels those introduced in chapter 1, with the following correspondences: $F \rightarrow A$, $^{18}F \rightarrow {}^{18}A$, $C_a \rightarrow p_a/P$, $C_c \rightarrow p_c/P$, $\alpha_d \rightarrow (1 + \bar{a})^{-1}$ and $R_c \rightarrow R_{eq}$. These are mostly new notations (to be more coherent with those used in the plant physiology literature) at the exception that R_c now does not necessarily refer to the CO_2 in equilibrium with leaf water.

Farquhar *et al*. further assumed that the oxygen isotope ratio of leaf water at the site of equilibration (i.e. in the chloroplast) could be approximated by the $^{18}O/^{16}O$ ratio at the evaporation site at the air-liquid interface. This assumption was based on the observation that chloroplasts, that are moving organelles, are often found appraised against the cell wall of mesophyll cells, thus minimising the transfer resistance for CO_2 uptake (Fig. 3.2). In this case, the $^{18}O/^{16}O$ ratio of the water at the CA site in the chloroplast can be approximated by the $^{18}O/^{16}O$ ratio of water at the evaporation site (R_{es}), and thus estimated from air and soil water isotope data using a physically-based model of leaf water isotopic enrichment during leaf transpiration (Dongmann *et al.*, 1974; Cernusak *et al.*, 2004; Farquhar & Cernusak, 2005).

From these estimates of R_{es}, we can calculate the $^{18}O/^{16}O$ ratio of CO_2 in full isotope equilibrium with leaf water at the CA site (noted Δ_{ea} when expressed relative to R_a):

$$\Delta_{ea} = \frac{R_{es}\alpha_{wc}}{R_a} - 1, \tag{3.6}$$

where α_{wc} denotes the equilibrium isotopic fractionation between CO_2 and leaf water. This fractionation is often taken equal to the one in pure water (1.042 at 20°C, Brenninkmeijer *et al.*, 1983).

Using simultaneous measurements of carbon isotope discrimination (to estimate p_c) and Δ_A, Farquhar *et al*. (1993) found that Eq. (3.5) broadly reproduced the relationship between Δ_A and p_c/p_a when the CO_2 in the chloroplast was assumed fully equilibrated with leaf water at the evaporative site (i.e. setting $\Delta_{ca} = \Delta_{ea}$). This simplification of Eq. (3.5) was then used to describe the influence of leaf photosynthesis on atmospheric $C^{18}OO$ using parameterizations of the ratio p_c/p_a and R_{es} describing how they vary with photosynthesis and transpiration across land surfaces (Farquhar *et al.*, 1993; Ciais *et al.*, 1997b; Peylin *et al.*, 1999).

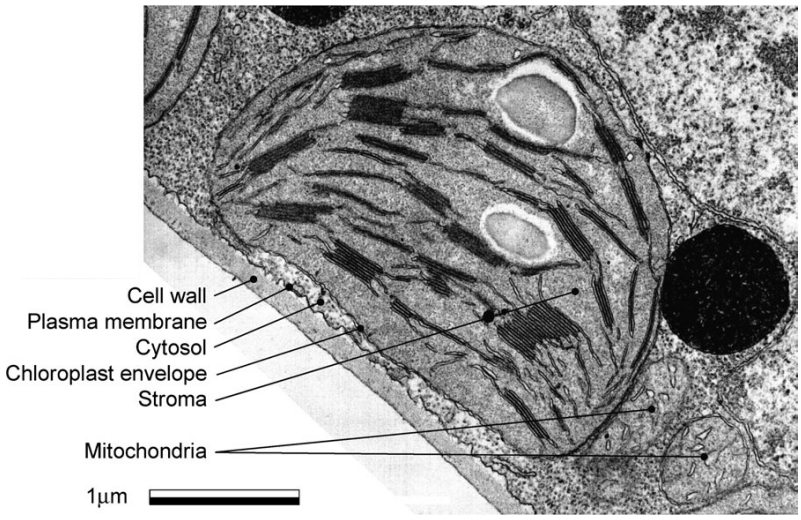

Figure 3.2 | Transmission electron micrograph of a chloroplast appraised against the cell wall of a mesophyll cell within a leaf of *Nicotiana tabacum* Adapted from Evans *et al.* (2009).

However, discrepancies were found and attributed to the different assumptions that were made. For example, Gillon and Yakir (2000a) found discrepancies between p_c obtained from ^{13}C discrimination that was always lower than that obtained from ^{18}O discrimination using Eq. (3.5). They partly attributed this difference to the fact that p_c and p_{CA} do not coincide as originally assumed, and used their results to partition mesophyll conductance between the conductance

through the cell wall, plasma membrane and cytosol (g_{cw}) and the conductance through the chloroplast envelop and stroma (g_{ch}). It was also recognised that the CO_2 at the CA site might not be fully equilibrated with leaf water if carbonic anhydrase is not present in large enough quantities and CO_2 assimilation is large, pulling non-equilibrated CO_2 inside the leaf chloroplast at a faster rate than the equilibration rate. It was also suggested that CO_2 produced during leaf photorespiration may not be in isotopic equilibrium with leaf water (Yakir *et al.*, 1994).

Farquhar and Lloyd (1993) revisited Eq. (3.5) and proposed an equation describing how respiration and competition between CO_2 hydration and carboxylation influence $C^{18}OO$ photosynthetic discrimination. For this, they assumed that CA and RuBisCO were still collocated but now competing for CO_2, and this competition was characterised by the ratio $\rho = V_c/V_{hc}$ of CO_2 carboxylation by RuBisCO (V_c) to CO_2 hydration by CA (V_{hc}). Formally, their derivation was based on the resistance scheme shown in Fig. 3.3A. Using this scheme they derived[17]:

$$\Delta_A \approx \frac{\bar{a}\left(1+3\rho\left(1-\frac{\Gamma}{p_c}\right)\right)+\frac{p_c}{p_a-p_c}\left(\Delta_{ea}+3\rho\left(b+\frac{\Gamma}{p_c}\Delta_{mc}\right)\right)}{1-\frac{p_c}{p_a-p_c}\Delta_{ea}+3\rho\left(1-\frac{\Gamma}{p_c}\right)\frac{p_a}{p_a-p_c}}, \quad (3.7)$$

where Γ (Pa) is the apparent compensation point, i.e., $A = V_c(1 - \Gamma/p_c)$, $\Delta_{mc} = R_{mi}/R_c - 1$ is a measure of the disequilibrium between chloroplastic and respired CO_2 and b is the oxygen isotope fractionation by RuBisCO during carboxylation. The latter is not known but is expected to be small because oxygen atoms of CO_2 molecules do not bind to RuBisCO (Farquhar & Lloyd, 1993). When CA activity is non-limiting, $\rho \to 0$ and Eq. (3.7) simplifies to Eq. (3.5). This model was tested in subsequent studies and led to estimates of ρ (assuming $\Delta_{mc} = 0$ and $b \approx 0$) around 1-3% (Flanagan *et al.*, 1994; Williams & Flanagan, 1996), except in anti-sense CA plants where it could increase to 50% (Williams *et al.*, 1996). It was also shown that, despite its small value, ignoring ρ could lead to errors on Δ_A up to 10-15‰ (Flanagan *et al.*, 1994).

The scheme shown in Fig. 3.3A is based on the idea that carbonic anhydrase in C_3 plants is mostly limited to the chloroplast compartment, a picture that has been contradicted since then (Moroney *et al.*, 2001; Fabre *et al.*, 2007). Besides, this scheme can only be applied to C_3 plants. Therefore, studies on $C^{18}OO$ discrimination by C_4 plants continued using Eq. (3.5) (because the flux-gradient relationships Eq. (3.4) from which it is derived are valid for both C_3 and C_4 plants), while accounting for a partial equilibration between CO_2 and leaf water by setting arbitrarily Δ_{ca} equal to $\theta_{eq}\Delta_{ea} + (1 - \theta_{eq})\Delta_{ca0}$, where θ_{eq} represents the 'degree of equilibration' of escaping CO_2 molecules and Δ_{ca0} represents the value of Δ_{ca} in the absence of any CA activity (Gillon & Yakir, 2000b; 2001; Cousins *et al.*, 2006a). The latter was deduced from equations similar to carbon isotope discrimination but neglecting isotope fractionation during carboxylation and respiration (Gillon & Yakir, 2000a). Alternatively, it can also be obtained from Eq. (3.7) with b and Δ_{mc} set to zero and taking the limit $\rho \to \infty$. Both approaches lead to $\Delta_A \to \bar{a}(1 - p_c / p_a)$ and combined with Eq. (3.5) lead to $\Delta_{ca0} = -\bar{a}(1 - p_c / p_a)$.

[17] The derivation of Eq. (3.7) proposed by Farquhar and Lloyd (1993) was not provided, even in subsequent publications. Besides, their equation contained a typographic error (J. Lloyd, personal communication). Later publications (e.g. Flanagan *et al.*, 1994) corrected the typo but introduced another one. We thus felt important to provide the derivation of their model which can be found in Appendix C of Ogée *et al.* (2018).

To derive an expression for θ_{eq}, Gillon and Yakir (2000b) revisited the work of Mills and Urey (1940) who showed that the $^{18}O/^{16}O$ ratio of CO_2 in closed aqueous solutions rapidly follows an ordinary differential equation, that can be re-written with the current notations as:

$$\frac{d\Delta_{ca}}{dt} = -k_{iso}\left(\Delta_{ca} - \Delta_{ea}\right), \tag{3.8}$$

where k_{iso} (s^{-1}) is the CO_2-H_2O isotopic exchange rate. The leaf mesophyll is not a closed system, but Gillon and Yakir assumed that Eq. (3.8) should describe well the dynamics of Δ_{ca}. This is justified only if the CO_2-H_2O isotopic exchange rate is much greater than any $C^{18}OO$ carboxylation flux, which is unlikely under high light or for CA-deficient leaves. Despite these caveats, it was proposed to estimate $\theta_{eq} = (\Delta_{ca} - \Delta_{ca0})/(\Delta_{ea} - \Delta_{ca0})$ by integrating Eq. (3.8) between time $t = 0$ and $t = \tau_{res}$, and assuming that Δ_{ca0} represents well the value of Δ_{ca} at time $t = 0$ (Gillon & Yakir, 2000b):

$$\theta_{eq} = 1 - \exp\left(-k_{iso}\tau_{res}\right). \tag{3.9}$$

This derivation is problematic as it uses a non-steady state formulation (integrated over the residence time τ_{res}) to describe steady-state gas exchange dynamics. Also considering that Δ_{ca0} represents well the value of Δ_{ca} at time $t = 0$ comes to assume that the leaf has been (initially) filled with unlabelled CO_2, which is not realistic even with a fluctuating environment because CA activity continuously resets Δ_{ca}. Yet, Eq. (3.9) has been used in several studies to link CA activity to Δ_A data (Gillon & Yakir, 2000b; 2001; Cousins *et al.*, 2006a; 2007). To do so, the exchange rate constant k_{iso} appearing in Eq. (3.9) is taken as one third of the CA-catalysed CO_2 hydration rate k_h and the residence time τ_{res} is taken as the ratio of the total amount of CO_2 inside the leaf to the one-way flux of CO_2 from the atmosphere into the leaf. However the ratio k_{iso}/k_h in a dynamic system equals one third only in acidic conditions (see chapter 2, Eq. (2.18)) and this definition of the residence time implicitly redefines the system boundaries to include not only the CA-containing leaf compartment but also other leaf compartments, including the inter-cellular air space. In this situation, k_{iso} should be replaced by a more complex expression that depends not only on pH but also on the volumes of the gas and liquid phases and the transfer conductance between these two phases, including the mesophyll conductance (see Appendix B in Ogée *et al.*, 2018)). Finally, Eq. (3.9) does not account for the competition between CO_2 hydration and carboxylation, or for the contribution of respiratory fluxes.

Although there were empirical indications that Eq. (3.9) was flawed (Cousins *et al.*, 2006a), it is only recently that we have understood the many reasons of its inapplicability (Ogée *et al.*, 2018). An alternative approach has been to use Eq. (3.5) (or its alternative including ternary corrections, see Ubierna *et al.*, 2017) and consider θ_{eq} (≤ 1) as a sensitivity parameter (Studer *et al.*, 2014; Barbour *et al.*, 2016; Ubierna *et al.*, 2017). However, this approach is a bit ill designed, as it requires an estimate of θ_{eq} to fully interpret the photosynthetic discrimination data, and can only be used to evaluate the sensitivity of the retrieved p_c (and mesophyll conductance) to variations in θ_{eq} (Barbour *et al.*, 2016). This is problematic especially for studying C_4 plants because the ^{18}O discrimination technique is one of the two techniques available that allows the estimation of mesophyll conductance for this group of plants. Carbon isotope discrimination cannot be used because of its weak relationship with p_i/p_a and chlorophyll fluorescence signals are also hard to interpret because the bundle sheath and mesophyll cells have different chloroplast populations (Evans & Cemmerer, 1996). A recent method derives mesophyll conductance by retrofitting the C_4 photosynthesis and ^{13}C discrimination models with gas exchange data, kinetic constants and *in*

vitro PEPC[18] activity measurements (Ubierna *et al.*, 2017). However this method is still at its infancy and needs other alternatives to verify its applicability for different environmental conditions and species.

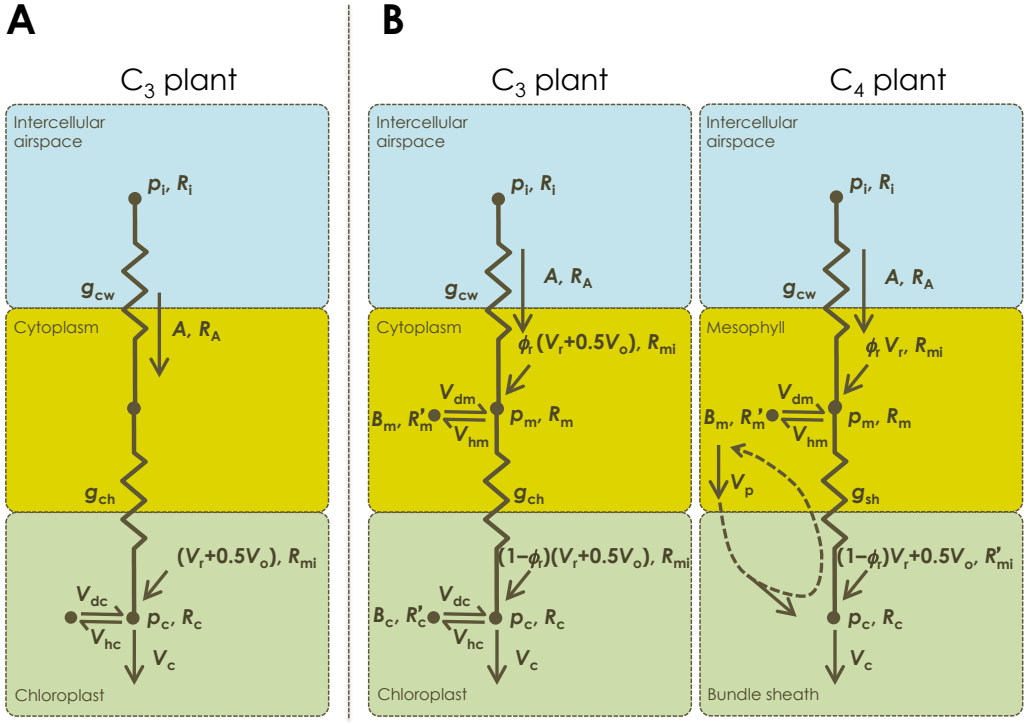

Fig. 3.3 | *In folio* transport and enzymatic reaction schemes for CO_2 and $C^{18}OO$, as proposed origininally by Farquhar and Lloyd (1993) to describe $C^{18}OO$ photosynthetic discrimination by C_3 plants (panel A) and recently extended to both C_3 and C_4 plants by Ogée *et al.* (2018) while including cytosolic CA activity and partial respired CO_2 recycling (panel B). In panel A, net photosynthesis (rate A, isotope ratio R_A) is driven by RuBisCO-driven carboxylation (rate V_c) that creates a CO_2 concentration gradient between the intercellular air space (partial pressure p_i, isotope ratio R_i) and the carboxylation site inside the cloroplast (partial pressure p_c, isotope ratio R_c). This gradient is imposed by a set of resistance to CO_2 transport across the cell wall, plasma membrane and the cytoplasm (g_{cw}) and across the chloroplast enveloppe and stroma (g_{ch}). The site of CA-driven CO_2 hydration and isotopic equilibration with leaf water is assumed to coincide with the site of carboxylation in the chloroplast. CO_2 equilibrates isotopically with chloroplastic water via CA-catalysed hydration of CO_2 (rate V_{hc}) and dehydration (rate V_{dc}) of bicarbonate (concentration B_c, isotope ratio R'_c). Respired CO_2 (isotope ratio R_{mi}) by mitochondria (rate V_r) and photo-respired CO_2 (rate V_o) are assumed to be fully recycled by the chloroplast. In panel B, CO_2 in the cytoplasm of mesophyll cells (partial pressure p_m, isotope ratio R_m) can also equilibrate isotopically with cytosolic water of mesophyll cells *via* CA-catalysed hydration of CO2 (rate V_{hm}) and dehydration (rate V_{dm}) of bicarbonate (concentration B_m, isotope ratio R'_m), while respired CO_2 is only partially recycled by CO_2 carboxylation (fraction 1 - ϕ_r). In C_4 plants, RuBisCO-related photorespiration occurs only in the bundle sheath cells and the CO_2 gradient between mesophyll and bundle sheath cells is imposed by a bundle sheath conductance (g_{sh}) allowing CO_2 to escape the bundle sheath ('leakiness'), counter acting its build up by C_4 acid synthesis from PEPC-driven bicarbonated carboxylation (rate V_p) and subsequent decarboxylation in the bundle sheath. For both C_3 and C_4 plants, the steady-state CO_2 mass balance leads to: $A = V_c - 0.5V_o - V_r$.

[18] PEPC stands for phosphorenolpyruvate (PEP) carboxylase.

For all these reasons, we extended the steady-state formulation of ^{18}O discrimination for C_3 plants by Farquhar and Lloyd (1993) to C_3 and C_4 photosynthesis pathways. The new model is schematically represented in Fig. 3.3B. It accounts for the competition between hydration and carboxylation, the influence of leaf respiration and photorespiration and the spatial separation of hydration and carboxylation sites as well as their difference in leaf water isotopic composition, especially important in C_4 species. It also applies to conditions of high leaf-to-air vapour pressure deficit, that require ternary corrections on the CO_2 and $C^{18}OO$ assimilation rates (Caemmerer & Farquhar, 1981; Farquhar & Cernusak, 2012).

For C_4 species, the main difficulties were to characterise the isotopic ratio of the water and CO_2 in the bundle sheath, and notably the contribution of the CO_2 released during the decarboxylation of C_4 acids in the bundle sheath. Those acids are synthesized in the mesophyll during PEP carboxylation, so that the net reaction is $HCO_3^- + PEP \rightarrow CO_2 + P_i +$ pyruvate. Because, out of the three oxygen atoms from the bicarbonate, one is lost to phosphate (P_i) and the other two are released as CO_2 without binding to any of the active sites of the different enzymes involved (PEPC, MDH, NAD-ME, or NADP-ME), we argued that oxygen fractionation by PEPC should be small and that the released CO_2 should have an isotope ratio equal to that of the bicarbonate in the mesophyll cells (R'_m). Finally, because this release of CO_2 is the main source of CO_2 in the bundle sheath cells, we argued that the isotope ratio of CO_2 in the bundle sheath (R_c) should be close to R'_m as well (Ogée *et al.*, 2018). Finally, ought to the small respiratory fluxes and the presence of CA in mitochondria, we assumed that CO_2 from respiration and photorespiration was fully equilibrated with leaf water. Such assumption is coherent with measurements of $C^{18}OO$ gas exchange data performed in the dark (Cernusak *et al.*, 2004; Farquhar & Cernusak, 2012).

With this new biochemical model, we can have a clearer representation of the mesophyll conductance (g_m) and CO_2 partial pressure (p_{CA}) that are required to model $\Delta^{18}O$ and the impact of leaf photosynthesis on atmospheric $C^{18}OO$ budgets (Ogée *et al.*, 2018). In C_4 plants, g_m corresponds to the conductance through the cell wall, plasma membrane and cytosol of mesophyll cells (i.e. $g_m = g_{cw}$) and p_{CA} should be closely related to the partial pressure in the cytosolic compartment of those cells (i.e. $p_{CA} = p_m$). In contrast, in C_3 plants, the CA site corresponds to the mean point of CA activity within the mesophyll cells (Ogée *et al.*, 2018):

$$p_{CA} = \frac{^{18}k_{hm}p_m + {}^{18}k_{hc}p_c}{^{18}k_{hm} + {}^{18}k_{hc}}. \tag{3.10}$$

where $^{18}k_{hm}p_m \approx V_{hm}$ and $^{18}k_{hc}p_c \approx V_{hc}$ and $^{18}k_{hm} + {}^{18}k_{hc} \approx k_{CA}$, the leaf CA activity estimated on leaf extracts. Given the more alkaline pH and higher CA concentration in the chloroplast stroma compared with the cytosol [pH 7.4 and [CA] around 0.1 mM for the cytosol and pH 8 and [CA] around 0.3 mM for the stroma; (Tholen & Zhu, 2011)], we should expect $^{18}k_{hc}$ to dominate over $^{18}k_{hm}$, so that $k_{CA} \approx {}^{18}k_{hc}$ and $p_{CA} \approx p_c$. In other words, in C_3 plants, g_m should be closely related to the mesophyll conductance for photosynthesis and $^{13}CO_2$ discrimination: $g_m \approx (1/g_{cw} + 1/g_{ch})^{-1}$.

Using this new modelling framework, we revisited a number of previously published datasets for C_3 and C_4 species, including CA-deficient mutants, and illustrated how to reconcile *in vitro* CA assays with online $\Delta^{18}O$ measurements whilst, at the same time, estimating g_m from $\Delta^{18}O$ data. A summary of these results will be provided further below.

Biochemical models of leaf COS uptake

In contrast to $C^{18}OO$ theory, much fewer biochemical models of COS uptake during photosynthesis exist in the literature. The first, and so far the most elaborate, model is the one

proposed by Protoschill-Krebs *et al.* (1992) and is schematically represented in Fig. 3.4. This model was based on enzymatic experiments at high COS concentrations (125-250 µM, more than one million times ambient concentrations, near toxic levels for mammals!) using mixtures of purified carboxylation enzymes (RuBisCO, from wheat leaves and PEPC, from corn leaves) and lyophilized α-CA (from bovine erythrocytes). They found that both RuBisCO and PEPC could take up COS, and that the uptake was enhanced in the presence of CA. However, the uptake by PEPC was very small. I estimated it at about 20 times the uncatalysed hydrolysis rate at 0.013 units(PEPC) mL^{-1} or about 1.3 µM of enzyme (Uedan & Sugiyama, 1976), leading to an equivalent k_{max}/K_m of about 1.7 10^{-3} s^{-1} μM^{-1}. Similarly the COS uptake by RuBisCO was very small with k_{max}/K_m of the order of 10^{-3} s^{-1} μM^{-1} as well, and confirming previous findings (Lorimer & Pierce, 1989). Compared to the k_{max}/K_m of plant β-CA around 2.4 s^{-1} μM^{-1} (see chapter 2) these enzymatic parameters of PEPC and RuBisCO were about 1000 times smaller, anticipating a COS uptake by these carboxylation enzymes about 2 orders of magnitude below the COS uptake by β-CA (the concentration ratios of activated RuBisCO or PEPC to CA have also to be taken into account).

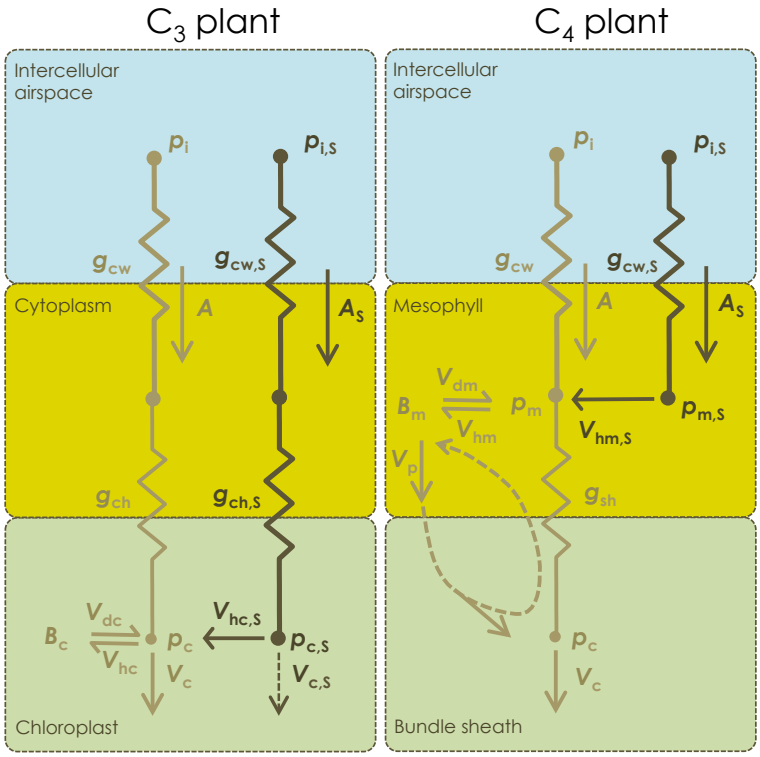

Fig. 3.4 | *In folio* transport and enzymatic reaction schemes of COS uptake by C_3 and C_4 plants, as proposed originally by Protoschill-Krebs *et al.* (1992). The net COS uptake rate (A_S) is driven by COS hydrolysis in the chloroplast of C_3 plants (rate $V_{hc,S}$) or in the cytoplasm of mesophyll cells of C_4 plants (rate $V_{hm,S}$). COS hydrolysis creates a COS concentration gradient between the intercellular air space (partial pressure $p_{i,S}$) and the site of hydrolysis in the chloroplast of C_3 plants (partial pressure $p_{c,S}$) or in the cytoplasm of C_4 plants (partial presure $p_{m,S}$). This gradient is imposed by a set of resistance to COS transport across the cell wall, plasma membrane and the cytoplasm ($g_{cw,S}$) and, for C_3 plants, across the chloroplast enveloppe and stroma ($g_{ch,S}$). Direct COS uptake by RuBisCO in the chloroplast of C_3 plants was also considered (rate $V_{c,S}$) but expected to be minor compared to COS hydrolysis.

Interestingly, Protoschill-Krebs *et al*. (1992) did not find large differences in COS uptake rates by PEPC, RuBisCO or CA. This is probably because they used α-CA, which is not very efficient at hydrolysing COS, with k_{max}/K_m values (Haritos & Dojchinov, 2005; Ogawa *et al*., 2013) similar to those found for PEPC and RuBisCO (i.e. also about 1000 times less efficient than β-CA). For this reason, Protoschill-Krebs *et al*. (1992) had to use large amounts of α-CA to see some enhancement on the COS uptake. It is only very recently that we know the large kinetic differences between α- and β-CAs for COS (Ogawa *et al*., 2013; Ogée *et al*., 2016; Meredith *et al*., 2019). It is probable that Protoschill-Krebs *et al*. anticipated the model shown in Fig. 3.4 based on the observations that (1) other studies had shown that plants were taking up large amounts of COS and (2) CA was already regarded as the key enzyme in COS metabolism by plants, notably after the $CO^{35}S$ plant fumigation experiments performed by Brown *et al*. (1986). In these experiments, it was found that the labelled ^{35}S was rapidly incorporated into sulphate, methionine, cysteine and glutathione, indicating that plants could metabolise COS. Because the formation of methionine and cysteine requires H_2S as an intermediate, and up to 17% of the initial radioactivity had been lost within 24h of fumigation, it was concluded that large amounts of $H_2{}^{35}S$ must have been produced (by CA-catalysed hydrolysis) and either metabolised or degassed (Brown *et al*., 1986).

A few years later, Protoschill-Krebs *et al*. performed similar experiments but on CA extracted from *Pisum sativum* leaves and found clear evidence that plant CAs were able to hydrolyse COS at very high rates and with a very high affinity (Protoschill-Krebs *et al*., 1996) . The k_{max}/K_m value of 2.4 s^{-1} μM^{-1} comes from a reanalysis of their dataset (Ogée *et al*., 2016). Further strong evidence that CA is the key enzyme explaining the COS uptake by foliage comes from more recent experiments by Stimler *et al*. on CA-antisense lines of C_3 and C_4 plants and showing that the COS uptake is completely suppressed in CA-deficient plants (Stimler *et al*., 2011; 2012)[19].

Based on the scheme shown in Fig. 3.4, the COS uptake rate should be (neglecting the uptake by RuBisCo in C_3 plants):

$$A_S = \left(\frac{1}{g_{s,S}/P} + \frac{1}{g_{m,S}/P} + \frac{1}{k_{CA,S}} \right) p_{a,S} \,. \tag{3.11}$$

where $g_{s,S}$ is the stomatal conductance for COS (about half that for water vapour), $g_{m,S}$ is the mesophyll conductance for COS (i.e. $g_{cw,S}$ in C_4 plants) and $k_{CA,S}$ is the CA activity for COS.

[19] An earlier study had reported some correlation between COS uptake by three C_3 species and leaf CA activity measured on crude leaf extracts (Yonemura *et al*., 2005). However, it seems that this correlation was a simple artifact as the differences in COS uptake were mostly driven by differences in stomatal conductance (see their Table 1). Actually the reported CA activity were not at all representative of CA activity *in vivo* relative to COS consumption as they were expressed as rates of CO_2 hydration at 2°C and 17.5mM of CO_2. In C_4 plants, we have $k_{CA,S} = V_{hm,S}/p_{m,S}$ which is expected to co-vary with the CA activity for CO_2 $k_{CA} = V_{hm}/p_m$, but not with V_{hm} divided by 25kPa (the partial pressure in the air corresponding to 17.5mM at 2°C). This is because, depending on stomatal and mesophyll conductances, the partial pressures of CO_2 (p_m) and COS ($p_{m,S}$) at the CA site will differ for the same COS uptake rate. Clearly, because of the between-species differences in stomatal conductances, the correlation between A_S and V_{hm} at 2°C shown by Yonemura *et al*. cannot be a strong proof that COS uptake is "based on the inherent capacity of CA" to scavenge COS, as was claimed by these authors.

As explained earlier, the model proposed by Protoschill-Krebs *et al*. (1992) is the most complete so far and is still used today to explain COS uptake by C_3 and C_4 plants (Stimler *et al*., 2011). However, we know now that C_3 plants also contain CA in their cytoplasm. As for the $C^{18}OO$ model, it would seem therefore more correct to consider that part of the COS in C_3 plants is hydrolysed by cytoplasmic, not chloroplastic CA. This would modify a bit the scheme shown in Fig. 3.4 but would change only slightly the interpretation of the site of hydrolysis in C_3 plants because of the higher CA activity in the chloroplast than in the cytosol (see discussion above). However, this would be more coherent with the new $C^{18}OO$ discrimination model (Ogée *et al*., 2018).

It is interesting to note that, according to the scheme shown in Fig. 3.4, the COS uptake induces a small disequilibrium between carboxylation and respiration ($V_c - 0.5V_o - V_r$) and the CO_2 supply (A). In other words, there is more CO_2 fixation than there is CO_2 uptake because of the extra CO_2 that is provided by COS hydrolysis. However, at natural abundance, this disequilibrium is negligible because COS is one million times less abundant than CO_2 in the atmosphere.

The degree of equilibration between CO_2 and leaf water is high even in C4 species

Using the $C^{18}OO$ discrimination model depicted in Fig. 3.3B, we revisited datasets to explore variations of the degree of equilibration between CO_2 and leaf water in different plant functional groups. As mentioned above, this degree of equilibration can be formally estimated as (Gillon & Yakir, 2000a):

$$\theta_{eq} = \frac{\Delta_{ca} - \Delta_{ca0}}{\Delta_{ea} - \Delta_{ca0}}, \tag{3.12}$$

where Δ_{ca0} represents the value of Δ_{ca} in the absence of any CA activity. Expressions for Δ_{ca0} have been derived with (Ubierna *et al*., 2017; Ogée *et al*., 2018) or without (Gillon & Yakir, 2000a; 2001) ternary corrections. The exact expression shows that Δ_{ca0} depends on p_{CA}, and therefore implicitly assumes that, despite the (putative) absence of CA activity, the carboxylation site coincides with the (true) CA site. This can be problematic, especially in C_4 plants. Fortunately, in most cases, θ_{eq} is expected to be close to unity and the exact knowledge of Δ_{ca0} becomes less critical. Most importantly, when using the models depicted in Fig. 3.3 (Farquhar & Lloyd, 1993; Ogée *et al*., 2018), the knowledge of Δ_{ca0} is only required to compute θ_{eq}. This is very different from the approach of Gillon and Yakir (Gillon & Yakir, 2000a; 2001) that proposed an independent (and flawed, see above) expression for θ_{eq} (Eq. (3.9)) which thus required knowledge of Δ_{ca0} to compute Δ_{ca} and then p_{CA} and g_m.

Revisiting the data from Barbour *et al*. (2016) on C_3 and C_4 plants with the model depicted in Fig. 3.3B led to a degree of equilibration near unity in all species (Fig. 3.5), and especially in C_3 plants. This partially justified the *a priori* assumption made by Barbour *et al*. (2016) that $\theta_{eq} = 1$. However, accounting for incomplete equilibration between CO_2 and leaf water led to $\Delta^{18}O$-derived g_m values that were significantly higher than those obtained assuming full isotopic equilibration (Fig. 3.5), and also higher than those derived from ^{13}C discrimination (Barbour *et al*., 2016), which seemed more compatible with the idea that the CA site was located at the chloroplast surface and, thus, upstream of the carboxylation site (Ogée *et al*., 2018). More importantly, the results shown in Fig. 3.5 clearly demonstrated that, as C_3 plants, C_4 plants must operate most of the time near full equilibration, with a lowest θ_{eq} around 0.75 reached only under high light (> 1500 µmol $m^{-}2$ s^{-1}) and well-watered conditions.

This result is only based on three C_4 species, compared to 14 species in Gillon and Yakir (2001). Although CA is essential for the functioning of the C_4 photosynthetic pathway (Badger & Price,

1994; Caemmerer *et al.*, 2004), significant differences in CA activity exist across evolutionary lineages of C_4 plants (Gillon & Yakir, 2001). This large variability is still largely unexplained but probably related to the specific environment to which a particular species has adapted (Studer *et al.*, 2014). In the dicot species *Flaveria bidentis*, it was found that CA was produced in high excess compared to its requirements to maintain net photosynthesis (Caemmerer *et al.*, 2004; Cousins *et al.*, 2006b; 2006a). Experiments on CA-knockout mutants showed that CO_2 assimilation rates were unaffected by a reduction in CA until CA activity was reduced below 10-20% of the wild type (Caemmerer *et al.*, 2004; Cousins *et al.*, 2006a; 2006b). This excess of CA activity may be advantageous when the CO_2 supply becomes limiting, i.e. during drought (because of stomatal closure) or under low CO_2 (C_4 plants expanded their range approximately 10 million years ago, when the global atmospheric CO_2 was below 300 ppm). This excess of CA activity in C_4 dicots may also explain why these species have the highest degree of equilibration amongst C_4 species (Gillon & Yakir, 2001), in agreement with our findings (Fig. 3.5).

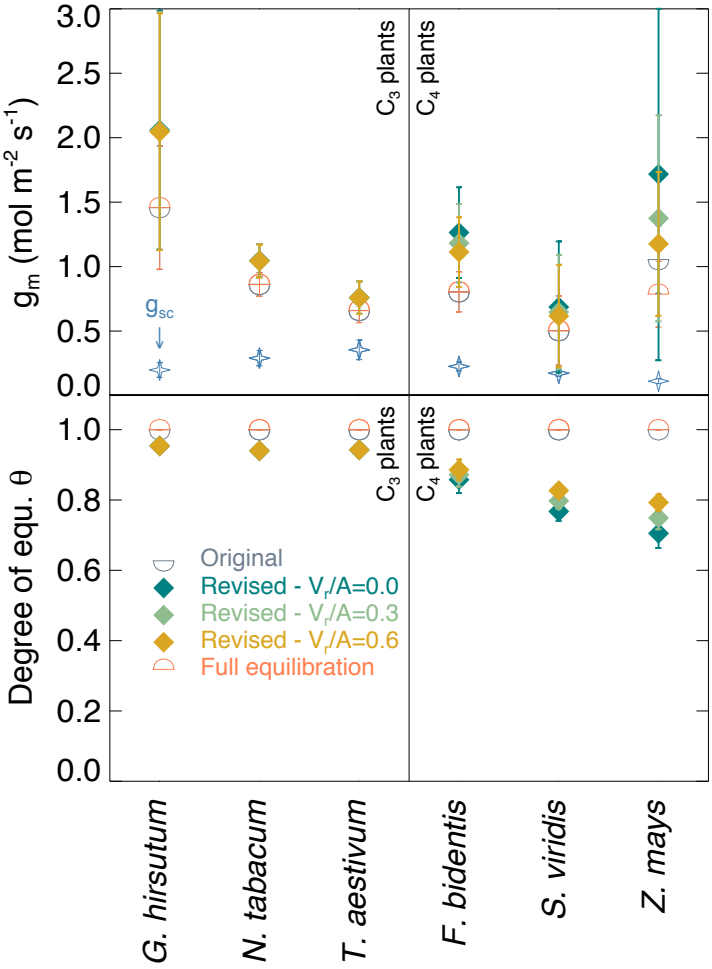

Figure 3.5 | Degree of isotopic equilibrium (θ_{eq}) and mesophyll conductance (g_m) for three C_3 (left) and three C_4 (right) plants studied by Barbour *et al.* (2016). Original values are taken from Barbour *et al.* and were obtained assuming full equilibration (θ_{eq} = 1). Revised values were obtained using the model depicted in Fig. 3.3B, with three different values of the respiratory fraction V_r/A and measured CA activity, or assuming full equilibration as in the original study. Taken from Ogée *et al.* (2018). Ternary corrections were fully accounted for in both studies. Higher respiration rates (V_r/A) leads to a higher degree of equilibration because respired CO_2 is assumed already fully equilibrated in the model.

However, our results suggest that the C_4 monocots *Setaria viridis* or *Zea mays* also exhibit a relatively high degree of equilibration (Fig. 3.5), which is in sharp contrast with what had been suggested before with values of θ_{eq} for these two species as low as 0.16 (Gillon & Yakir, 2001). The reasons for these discrepancies seem mostly methodological. First, the derivation of Eq. (3.9) used in Gillon and Yakir (2001) is in many aspects problematic (see above). There are also large uncertainties on the CA activity measurements. The pH method used previously has been shown to be sensitive to the buffer solution used (Hatch & Burnell, 1990) and must be performed at 2°C and saturating CO_2, i.e., very far from physiological conditions. Another method, using doubly-labelled CO_2, can be performed at 25°C and ambient CO_2 concentrations, and tends to give higher CA activities for C_4 monocots such as *S. viridis* or *Z. mays* (Cousins *et al.*, 2006a; Studer *et al.*, 2014; Barbour *et al.*, 2016; Ubierna *et al.*, 2017). The datasets that we revisited all used this new method, and thus exhibited higher intrinsic CA activities than reported in Gillon and Yakir (2001).

Even with the same methodology, reported CA activities can vary also greatly within one species. Because CA activity of corn leaves was not measured by Barbour *et al.* (2016), we had to estimate its value from the literature. Results shown in Fig. 3.5 were obtained with k_{CA} set to 34 mmol m^{-2} s^{-1} Pa^{-1} according to Cousins *et al.* (Cousins *et al.*, 2006a). However Studer et al. (2014) reported CA activity for *Z. mays* about 2 to 3 times higher. Using their CA activity value for *Z. mays* results in even higher degrees of equilibration.

From the analysis above, it seems clear that the degree of equilibration must be high in both C_3 and C_4 species. The minimum value for θ_{eq} we found corresponds roughly to the global mean value used in atmospheric $C^{18}OO$ budgets (Cuntz *et al.*, 2003b; Welp *et al.*, 2011) and based on the global map by Gillon and Yakir (2001). A higher degree of equilibration in C_4 species should increase the influence of C_4 photosynthesis on atmospheric $C^{18}OO$, with substantial changes on the seasonal cycle at most stations (Cuntz *et al.*, 2003b).

Importance of ternary corrections for mesophyll conductance estimates

In Fig. 3.5, the values for g_m that we estimated with our model assuming full equilibration were in perfect agreement with the mesophyll conductance values reported by Barbour *et al.* (2016). This is because in both studies, ternary corrections had been applied when interpreting both the gas exchange data (to estimate p_i, Eq. (3.2)) and the $\Delta^{18}O$ discrimination data (to estimate R_i, Eq. (3.3)). When accounting for incomplete equilibration of the CO_2 coming out of the leaf, our model predicted higher g_m (i.e. higher p_{CA}) because, to explain the same $\Delta^{18}O$ measurement with less equilibration, more CO_2 had to come out of the leaf. The results were very different when we revisited datasets where ternary corrections had been applied to the gas exchange data only. For example, when revisiting the light response data from Cousins *et al.* (2006a), we obtained significantly lower g_m values for *F. bidentis* compared to the original estimate, even at low light (Fig. 3.6). This was despite the fact that, in both cases, full isotopic equilibration was reached (an assumption in the case of Cousins *et al.* (2006a) and a prediction in this study). This apparent contradiction arises from the ternary corrections. Cousins *et al.* (2006a) applied ternary corrections to estimate p_i but not to interpret $C^{18}OO$ discrimination data, as was common practice at the time. Farquhar and Cernusak (2012) have since shown that such a practice can lead to erroneous $\Delta^{13}C$-derived g_m estimates We show here the same happens when interpreting $\Delta^{18}O$ discrimination data. Indeed, when ternary corrections are only applied to compute p_i, then our model predicts the exact original g_m value at low irradiance, but much lower g_m values with increasing light [see Supplemental Fig. S1 in Ogée *et al.* (2018)]. On the other hand, not applying ternary corrections at all leads to g_m values almost identical to those shown in Fig. 3.6. [see

Supplemental Fig. S1 in Ogée *et al.* (2018)], a result also predicted by Farquhar and Cernusak (2012) for $\Delta^{13}C$-derived g_m.

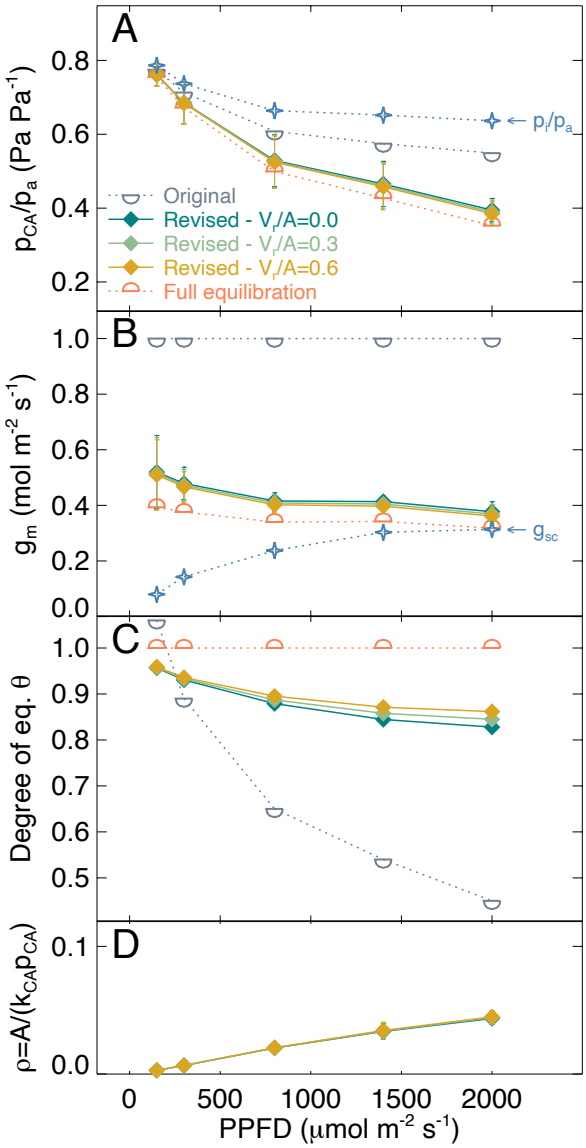

Figure 3.6 | Light response of gas-exchange parameters in *Flaveria bidentis* leaves exposed to increasing levels of photosynthetic photon flux density (PPFD). (A) CO_2 partial pressure ratio p_{CA}/p_a, (B) $\Delta^{18}O$-derived mesophyll conductance (g_m), (C) $\Delta^{18}O$-derived degree of isotopic equilibrium (θ) and (D) the ratio ρ = $A/(k_{CA}p_{CA})$. Data taken from Cousins et al. (2006a). Original and revised values, with three different values of the respiratory fraction V_r/A, or assuming full equilibration, are shown. The CO_2 partial pressure ratio p_i/p_a and the stomatal conductance to CO_2 (g_{sc}) are also shown, in panels (A) and (B) respectively.

To summarise, once ternary corrections are applied consistently, i.e. either completely or not at all, then our model predicts a rather small mesophyll conductance that varies little, and thus becomes increasingly limiting, when light intensity increases. At high light, stomatal conductance

for CO_2 is only slightly lower than g_m. This prediction that g_m is light-independent is based on the idea that k_{CA} is also constant as light increases and both are consistent with Eq. (3.11) and COS studies showing that leaf COS uptake is mostly under stomatal control (Yonemura *et al.*, 2005; Stimler *et al.*, 2011).

3.3 Remaining questions and future directions

What is the link between COS exchange and stomatal conductance?

For a global modelling perspective, the idea that COS uptake by foliage is under strong stomatal control is very attractive because it means that atmospheric COS is an excellent tracer for water and carbon fluxes. It is coherent with our understanding of COS uptake by plants (Eq. 3.11) and the idea that mesophyll or CA activity are not responding to light. However, both g_m (Ubierna *et al.*, 2017) and CA (Boyd *et al.*, 2015) will respond positively to an increase in temperature. Several studies report also an increase of g_m to a short-term reduction in CO_2 concentrations (Douthe *et al.*, 2011; Flexas *et al.*, 2012; Osborn *et al.*, 2016; Ubierna *et al.*, 2018). The mechanisms for this response are not known and were even suggested to be exaggerated by methodological artefacts (Gu & Sun, 2014). However, new independent methods have recently been developed and seem to confirm that g_m increases in response to a rapid drop in CO_2 levels (Ubierna *et al.*, 2018). **It would be interesting to perform experiments with COS measurements to verify whether mesophyll conductance for COS ($g_{m,S}$) also responds to CO_2**. These responses of $g_{m,S}$ and CA activity to temperature and maybe CO_2 will complicate the relationships between COS uptake and stomatal conductance.

More surprisingly, some studies reported a direct influence of COS concentration on stomatal conductance, whereby an increase in COS mixing ratio (from sub-ambient levels to 2500 pmol mol^{-1}) led to higher stomatal conductance (Stimler *et al.*, 2010; 2012). An early study had reported a reduction of the resistance to COS uptake (i.e. the inverse of $A_S/p_{a,S}$ in Eq. 3.11) in several crops when the COS concentration ($p_{a,S}$) was increased (Goldan *et al.*, 1988). If this resistance to COS uptake was mostly controlled by changes in stomatal conductance (see above), these results would also imply that stomatal conductance responds to COS concentration. Alternatively, low COS emissions from these cultivated plants (Kesselmeier & Merk, 1993) may have counter-acted COS uptake at low COS concentrations leading to a higher (apparent) resistance.

The results reported by Stimler *et al.* are different because they are reporting the direct response of stomatal conductance to water vapour (g_{sw}), measured from classical gas exchange methods and analysers. Interestingly, the enhancement of g_{sw} with increasing COS mixing ratio was differently expressed depending on the plant species (Stimler *et al.*, 2012). About 25% of the studied species showed no stomatal response to COS levels but more than half of them exhibited a strong response. There seemed to be no clear relationship between the sensitivity of stomata to COS and the rate of COS uptake (Stimler *et al.*, 2012). However, it was found that the opening of stomata at higher COS levels was inhibited in CA-knockout mutants using either the C_3 (*Nicotina tabacum*) or C_4 (*Flaveria bidentis*) photosynthetic pathway (Stimler *et al.*, 2012). This led Stimer *et al.* to propose that the enhancement was driven by H_2S production following CA-catalysed COS hydrolysis (Stimler *et al.*, 2012).

The exact mechanisms linking H_2S production and stomatal opening is not known at present but several studies have reported that high levels of H_2S (up to parts per million) could cause both opening and closing of stomata (see references in Stimler *et al.*, 2012). H_2S is also known to modify the cationic flow across the cell membrane of mammalian cells (Jiang *et al.*, 2010),

suggesting that similar mechanisms may also exist in plants (Stimler *et al.*, 2012). This was demonstrated at least for other inorganic sulphur compounds such as sulphites that were shown (at micromolar levels) to inhibit malate production in epidermal cells that usually counter-acts the movements of K^+ in guard cells in response to light (Rao & Anderson, 1983; Rennenberg, 1984). However, the levels of H_2S expected in sub-stomatal cavities seem low (parts per billion or less) compared to the levels required to affect stomatal conductance. It is also not clear why the effect is so variable among plant species. Depending on the class of CA that are present (α- vs. β-CA, see above) and their activity and location inside the leaf mesophyll, different production rates of H_2S could be produced, consumed in sulphur metabolism, or released through the stomata. This could explain the inter-species difference reported by Stimler *et al*. (2012).

Based on their observations, Stimler *et al*. suggested that COS concentration may be a significant and unrecognized variable in laboratory studies on stomatal conductance, because uncontrolled COS concentrations could complicate their interpretations. **Clearly, the basis for the stomatal response to COS concentration and its inter-species variability needs to be further explored**. This may provide insights into the mechanisms regulating stomatal conductance, and help revisit and better interpret laboratory studies on stomatal responses to light and CO_2, notably those on CA knock-out mutants (e.g. Kolbe *et al.*, 2018).

Predicting changes in CA activity and mesophyll conductance

A long-term increase in CO_2 is expected to be accompanied by a reduction in stomatal conductance (Ainsworth & Rogers, 2007; De Kauwe *et al.*, 2013; Medlyn & De Kauwe, 2013) and thus a reduction in COS uptake (Sandoval-Soto *et al.*, 2012). The effect on the $C^{18}OO$ exchange is unclear because a reduction in stomatal conductance also increases the isotopic fractionation during diffusion of water vapour and CO_2 across the stomata, thereby increasing the extent of leaf water isotopic enrichment (Farquhar *et al.*, 2007).

Increasing CO_2 should also be accompanied by a reduction in the requirements for CA (Badger & Price, 1994; Protoschill-Krebs *et al.*, 1995; Sandoval-Soto *et al.*, 2012; Studer *et al.*, 2014) and RuBisCO (Ainsworth *et al.*, 2004; Long *et al.*, 2004), particularly in N-limited ecosystems (Ainsworth & Rogers, 2007). In fact, lines of evidence suggest that CA should scale with photosynthetic capacity in response to CO_2 acclimation (Badger & Price, 1994 and references therein). Mesophyll conductance was also reported to scale with RuBISCO contents in tobacco plants (Evans *et al.*, 1994) and to decrease with leaf age in both C_3 and C_4 plants (Barbour *et al.*, 2016), or after an acclimation to high CO_2 levels (Barbour, 2016).

Following this argument, Berry *et al*. (2013) proposed a scaling of the COS uptake rates with photosynthetic capacity (V_{cmax}). Precisely, they proposed to scale the 'internal' COS conductance, defined as $g_{i,S} = (P/g_{m,S} + 1/k_{CA,S})^{-1}$ (Eq. 3.11), with V_{cmax}: $g_{i,S} = 1200V_{cmax}$ (C_3 plants) and $g_{i,S} = 13000V_{cmax}$ (C_4 plants). With this parameterisation, they were able to reproduce without bias the observed leaf COS fluxes from Stimler *et al*. (2012) (Berry *et al.*, 2013). The idea of scaling CA activity and mesophyll conductance with V_{cmax} is very attractive because V_{cmax} is a parameter that is readily available in all land surface models. However it is not clear how these parameterisations derived for COS would translate for the 'internal' conductance relevant for CO_2 and $C^{18}OO$.

The k_{CA} and g_m datasets revisited in Ogée *et al*. (Ogée *et al.*, 2018) may help address this question. We first performed a normalisation of these two parameters at 25°C, using published temperature responses (Boyd *et al.*, 2015; Ubierna *et al.*, 2017). We then derived V_{cmax} at 25°C from net CO_2 assimilation data following previous approaches, i.e., assuming photosynthesis at high light is RuBISCO-limited (Lloyd *et al.*, 1992; Caemmerer, 2013). For this we used published

temperature responses for V_{cmax} and for the Michaelis-Menten constants of RuBISCO for CO_2 and O_2 and its CO_2/O_2 specificity (Bernacchi *et al.*, 2001). Results are shown in Fig. 3.7, where C_3 and C_4 species are treated separately. We found no clear correlation between $g_{m,25}$ and $V_{cmax,25}$ for C_4 plants, but a linear increase of $k_{CA,25}$ with $V_{cmax,25}$ in both plant groups. We also found a significant increase of $g_{m,25}$ with $V_{cmax,25}$ in C_3 plants. These results are still preliminary but support well the idea that the 'internal' conductance for $C^{18}OO$ and CO_2 should scale with photosynthetic capacity.

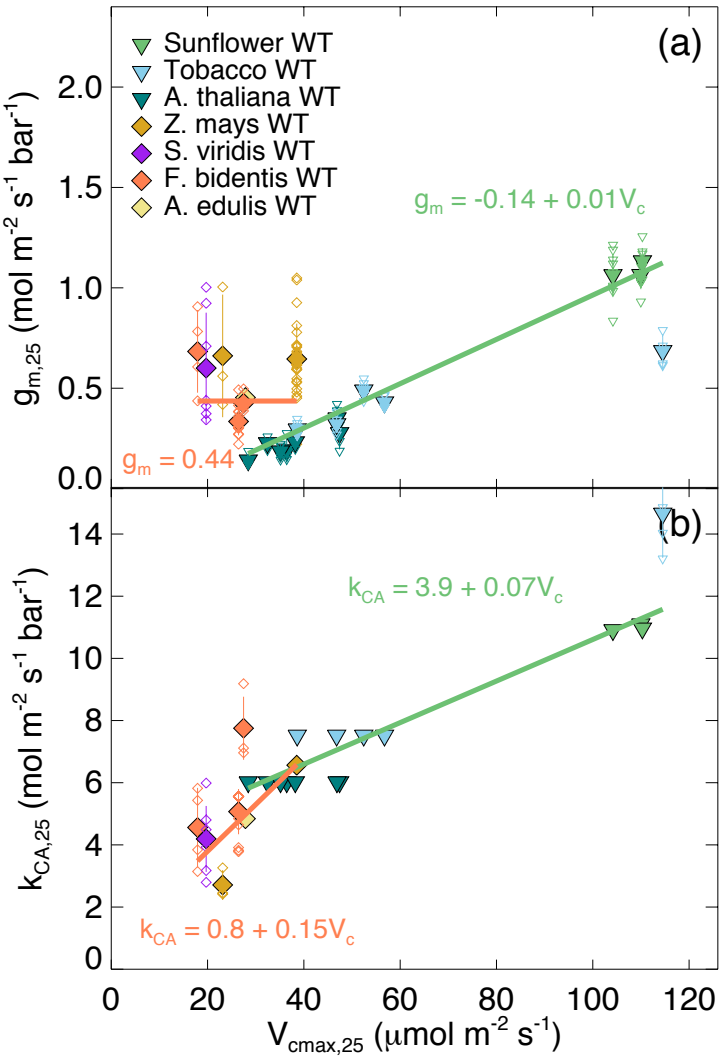

Figure 3.7 | Correlations between carboxylation capacity and (a) $\Delta^{18}O$-derived mesophyll conductance or (b) CA activity in different plants. All parameters are normalised at 25°C (see text). Datasets taken from Ogée *et al.* (2018), except for *Helianthus annuus* (sunflower) and *Arabidopsis thaliana* that are original datasets (West *et al.* unpublished data).

The parameterisations of g_m and k_{CA} presented above could be implemented in land surface models to predict $C^{18}OO$ photosynthetic discrimination. However the $\Delta^{18}O$ theory presented in Ogée *et al.* (2018) is difficult to implement in land surface models. One difficulty is to account for the ternary corrections. As noted earlier land surface models do not implement ternary corrections for water or CO_2 fluxes from foliage. Their parameterizations of photosynthetic parameters have been tuned to simulate realistic fluxes without having to take these complications into account explicitly. This means that the CO_2 partial pressure in the intercellular air space simulated by these models is the one we would estimate without ternary corrections but the correct CO_2 assimilation rate: $p_i' = p_a - A/g_{sc}$. Noting that the $\Delta^{18}O$ theory presented in Ogée *et al.* (2018) predicted almost the same results when ternary corrections were ignored consistently when computing CO_2 gas exchange and isotope data, we explored the idea of using p_i' and

computing $\Delta^{18}O$ without ternary corrections. In this case, and neglecting also respiratory terms, the $C^{18}OO$ photosynthetic discrimination follows an expression very similar to Eq. (3.5):

$$\Delta_A \approx \frac{\bar{a}(1+3\rho_A)+\kappa_c(\delta_{eq}-\delta_a)}{1-\kappa_c(\delta_{eq}-\delta_a)+3\rho_A(1+\kappa_c)} \approx \frac{\bar{a}(1+3\rho_A)+\kappa_c(\delta_{eq}-\delta_a)}{1+3\rho_A(1+\kappa_c)}, \tag{3.13}$$

with $\rho_A = A/(k_{CA}p_{CA})$, $\kappa_c = p_{CA}/(p_a - p_{CA})$, $p_{CA} \approx p_i' - A/g_m$ and:

$$\bar{a} = \frac{a_b(p_a - p_s) + a_s(p_s - p_i') + a_w(p_i' - p_{CA})}{p_a - p_{CA}}, \tag{3.14}$$

where a_b (5.9‰) and a_s (8.8‰) are the fractionation during CO_2 diffusion through the leaf boundary layer and the stomatal pores, respectively, and a_w is the fractionation during CO_2 dissolution (at the air-liquid interface) and diffusion in the liquid phase (from this interface to the CA site). The latter accounts for the fact that the solubility of $C^{18}OO$ in water differs slightly from that of CO_2 and that $C^{18}OO$ also diffuses more slowly than CO_2. The effect is small however and a_w is often taken equal to 0.8‰ irrespective of temperature (Farquhar & Lloyd, 1993; Farquhar & Cernusak, 2012; Barbour *et al.*, 2016).

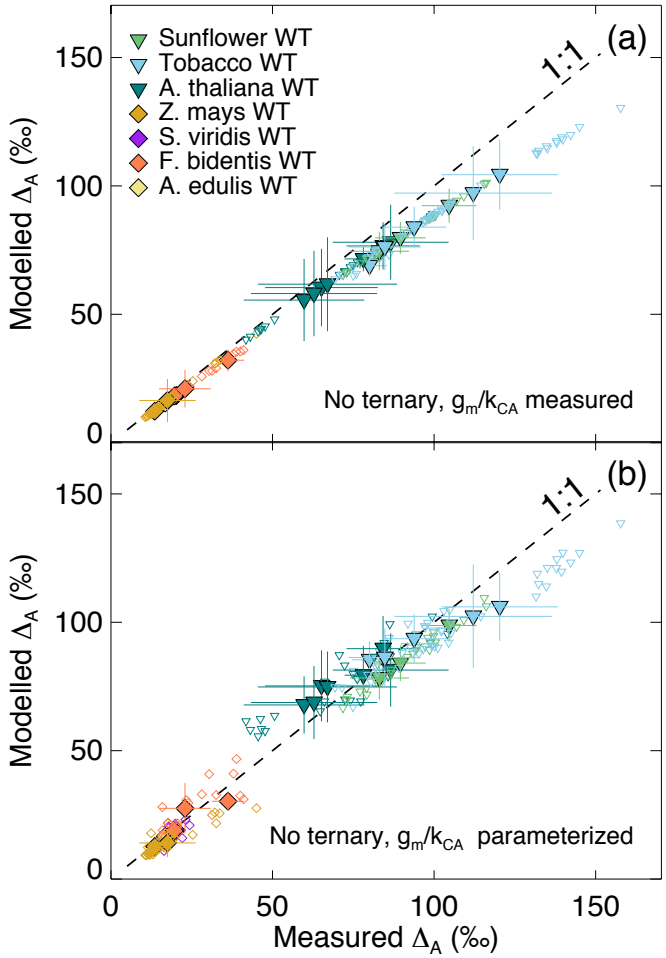

Figure 3.8 | Modelled *vs.* Measured $C^{18}OO$ photosynthetic discrimination using Eq. (3.13) with (a) or without (b) the isotopic disequilibrium term in the denominator. Datasets taken from Ogée *et al.* (2018), except for *Helianthus annuus* (sunflower) and *Arabidopsis thaliana* that are original datasets (West *et al.*, unpublished data).

Using measurements of k_{CA} and g_m, the first expression in Eq. (3.13) (i.e. with the disequilibrium $\delta_{eq} - \delta_a$ in the denominator) reproduces almost perfectly ($r^2 = 1$; mean absolute error = 2‰) the variability in the $C^{18}OO$ photosynthetic discrimination measurements. This demonstrates that,

when ternary corrections are ignored consistently, similar k_{CA} and g_m and stomatal conductance and photosynthetic rates would produce similar discrimination. Neglecting the disequilibrium δ_{eq} - δ_a in the denominator (i.e. using the second expression in Eq. (3.13)) creates a negative bias because large disequilibria are associated with large discriminations (Fig. 3.8a). When doing the same but with g_m and k_{CA} values estimated from the regressions shown in Fig. 3.7 the same bias persists with a larger spread around the 1:1 line (Fig. 3.8b).

By neglecting the disequilibrium in the denominator of Eq. (3.13) we end up with a linear relationship between $C^{18}OO$ discrimination (Δ_A) and the $^{18}O/^{16}O$ composition of atmospheric CO_2 (δ_a). This is important because, when implemented in a global model, δ_a is computed interactively by sending the $C^{18}OO$ fluxes to the atmosphere. Having fluxes that are not linearly related to the atmospheric concentration would require iterations. The disequilibrium δ_{eq} - δ_a from the measured datasets is large because the CO_2 on the inlet of the gas exchange systems comes from gas bottles with very depleted $^{18}O/^{16}O$ ratios compared to atmospheric levels. In nature, the disequilibrium should be smaller and the negative bias should partly disappear. We should thus consider Eq. (3.13) as an excellent approximation of the $C^{18}OO$ discrimination model presented in Ogée *et al*. (2018).

Linking leaf COS and $C^{18}OO$ fluxes

Although the parallel between the diffusional and enzymatic processes governing COS and $C^{18}OO$ exchange by foliage is evident, very few studies have attempted to link the two tracers together. Yonemura *et al*. (2005) attempted to link leaf COS flux measurements to CA activity assays relevant to CO_2 hydration. Eddy covariance measurements of COS (Commane *et al*., 2015; Wehr *et al*., 2017) and $C^{18}OO$ (Wehr *et al*., 2013) fluxes from one temperate broadleaf forest (Harvard forest) have also been reported but their diurnal or seasonal dynamics were never compared, except at conferences (Ogée *et al*., EGU 2016).

The only study so far that directly compared leaf COS uptake rates (A_S) and photosynthetic $C^{18}OO$ discrimination (Δ_A) is the one from Stimler *et al*. (Stimler *et al*., 2011). They reported a "decoupling between A_S and Δ_A in comparing C_3 and C_4 plants", with reduced Δ_A but similar A_S in C_4 plants compared to those found C_3 plants. They explained their results by suggesting that C_4 plants must have (1) higher mesophyll conductance than C_3 plants despite lower CA activity (thus maintaining similar A_S, Eq. (3.11)), and (2) a high PEPC/CA activity ratio that would reduce the ^{18}O exchange efficiency between CO_2 and water and lower Δ_A compared to C_3 plants. A higher g_m in C_4 plants compared to C_3 plants is broadly coherent with Fig. 3.7. A decrease in Δ_A with high PEPC/CA activity ratio is also coherent with results by Cousins *et al*. (2007) on PEPC-deficient mutants of the C_4 dicot *Amaranthus edulis* that show a sharp increase in Δ_A (and a decrease in CO_2 assimilation A) when PEPC activity is reduced by more than 90% (but RuBISCO and CA activity are maintained).

The model shown in Fig. 3.8B takes into account the competition between PEPC and CA in C_4 plants but the derived Δ_A does not depend on PEPC activity (V_p) because we have assumed that the isotope ratio of the CO_2 in the bundle sheath (R_c) is well approximated by the CO_2 that is released from PEPC activity (R_p) because it constitutes its main CO_2 source. However, in PEPC-deficient mutants, this is not the case and a better approximation would be to assume that R_c is well approximated by the isotope ratio of respired CO_2 in the bundle sheath. This would create a strong increase in Δ_A, as observed by Cousins *et al*. (2007).

The link between $C^{18}OO$ and COS fluxes can also be explored at the global scale using the parameterisation of k_{CA} and g_m shown in Fig. (3.8) and extrapolating their values for COS.

Assuming that plant CAs are mostly β-CA, the ratio of $k_{CA,S}/k_{CA}$ should be equal to the differences in k_{max}/K_m of plant β-CA for COS and CO_2 (about 0.05). Similarly, the ratio $g_{m,S}/g_m$ should be equal to the ratio of solubility and diffusivity of CO_2 and COS in aqueous solutions (around 0.59-0.62 over 0-40°C). Using these conversion factors, we could then use the relationships shown in Fig. 3.7 and calculate how $g_{m,S}$ and $k_{CA,S}$ would vary with carboxylation capacity. We implemented these relationships in the global land C cycle model MECBETH, coupled to the climate and atmospheric transport model ECHAM (Cuntz *et al.*, 2003a). The yearly mean plant COS uptake distribution that resulted from this parameterisation is shown in Fig. 3.7. We also performed a run using the parameterisation proposed by Berry *et al.* (2013) and based on COS data only: $g_{i,S} = (P/g_{m,S} + 1/k_{CA,S})^{-1} = 1200V_{cmax}$ (C_3 plants) and $g_{i,S} = 13000V_{cmax}$ (C_4 plants). Based on results shown in Fig. 3.9, it seems clear that the two parameterisations predict very similar global distributions of the COS uptake, and also very similar global totals (864 *vs.* 889 GtS yr^{-1}). This is reassuring and demonstrates that the COS uptake and one way $C^{18}OO$ fluxes from foliage are well correlated and one can be deduced from the other using the conversion factors proposed here, by splitting $g_{i,S}$ explicitly into its diffusive ($g_{m,S}$) and enzymatic ($k_{CA,S}$) components.

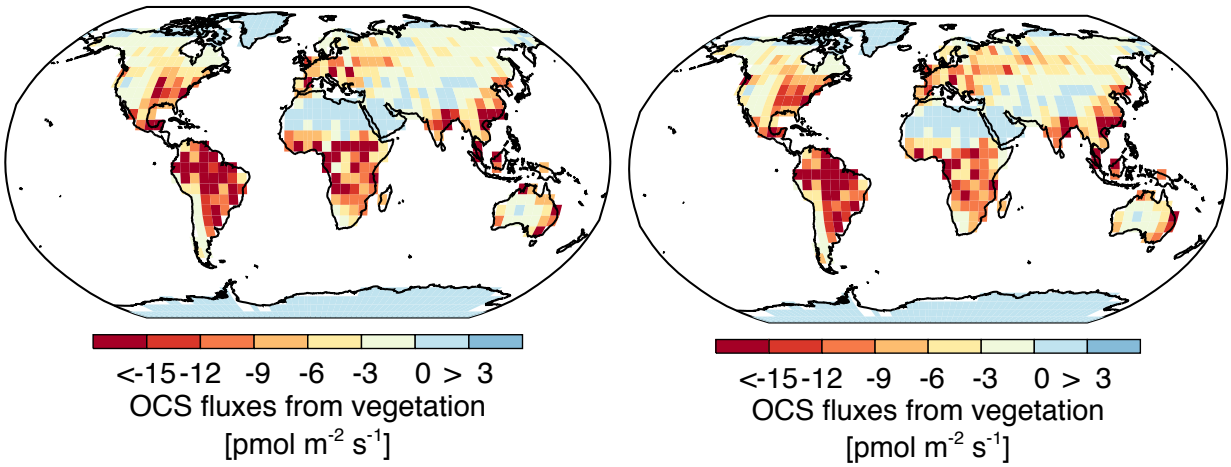

Fig. 3.9 | Yearly mean plant COS uptake distribution simulated by the global land C cycle model MECBETH (climatological mean for the 1970s). Left: parameterisation of $g_{m,S}$ and $k_{CA,S}$ based on CO_2 isotope data (Fig. 3.7) and conversion factors accounting for differences in enzyme kinetics and diffusivities between the two gases. Right: parameterisation of $g_{m,S}$ and $k_{CA,S}$ based on COS leaf cuvette measurements as proposed by Berry *et al.* (2013).

The preliminary results shown in Fig. 3.9 are encouraging but also call for more investigations. The correspondence between k_{CA} and $k_{CA,S}$ that we have used is based on measurements of the k_{max}/K_m for COS and CO_2 of only one plant β-CA from pea leaves (Protoschill-Krebs *et al.*, 1996). Plants contain many different types of β-CAs, and also α- and γ-CAs (Fabre *et al.*, 2007; DiMario *et al.*, 2016). Although β-CAs seem to be the most expressed and abundant class in plants (DiMario *et al.*, 2016), if other CAs are present and abundant, for example in the cell wall of the mesophyll cells, their influence on the COS and $C^{18}OO$ exchange may be large, and we could observe large divergences between k_{CA} and $k_{CA,S}$. We would need to carry experiments where both tracers are measured with different plant types and experiment conditions to verify the generality of our approach.

Chapter 4 – Perspectives

As I was writing this thesis, I slowly realised that it was very difficult to synthesise in a short document all the experimental and theoretical work that had been done on $C^{18}OO$ and COS exchange in soils and leaves. My initial intention was not to write nearly 100 pages on the subject, and I apologise to the reader and the jury member if they felt I was not concise enough. However, I did not want to hide the difficulties that had to be faced, nor the possible complications that have not been fully resolved. Instead, I tried to be as exhaustive as possible, while keeping the focus on approaches and theories that could still be implemented in large-scale models. Clearly microbial life is not one-dimensional and plant function cannot be resumed to electric circuits. Yet, this is how they are represented in even the most sophisticated land surface models.

In Chapter 2, I summarised the current state of knowledge regarding our understanding of COS and $C^{18}OO$ fluxes from oxic soil surfaces. We have now physical and ecological models of how these fluxes respond to rapid changes in soil moisture and temperature and how microbial biomass, soil pH and nutrient availability play on these fluxes. There are still uncertainties, notably regarding the exact role of community structure in regulating COS uptake, or the role of soil texture, chemistry and pH on the ^{18}O exchange rate and soil water isotopic heterogeneity. Yet, compared to previous approaches based on a couple of measurements, we are now in a position to describe with better realism the spatial and seasonal changes of COS and $C^{18}OO$ fluxes. We are now doing it using static maps of soil pH, N content and microbial biomass (Fig. 4.1). However, the direct link between these fluxes and soil microbial biomass and nitrogen content brings a new constraint on land surface models predictions of soil heterotrophic respiration and nutrient availability. Taking this constraint into account would bring more coherence and dynamic relationships between the atmospheric budgets of COS and $C^{18}OO$ and the soil C and nutrient pools predicted by the land surface models.

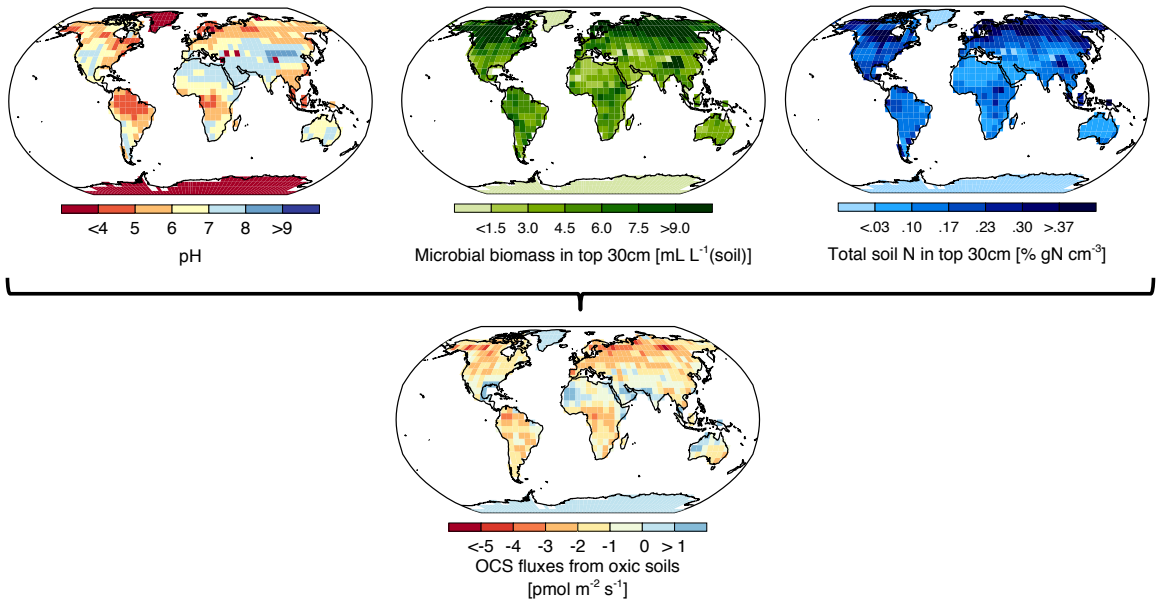

Fig. 4.1 | Global distributions of soil pH and microbial biomass C and soil N in the top 30cm were combined in the land surface model MECBETH to produce a map of yearly mean soil COS fluxes (climatological mean for the 1970s).

In chapter 3, we summarised our latest understanding of the COS and $C^{18}OO$ gas exchange in leaves and their relationship with leaf stomatal conductance. We have seen that both leaf CA

activity and mesophyll conductance for $C^{18}OO$ could be related to the leaf carboxylation capacity (V_{cmax}) and implemented in a simple linearised model to reproduce $C^{18}OO$ discrimination data with a good accuracy. We have also seen that these relationships can be transposed to predict COS uptake. This link the two tracers have to stomatal conductance and the carboxylation capacity of the plant brings a new constraint on land surface model predictions of leaf nitrogen use and stomatal regulation. Taking this new constraint into account would bring more coherence and dynamic relationships between the atmospheric budgets of COS and $C^{18}OO$ and leaf photosynthesis and transpiration predicted by the land surface models.

In chapter 1, we have seen how fluctuations in atmospheric $C^{18}OO$ were related to ENSO cycles and strongly shaped by Northern hemisphere ecosystems. By developing algorithms that could be implemented directly in LSMs or used offline provided that all the necessary output variables are available, we could transport the different tracers and explore how the different LSMs predict their seasonal and inter-annual variability in the atmosphere. By identifying those models that capture best the atmospheric observations, we should be able to reduce our uncertainties on the future of the C cycle and the associated climate change.

Bibliography

Ahlström A, Raupach MR, Schurgers G et al. (2015) The dominant role of semi-arid ecosystems in the trend and variability of the land CO_2 sink. *Science*, **348**, 895.

Ainsworth EA, Rogers A (2007) The response of photosynthesis and stomatal conductance to rising [CO_2]: mechanisms and environmental interactions. *Plant Cell and Environment*, **30**, 258–270.

Ainsworth EA, Long SP (2004) What have we learned from 15 years of free-air CO_2 enrichment (FACE)? A meta-analytic review of the responses of photosynthesis, canopy properties and plant production to rising CO_2. *New Phytologist*, **165**, 351–372.

Allison G, Barnes C, Hughes M (1983) The distribution of deuterium and ^{18}O in dry soils 2. Experimental. *Journal of Hydrology*, **64**, 377–397.

Amundson R, Stern L, Baisden W, Wang Y (1998) The isotopic composition of soil and soil-respired CO_2. *Geoderma*, **82**, 83–114.

Anav A, Friedlingstein P, Beer C et al. (2015) Spatiotemporal patterns of terrestrial gross primary production: A review. *Reviews of Geophysics*, **53**, 785–818.

Asaf D, Rotenberg E, Tatarinov F, Dicken U, Montzka SA, Yakir D (2013) Ecosystem photosynthesis inferred from measurements of carbonyl sulphide flux. *Nature Geoscience*.

Badger MR, Price GD (1994) The role of carbonic anhydrase in photosynthesis. *Annual Review of Plant Physiology and Plant Molecular Biology*, **45**, 369–392.

Baldocchi D, Falge EM, Gu L et al. (2001) FLUXNET: A New Tool to Study the Temporal and Spatial Variability of Ecosystem-Scale Carbon Dioxide, Water Vapor, and Energy Flux Densities. *Bulletin of the American Meteorological Society*, **82**, 2415–2434.

Barbour MM (2016) Understanding regulation of leaf internal carbon and water transport using online stable isotope techniques. *The New phytologist*, **213**, 83–88.

Barbour MM, Cernusak LA, Whitehead D, Griffin K, Turnbull M, Tissue D, Farquhar GD (2005) Nocturnal stomatal conductance and implications for modeling $\delta 18O$ of leaf-respired CO_2 in temperate tree species. *Functional Plant Biology*, **32**, 1107–1121.

Barbour MM, Evans JR, Simonin KA, Caemmerer von S (2016) Online CO_2 and H_2O oxygen isotope fractionation allows estimation of mesophyll conductance in C_4 plants, and reveals that mesophyll conductance decreases as leaves age in both C_4 and C_3 plants. *The New phytologist*, **210**, 875–889.

Bastos A, Friedlingstein P, Sitch S et al. (2018) Impact of the 2015/2016 El Niño on the terrestrial carbon cycle constrained by bottom-up and top-down approaches. *Philosophical Transactions of the Royal Society B: Biological Sciences*, **373**, 20170304.

Bastos A, Janssens IA, Gouveia CM et al. (2016) European land CO_2 sink influenced by NAO and East-Atlantic Pattern coupling. *Nature Communications*, **7**, 10315.

Beer C, Reichstein M, Tomelleri E et al. (2010) Terrestrial Gross Carbon Dioxide Uptake: Global Distribution and Covariation with Climate. *Science*, **329**, 834–838.

Belviso S, Schmidt M, Yver C, Ramonet M, Gros V, Launois T (2013) Strong similarities between night-time deposition velocities of carbonyl sulphide and molecular hydrogen inferred from semi-continuous atmospheric observations in Gif-sur-Yvette, Paris region. *Tellus B*, **65**, 20719.

Berkelhammer M, Asaf D, Still C et al. (2014) Constraining surface carbon fluxes using in situ measurements of carbonyl sulfide and carbon dioxide. *Global Biogeochemical Cycles*, **28**, 161–179.

Bernacchi CJ, Singsaas EL, Pimentel C, Portis AR, Long S (2001) Improved temperature response functions for models of Rubisco-limited photosynthesis. *Plant Cell and Environment*, **24**, 253–259.

Berry JA, Wolf A, Campbell JE et al. (2013) A coupled model of the global cycles of carbonyl sulfide and CO_2: A possible new window on the carbon cycle. *Journal of Geophysical*

Research: Biogeosciences, **118**, 842–852.

Bird RB, Stewart WE, Lightfoot EN (2002) *Transport phenomena*. John Wiley & Sons, 897 p.

Blezinger S, Wilhelm C, Kesselmeier J (2000) Enzymatic consumption of carbonyl sulfide (COS) by marine algae. *Biogeochemistry*, **48**, 185–197.

Bloem E, Haneklaus S, Kesselmeier J, Schnug E (2012) Sulfur Fertilization and Fungal Infections Affect the Exchange of H_2S and COS from Agricultural Crops. *Journal of Agricultural and Food Chemistry*, **60**, 7588–7596.

Bolin B, Keeling CD (1963) Large-scale atmospheric mixing as deduced from the seasonal and meridional variations of carbon dioxide. *Journal of Geophysical Research*, **68**, 3899–3920.

Bonan GB (1991) Atmosphere-biosphere exchange of carbon dioxide in boreal ecosystems. *Journal of Geophysical Research*, **96**, 7301–7312.

Bousquet P, Peylin P, Ciais P, Le Quéré C, Friedlingstein P, Tans PP (2000) Regional Changes in Carbon Dioxide Fluxes of Land and Oceans Since 1980. *Science*, **290**, 1342–1346.

Bowling DR, Tans PP, Monson RK (2001) Partitioning net ecosystem carbon exchange with isotopic fluxes of CO_2. *Global Change Biology*, **7**, 127–145.

Boyd RA, Gandin A, Cousins AB (2015) Temperature response of C_4 photosynthesis: biochemical analysis of Rubisco, Phosphoenolpyruvate Carboxylase and Carbonic Anhydrase in *Setaria viridis*. *Plant Physiology*, pp.00586.2015.

Boyer JS (2015) Turgor and the transport of CO_2 and water across the cuticle (epidermis) of leaves. *Journal of Experimental Botany*, **66**, 2625–2633.

Boyer JS, Kawamitsu Y (2011) Photosynthesis gas exchange system with internal CO_2 directly measured. *Environmental Control in Biology*.

Boyer JS, Wong SC, Farquhar GD (1997) CO_2 and water vapor exchange across leaf cuticle (epidermis) at various water potentials. *Plant Physiology*, **114**, 185–191.

Brenninkmeijer C, Kraft P, Mook W (1983) Oxygen isotope fractionation between CO_2 and H_2O. *Isotope Geoscience*, **1**, 181–190.

Broecker WS, Takahashi T, Simpson HJ, Peng TH (1979) Fate of Fossil Fuel Carbon Dioxide and the Global Carbon Budget. *Science*, **206**, 409.

Brown KA, Kluczewski SM, Bell JNB (1986) Metabolism of [35S]-carbonyl sulphide in perennial ryegrass (Lolium perenne L.) and radish (Raphanus sativus L.). *Environmental and Experimental Botany*, **26**, 355–364.

Buenning N, Noone D et al. (2014) The response of the $^{18}O/^{16}O$ composition of atmospheric CO_2 to changes in environmental conditions. *Journal of Geophysical Research: Biogeosciences*, **119**, 55–79.

Bunk R, Behrendt T, Yi Z, Andreae MO, Kesselmeier J (2017) Exchange of carbonyl sulfide (OCS) between soils and atmosphere under various CO_2 concentrations. *Journal of Geophysical Research: Biogeosciences*, **122**, 1343–1358.

Bunk R, Yi Z, Behrendt T, Wu D, Andreae MO, Kesselmeier J (2018) Carbonyl sulfide (OCS) exchange between soils and the atmosphere affected by soil moisture and compensation points. *Biogeosciences Discussions*, 1–29.

Burnell JN, Hatch MD (1988) Low bundle sheath carbonic anhydrase is apparently essential for effective C_4 pathway operation. *Plant Physiology*, **86**, 1252–1256.

Caemmerer von S (2013) Steady-state models of photosynthesis. *Plant Cell and Environment*, **36**, 1617–1630.

Caemmerer von S, Farquhar GD (1981) Some relationships between the biochemistry of photosynthesis and the gas exchange of leaves. *Planta*, **153**, 376–387.

Caemmerer von S, Farquhar GD, Berry JA (2009) Biochemical model of C_3 photosynthesis. In:

Photosynthesis in silico, pp. 209–230. Springer.

Caemmerer von S, Quinn V, Hancock NC, Price GD, Furbank RT, Ludwig M (2004) Carbonic anhydrase and C_4 photosynthesis: a transgenic analysis. *Plant Cell and Environment*, **27**, 697–703.

Callendar GS (1938) The artificial production of carbon dioxide and its influence on temperature. *Quaterly Journal of the Royal Meteorological Society*, **64**, 223.

Campbell JE, Berry JA, Seibt U et al. (2017) Large historical growth in global terrestrial grossprimary production. *Nature*, **544**, 84–87.

Campbell JE, Carmichael GR, Chai T et al. (2008) Photosynthetic Control of Atmospheric Carbonyl Sulfide During the Growing Season. *Science*, **322**, 1085–1088.

Cernusak LA, Farquhar GD, Wong SC, Stuart-Williams H (2004) Measurement and interpretation of the oxygen isotope composition of carbon dioxide respired by leaves in the dark. *Plant Physiology*, **136**, 3350.

Chen G, Auerswald K, Schnyder H (2016) ^{2}H and ^{18}O depletion of water close to organic surfaces. *Biogeosciences*, **13**, 3175–3186.

Ciais P, Canadell JG, Luyssaert S et al. (2010) Can we reconcile atmospheric estimates of the Northern terrestrial carbon sink with land-based accounting? *Current Opinion in Environmental Sustainability*, **2**, 225–230.

Ciais P, Denning AS, Tans P et al. (1997a) A three-dimensional synthesis study of $\delta^{18}O$ in atmospheric CO_2 1. Surface fluxes. *Journal of Geophysical Research*, **102**, 5857–5872.

Ciais P, Reichstein M, Viovy N et al. (2005) Europe-wide reduction in primary productivity caused by the heat and drought in 2003. *Nature*, **437**, 529–533.

Ciais P, Tan J, Wang X et al. (2019) Five decades of northern land carbon uptake revealed by the interhemispheric CO_2 gradient. *Nature*, 1–17.

Ciais P, Tans P, Denning AS et al. (1997b) A three-dimensional synthesis study of $\delta^{18}O$ in atmospheric CO_2 2. Simulations with the TM2 transport model. *Journal of Geophysical Research*, **102**, 5873–5883.

Ciais P, Tans PP, White JW et al. (1995) Partitioning of ocean and land uptake of CO_2 as inferred by $\delta^{13}C$ measurements from the NOAA/CMDL global air sampling network. *Journal of Geophysical Research*, **100**, 5051–5070.

Commane R, Meredith LK, Baker IT et al. (2015) Seasonal fluxes of carbonyl sulfide in a midlatitude forest. *Proceedings of the National Academy of Sciences of the United States of America*, 201504131.

Conway TJ, Conway TJ, Tans P et al. (1994) Evidence for interannual variability of the carbon cycle from the National Oceanic and Atmospheric Administration/Climate Monitoring and Diagnostics Laboratory global air sampling network. *Journal of Geophysical Research*, **99**, 22831–22855.

Cousins AB, Badger MR, Caemmerer von S (2006a) A transgenic approach to understanding the influence of carbonic anhydrase on $C^{18}OO$ discrimination during C_4 photosynthesis. *Plant Physiology*, **142**, 662–672.

Cousins AB, Badger MR, Caemmerer von S (2006b) Carbonic Anhydrase and Its Influence on Carbon Isotope Discrimination during C_4 Photosynthesis. Insights from Antisense RNA in *Flaveria bidentis*. *Plant Physiology*, **141**, 232–242.

Cousins AB, Baroli I, Badger MR, Ivakov A, Lea PJ, Leegood RC, Caemmerer von S (2007) The Role of Phosphoenolpyruvate Carboxylase during C_4 Photosynthetic Isotope Exchange and Stomatal Conductance. *Plant Physiology*, **145**, 1006–1017.

Cowan IR, Farquhar GD (1977) Stomatal function in relation to leaf metabolism and environment (ed Jennings DH). *Symposia of the Society for Experimental Biology*, **31**, 471–505.

Cox PM, Betts RA, Jones CD, Spall SA, Totterdell IJ (2000) Acceleration of global warming due to carbon-cycle feedbacks in a coupled climate model. *Nature*, **408**, 184–187.

Cuntz M (2011) A dent in carbon's gold standard. *Nature*, **477**, 547–548.

Cuntz M, Ciais P, Hoffmann G, Knorr W (2003a) A comprehensive global three-dimensional model of $\delta^{18}O$ in atmospheric CO_2: 1. Validation of surface processes. *Journal of Geophysical Research*, **108**, 4527.

Cuntz M, Ciais P, Hoffmann G et al. (2003b) A comprehensive global three-dimensional model of $\delta^{18}O$ in atmospheric CO_2: 2. Mapping the atmospheric signal. *Journal of Geophysical Research*, **108**, 4528.

Daniel RM, Peterson ME, Danson MJ et al. (2010) The molecular basis of the effect of temperature on enzyme activity. *The Biochemical journal*, **425**, 353–360.

De Kauwe MG, Medlyn BE et al. (2013) Forest water use and water use efficiency at elevated CO_2: a model-data intercomparison at two contrasting temperate forest FACE sites. *Global Change Biology*, **19**, 1759–1779.

Deepagoda TKKC, Moldrup P, Schjønning P, Wollesen de Jonge L, Kawamoto K, Komatsu T (2011) Density-Corrected Models for Gas Diffusivity and Air Permeability in Unsaturated Soil. *Vadose Zone Journal*, **10**, 226–238.

Del Prete S, Vullo D, Fisher GM, Andrews KT, Poulsen S-A, Capasso C, Supuran CT (2014) Bioorganic & Medicinal Chemistry Letters. *Bioorganic & Medicinal Chemistry Letters*, **24**, 4389–4396.

Devai I, Delaune RD (1995) Formation of volatile sulfur compounds in salt marsh sediment as influenced by soil redox condition. *Organic Geochemistry*, **23**, 283–287.

DiMario RJ, Quebedeaux JC, Longstreth DJ, Dassanayake M, Hartman MM, Moroney JV (2016) The cytoplasmic carbonic anhydrases βCA2 and βCA4 are required for optimal plant growth at low CO_2. *Plant Physiology*, **171**, 280–293.

Dongmann G, Nürnberg HW, Förstel H, Wagener K (1974) On the enrichment of $H_2{}^{18}O$ in the leaves of transpiring plants. *Radiation and Environmental Biophysics*, **11**, 41–52.

Douthe C, Dreyer E et al. (2011) Mesophyll conductance to CO_2, assessed from online TDL-AS records of $^{13}CO_2$ discrimination, displays small but significant short-term responses to CO_2 and irradiance in Eucalyptus seedlings. *Journal of Experimental Botany*, **62**, 5335–5346.

Dufresne JL, Fairhead L, Le Treut H et al. (2002) On the magnitude of positive feedback between future climate change and the carbon cycle. *Geophysical Research Letters*, **29**, 43–1–43–4.

Elliott S, Lu E, Rowland FS (1989) Rates and mechanisms for the hydrolysis of carbonyl sulfide in natural waters. *Environmental Science & Technology*, **23**, 458–461.

Evans JR, Cemmerer von S (1996) Carbon dioxide diffusion inside leaves. *Plant Physiology*, **110**, 339–346.

Evans JR, Caemmerer SV, Setchell BA, Hudson GS (1994) The Relationship Between CO_2 Transfer Conductance and Leaf Anatomy in Transgenic Tobacco With a Reduced Content of Rubisco. *Functional Plant Biol.*, **21**, 475–495 KW –.

Evans JR, Evans JR, Sharkey T et al. (1986) Carbon isotope discrimination measured concurrently with gas exchange to investigate CO_2 diffusion in leaves of higher plants. *Australian Journal of Plant Physiology*, **13**, 281–292.

Evans JR, Kaldenhoff R, Genty B, Terashima I (2009) Resistances along the CO_2 diffusion pathway inside leaves. *Journal of Experimental Botany*, **60**, 2235–2248.

Fabre N, Reiter IM, Becuwe-Linka N, Genty B, Rumeau D (2007) Characterization and expression analysis of genes encoding a and b carbonic anhydrases in Arabidopsis. *Plant Cell and Environment*, **30**, 617–629.

Farquhar GD, Cernusak LA (2005) On the isotopic composition of leaf water in the non-steady state. *Functional Plant Biology*, **32**, 293–303.

Farquhar GD, Cernusak LA (2012) Ternary effects on the gas exchange of isotopologues of carbon dioxide. *Plant Cell and Environment*, **35**, 1221–1231.

Farquhar GD, Lloyd J (1993) Carbon and oxygen isotope effects in the exchange of carbon dioxide between terrestrial plants and the atmosphere. In: *Stable Isotopes and Plant Carbon–Water Relations* (eds Ehleringer JR, Hall AE, Farquhar GD), pp. 47–70. Academic Press, San Diego.

Farquhar GD, Caemmerer von S, Berry JA (1980) A biochemical model of photosynthetic CO_2 assimilation in leaves of C_3 species. *Planta*, **149**, 78–90.

Farquhar GD, Cernusak LA, Barnes B (2007) Heavy Water Fractionation during Transpiration. *Plant Physiology*, **143**, 11–18.

Farquhar GD, Lloyd J, Taylor JA et al. (1993) Vegetation effects on the isotope composition of oxygen in atmospheric CO_2. *Nature*, **363**, 439–443.

Farquhar GD, O'leary M, Berry JA (1982) On the relationship between carbon isotope discrimination and the intercellular carbon dioxide concentration in leaves. *Australian Journal of Plant Physiology*, **9**, 121–137.

Flanagan LB, Phillips SL, Ehleringer JR, Lloyd J, Farquhar GD (1994) Effect of changes in leaf water oxygen isotopic composition on discrimination against $C^{16}O^{18}O$ during photosynthetic gas-exchange. *Australian Journal of Plant Physiology*, **21**, 221–234.

Flexas J, Barbour MM, Brendel O et al. (2012) Mesophyll diffusion conductance to CO_2: An unappreciated central player in photosynthesis. *Plant Science*, **193-194**, 70–84.

Francey RJ, Tans PP (1987) Latitudinal varion in oxygen-18 of atmospheric CO_2. *Nature*, **327**, 495–497.

Francey RJ, Tans PP, Allison CE, Enting IG, White JWC, Trolier M (1995) Changes in oceanic and terrestrial carbon uptake since 1982. *Nature*, **373**, 326–330.

Friedli H, Siegenthaler U, Rauber D, Oeschger H (1987) Measurements of concentration, $^{13}C/^{12}C$ and $^{18}O/^{16}O$ ratios of tropospheric carbon dioxide over Switzerland. *Tellus B*, **39**, 80–88.

Friedlingstein P, Prentice IC (2010) Carbon-climate feedbacks: a review of model and observation based estimates. *Current Opinion in Environmental Sustainability*, **2**, 251–257.

Friedlingstein P, Bopp L, Rayner P et al. (2006) Climate-carbon cycle feedback analysis: Results from the C4MIP model intercomparison. *Journal of climate*, **19**, 3337–3353.

Friedlingstein P, Dufresne JL, Cox PM, Rayner P (2003) How positive is the feedback between climate change and the carbon cycle? *Tellus B*, **55**, 692–700.

Friedlingstein P, Meinshausen M, Arora VK, Jones CD, Anav A, Liddicoat SK, Knutti R (2014) Uncertainties in CMIP5 Climate Projections due to Carbon Cycle Feedbacks. *Journal of climate*, **27**, 511–526.

Friend AD, Arneth A, Kiang NY et al. (2007) FLUXNET and modelling the global carbon cycle. *Global Change Biology*, **13**, 610–633.

Gamnitzer U, Moyes AB, Bowling DR, Schnyder H (2011) Measuring and modelling the isotopic composition of soil respiration: insights from a grassland tracer experiment. *Biogeosciences*, **8**, 1333–1350.

Genty B, Meyer S, Piel C, Badeck F, Liozon R (1998) CO_2 Diffusion Inside Leaf Mesophyll of Ligneous Plants. In: *Photosynthesis: Mechanisms and Effects: Volume I–V: Proceedings of the XIth International Congress on Photosynthesis, Budapest, Hungary, August 17–22, 1998* (ed Garab G), pp. 3961–3966. Springer Netherlands, Dordrecht.

Gerster R (1971) Kinetics of oxygen exchange between gaseous $C^{18}O_2$ and water (*in french*). *International Journal of Applied Radiation and Isotopes*, **22**, 339–348.

Gillon J, Yakir D (2000a) Internal Conductance to CO_2 Diffusion and $C^{18}OO$ Discrimination in C_3 Leaves. *Plant Physiology*, **123**, 201–213.

Gillon J, Yakir D (2000b) Naturally low carbonic anhydrase activity in C_4 and C_3 plants limits discrimination against $C^{18}OO$ during photosynthesis. *Plant Cell and Environment*, **23**, 903–915.

Gillon J, Yakir D (2001) Influence of carbonic anhydrase activity in terrestrial vegetation on the ^{18}O content of atmospheric CO_2. *Science*, **291**, 2584–2587.

Gimeno TE, Ogée J, Royles J et al. (2017) Bryophyte gas-exchange dynamics along varying hydration status reveal a significant carbonyl sulphide (COS) sink in the dark and COS source in the light. *The New phytologist*, **180**, 864.

Goldan PD, Fall R, Kuster WC, Fehsenfeld FC (1988) Uptake of COS by Growing Vegetation - a Major Tropospheric Sink. *Journal Geophysical Research Atmosphere*, **93**, 14186–14192.

Goulden ML, Munger JW, Fan S, Daube BC, Wofsy SC (1996) Exchange of carbon dioxide by a deciduous forest: response to internannual climate variability. *Science*, **271**, 1576–1578.

Gu L, Sun Y (2014) Artefactual responses of mesophyll conductance to CO_2 and irradiance estimated with the variable J and online isotope discrimination methods. *Plant Cell and Environment*, **37**, 1231–1249.

Haritos VS, Dojchinov G (2005) Carbonic anhydrase metabolism is a key factor in the toxicity of CO_2 and COS but not CS_2 toward the flour beetle *Tribolium castaneum* [Coleoptera: Tenebrionidae]. *Comparative Biochemistry and Physiology Part C: Toxicology & Pharmacology*, **140**, 139–147.

Hatch MD, Burnell JN (1990) Carbonic anhydrase activity in leaves and its role in the first step of C_4 photosynthesis. *Plant Physiology*, **93**, 825–828.

Hesterberg R, Siegenthaler U (1991) Production and stable isotopic composition of CO_2 in a soil near Bern, Switzerland. *Tellus B*, **43**, 197–205.

Houghton RA, Hobbie JE, Melillo JM, Moore B, Peterson BJ, Shaver GR, Woodwell GM (1983) Changes in the carbon content of terrestrial biota and soils between 1860 and 1980: a net release of CO_2 to the atmosphere. *Ecologicala Monogrpahs*, **53**, 235–262.

Hsieh J, Savin S, Kelly E, Chadwick O (1998) Measurement of soil-water $\delta^{18}O$ values by direct equilibration with CO2. *Geoderma*, **82**, 255–268.

Isik S, Kockar F, Aydin M et al. (2009) Carbonic anhydrase inhibitors: inhibition of the beta-class enzyme from the yeast *Saccharomyces cervevisiae* with sulfonamides and sulfamates. *Bioorganic & Medicinal Chemistry*, **17**, 1158–1163.

Jarman PD (1974) The Diffusion of Carbon Dioxide and Water Vapour through Stomata. *Journal of Experimental Botany*, **25**, 927–936.

Jiang B, Tang G, Cao K, Wu L, Wang R (2010) Molecular Mechanism for H_2S-Induced Activation of K ATP Channels. *Antioxidants & Redox Signaling*, **12**, 1167–1178.

Jones SP, Ogée J, Sauze J et al. (2017) Non-destructive estimates of soil carbonic anhydrase activity and associated soil water oxygen isotope composition. *Hydrology and Earth System Sciences*, **21**, 6363–6377.

Jouzel J, Koster RD, Suozzo RJ, Russell GL, White JWC, Broecker WS (1991) Simulations of the HDO and $H_2{}^{18}O$ atmospheric cycles using the NASA GISS general circulation model: Sensitivity experiments for present-day conditions. *Journal of Geophysical Research*, **96**, 7495.

Kaisermann A, Jones SP, Wohl S, Ogée J, Wingate L (2018a) Nitrogen fertilization reduces the capacity of soils to take up atmospheric carbonyl sulphide. *Soil Systems*, **2**, 62.

Kaisermann A, Ogée J, Sauze J, Wohl S, Jones SP, Gutierrez A, Wingate L (2018b) Disentangling

the rates of carbonyl sulfide (COS) production and consumption and their dependency on soil properties across biomes and land use types. *Atmospheric Chemistry and Physics*, **18**, 9425–9440.

Kapiluto Y, Yakir D, Tans P, Berkowitz B (2007) Experimental and numerical studies of the ^{18}O exchange between CO_2 and water in the atmosphere-soil invasion flux. *Geochimica et Cosmochimica Acta*, **71**, 2657–2671.

Keeling CD (1958) The concentration and isotopic abundances of atmospheric carbon dioxide in rural areas. *Geochimica et Cosmochimica Acta*, **13**, 322–334.

Keeling CD (1960) The concentration and isotopic abundances of carbon dioxide in the atmosphere. *Tellus B*, **2**, 200–203.

Keeling CD, Whorf TP, Wahlen M, van der Plichtt J (1995) Interannual extremes in the rate of rise of atmospheric carbon dioxide since 1980. *Nature*, **375**, 666–670.

Keeling RF, Graven HD, Welp LR et al. (2017) Atmospheric evidence for a global secular increase in carbon isotopic discrimination of land photosynthesis. *Proceedings of the National Academy of Sciences of the United States of America*, **114**, 10361–10366.

Keeling RF, Piper SC, Heimann M (1996) Global and hemispheric CO_2 sinks deduced from changes in atmospheric O_2 concentration. *Nature*, **381**, 218–221.

Kesselmeier J, Merk L (1993) Exchange of carbonyl sulfide (COS) between agricultural plants and the atmosphere: Studies on the deposition of COS to peas, corn and rapeseed. *Biogeochemistry*, **23**, 47–59.

Kesselmeier J, Teusch N, Kuhn U (1999) Controlling variables for the uptake of atmospheric carbonyl sulfide by soil. *Journal of Geophysical Research*, **104**, 11,577–11,584.

Kettle AJ, Kuhn U, Hobe von M, Kesselmeier J, Andreae MO (2002) Global budget of atmospheric carbonyl sulfide: Temporal and spatial variations of the dominant sources and sinks. *Journal of Geophysical Research*, **107**, 4658.

Kitz F, Gerdel K, Hammerle A, Laterza T, Spielmann FM, Wohlfahrt G (2017) In situ soil COS exchange of a temperate mountain grassland under simulated drought. *Oecologia*, 1–10.

Kolbe AR, Brutnell TP, Cousins AB, Studer AJ (2018) Carbonic Anhydrase Mutants in *Zea mays* Have Altered Stomatal Responses to Environmental Signals. *Plant Physiology*, **177**, 980–989.

Kooijmans LMJ, Maseyk K, Seibt U et al. (2017) Canopy uptake dominates nighttime carbonyl sulfide fluxes in a boreal forest. *Atmospheric Chemistry and Physics*, **17**, 11453–11465.

Kooijmans LMJ, Sun W, Aalto J et al. (2019) Influences of light and humidity on carbonyl sulfide-based estimates of photosynthesis. *Proceedings of the National Academy of Sciences of the United States of America*, **116**, 2470–2475.

Krinner G, Viovy N, De Noblet-Ducoudré N et al. (2005) A dynamic global vegetation model for studies of the coupled atmosphere-biosphere system. *Global Biogeochemical Cycles*, **19**, GB1015.

Krulwich TA, Sachs G, Padan E (2011) Molecular aspects of bacterial pH sensing and homeostasis. *Nature Reviews Microbiology*, **9**, 330–343.

Lasslop G, Reichstein M, Papale D et al. (2010) Separation of net ecosystem exchange into assimilation and respiration using a light response curve approach: critical issues and global evaluation. *Global Change Biology*, **16**, 187–208.

Launois T, Peylin P, Belviso S, Poulter B (2015) A new model of the global biogeochemical cycle of carbonyl sulfide – Part 2: Use of OCS to constrain gross primary productivity of current vegetation models. *Atmos. Chem. Phys.*, **15**, 9285–9312.

Le Quéré C, Aumont O, Bopp L et al. (2003) Two decades of ocean CO_2 sink and variability. *Tellus B*, **55**, 649–656.

Le Quéré C, Moriarty R, Andrew RM et al. (2015) Global Carbon Budget 2015. *Earth System*

Science Data, **7**, 349–396.

Lehmann S, Conrad R (1996) Characteristics of turnover of carbonyl sulfide in four different soils. *Journal of Atmospheric Chemistry*, **23**, 193–207.

Liang LL, Arcus VL, Heskel MA et al. (2017) Macromolecular rate theory (MMRT) provides a thermodynamics rationale to underpin the convergent temperature response in plant leaf respiration. *Global Change Biology*, **24**, 1538–1547.

Lin Y, Horita J, Abe O (2018) Adsorption isotope effects of water on mesoporous silica and alumina with implications for the land-vegetation-atmosphere system. *Geochimica et Cosmochimica Acta*, **223**, 520–536.

Lloyd J, Syvertsen J, Kriedemann P, Farquhar GD (1992) Low conductances for CO_2 diffusion from stomata to the sites of carboxylation in leaves of woody species. *Plant Cell and Environment*, **15**, 873–899.

Long SP, Ainsworth EA, Rogers A, Ort DR (2004) Rising atmospheric carbon dioxide: plants FACE the future. *Annual Review of Plant Biology*, **55**, 591–628.

Lorimer GH, Pierce J (1989) Carbonyl sulfide: an alternate substrate for but not an activator of ribulose-1,5-bisphosphate carboxylase. *The Journal of biological chemistry*, **264**, 2764–2772.

Maier M, Schack-Kirchner H, Aubinet M, Goffin S, Longdoz B, Parent F (2012) Turbulence Effect on Gas Transport in Three Contrasting Forest Soils. *Soil Science Society of America Journal*, **76**, 1518.

Manzoni S, Katul GG (2014) Invariant soil water potential at zero microbial respiration explained by hydrological discontinuity in dry soils. *Geophysical Research Letters*, **41**, 7151–7158.

Marrero TR, Mason EA (1972) Gaseous Diffusion Coefficients. *Journal of Physical and Chemical Reference Data*, **1**, 3–118.

Maseyk K, Berry JA, Billesbach D, Campbell JE, Torn MS, Zahniser M, Seibt U (2014) Sources and sinks of carbonyl sulfide in an agricultural field in the Southern Great Plains. *Proceedings of the National Academy of Sciences of the United States of America*, **111**, 9064–9069.

Massman WJ, Sommerfeld RA, Mosier AR, Zeller KF, Hehn TJ, Rochelle SG (1997) A model investigation of turbulence-driven pressure-pumping effects on the rate of diffusion of CO_2, N_2O, and CH_4 through layered snowpacks. *Journal of Geophysical Research: Atmospheres (1984–2012)*, **102**, 18851–18863.

Meadows DH, Meadows D, Randers J, Behrens WW III (1972) *The Limits to Growth*, Potomac Asociates Book edn. Universe Books, New York, 1 p.

Medlyn B, De Kauwe M (2013) Carbon dioxide and water use in forests. *Nature*, **499**, 287–289.

Mello WZ, Hines ME (1994) Application of static and dynamic enclosures for determining dimethyl sulfide and carbonyl sulfide exchange in *Sphagnum* peatlands: Implications for the magnitude and direction of flux. *Journal of Geophysical Research*, **99**, 14–601–14–607.

Meredith LK, Boye K, Youngerman C, Whelan M, Ogée J, Sauze J, Wingate L (2018) Coupled Biological and Abiotic Mechanisms Driving Carbonyl Sulfide Production in Soils. *Soil Systems*, **2**, 37.

Meredith LK, Ogée J, Boye K et al. (2019) Soil exchange rates of COS and $CO^{18}O$ differ with the diversity of microbial communities and their carbonic anhydrase enzymes. *The ISME Journal*, **13**, 290–300.

Merlin C, Masters M, McAteer S, Coulson A (2003) Why Is Carbonic Anhydrase Essential to *Escherichia coli*? *Journal of bacteriology*, **185**, 6415–6424.

Miller J, Yakir D, White J, Tans P (1999) Measurement of 18O/16O in the soil-atmosphere CO2 flux. *Global Biogeochemical Cycles*, **13**, 761–774.

Mills GA, Urey HC (1940) The Kinetics of Isotopic Exchange between Carbon Dioxide, Bicarbonate Ion, Carbonate Ion and Water. *Journal of the American Chemical Society*, **62**,

1019–1026.

Moldrup P, Olesen T, Komatsu T, Yoshikawa S, Schjønning P, Rolston DE (2003) Modeling diffusion and reaction in soils: X. A unifying model for solute and gas diffusivity in unsaturated soil. *Soil science*, **168**, 321–337.

Monteith JL (1977) Climate and the Efficiency of Crop Production in Britain. *Philosophical Transactions of the Royal Society B: Biological Sciences*, **281**, 277–294.

Montzka SA, Calvert P, Hall BD, Elkins JW, Conway TJ, Tans PP, Sweeney C (2007) On the global distribution, seasonality, and budget of atmospheric carbonyl sulfide (COS) and some similarities to CO_2. *Journal of Geophysical Research*, **112**, D09302.

Morales P, Sykes MT, Prentice IC et al. (2005) Comparing and evaluating process-based ecosystem model predictions of carbon and water fluxes in major European forest biomes. *Global Change Biology*, **11**, 2211–2233.

Morison JIL, Lawson T (2007) Does lateral gas diffusion in leaves matter? *Plant Cell and Environment*, **30**, 1072–1085.

Moroney JV, Bartlett SG, Samuelsson G (2001) Carbonic anhydrases in plants and algae. *Plant Cell and Environment*, **24**, 141–153.

Myneni R, Myneni R, Keeling C et al. (1997) Increased plant growth in the northern high latitudes from 1981 to 1991. *Nature*, **386**, 698–702.

Ogawa T, Kato H, Higashide M, Nishimiya M, Katayama Y (2016) Degradation of carbonyl sulfide by Actinomycetes and detection of clade D of β-class carbonic anhydrase. *FEMS Microbiology letters*.

Ogawa T, Noguchi K, Saito M et al. (2013) Carbonyl Sulfide Hydrolase from *Thiobacillus thioparus* Strain THI115 Is One of the β-Carbonic Anhydrase Family Enzymes. *Journal of the American Chemical Society*, **135**, 3818–3825.

Ogée J, Peylin P, Ciais P et al. (2003) Partitioning net ecosystem carbon exchange into net assimilation and respiration using $^{13}CO_2$ measurements: a cost-effective sampling strategy. *Global Biogeochemical Cycles*, **17**, 1070.

Ogée J, Peylin P, Cuntz M et al. (2004) Partitioning net ecosystem carbon exchange into net assimilation and respiration with canopy-scale isotopic measurements: an error propagation analysis with $^{13}CO_2$ and $CO^{18}O$ data. *Global Biogeochemical Cycles*, **18**, GB2019.

Ogée J, Sauze J, Kesselmeier J, Genty B, Van Diest H, Launois T, Wingate L (2016) A new mechanistic framework to predict OCS fluxes from soils. *Biogeosciences*, **13**, 2221–2240.

Ogée J, Wingate L, Genty B (2018) Estimating mesophyll conductance from measurements of $C^{18}OO$ photosynthetic discrimination and carbonic anhydrase activity. *Plant Physiol.*, **178**, 728–752.

Osborn HL, Alonso-Cantabrana H, Sharwood RE, Covshoff S, Evans JR, Furbank RT, Caemmerer von S (2016) Effects of reduced carbonic anhydrase activity on CO_2 assimilation rates in *Setaria viridis*: a transgenic analysis. *Journal of Experimental Botany*, erw357.

Parkhurst DF, Wong SC, Farquhar GD, Cowan IR (1988) Gradients of Intercellular CO_2 Levels Across the Leaf Mesophyll. *Plant Physiology*, **86**, 1032–1037.

Peylin P, Ciais P, Denning AS, Tans P, Berry JA, White J (1999) A 3-dimensional study of $\delta^{18}O$ in atmospheric CO_2: contribution of different land ecosystems. *Tellus B*, **51**, 642–667.

Placella SA, Brodie EL, Firestone MK (2012) Rainfall-induced carbon dioxide pulses result from sequential resuscitation of phylogenetically clustered microbial groups. *Proceedings of the National Academy of Sciences of the United States of America*, **109**, 10931–10936.

Poulter B, Frank D, Ciais P et al. (2014) Contribution of semi-arid ecosystems to interannual variability of the global carbon cycle. *Nature*, 1–17.

Protoschill-Krebs G, Kesselmeier J (1992) Enzymatic Pathways for the Consumption of Carbonyl

Sulphide (COS) by Higher Plants. *Botanica Acta*, **105**, 206–212.

Protoschill-Krebs G, Wilhelm C, Kesselmeier J (1995) Consumption of Carbonyl Sulphide by *Chlamydomonas reinhardtii* with Different Activities of Carbonic Anhydrase (CA) Induced by Different CO_2 Growing Regimes. *Botanica Acta*, **108**, 445–448.

Protoschill-Krebs G, Wilhelm C, Kesselmeier J (1996) Consumption of carbonyl sulphide (COS) by higher plant carbonic anhydrase (CA). *Atmospheric Environment*, **30**, 3151–3156.

Rao IM, Anderson LE (1983) Light and Stomatal Metabolism : II. Effects of Sulfite and Arsenite on Stomatal Opening and Light Modulation of Enzymes in Epidermis. *Plant Physiology*, **71**, 456–459.

Reichstein M, Ciais P, Papale D et al. (2007) Reduction of ecosystem productivity and respiration during the European summer 2003 climate anomaly: a joint flux tower, remote sensing and modelling analysis. *Global Change Biology*, **13**, 634–651.

Reichstein M, Falge E, Baldocchi D et al. (2005) On the separation of net ecosystem exchange into assimilation and ecosystem respiration: review and improved algorithm. *Global Change Biology*, **11**, 1424–1439.

Rennenberg H (1984) The Fate of Excess Sulfur in Higher Plants. *Annual Review of Plant Physiology*, **35**, 121–153.

Revelle R, Suess HE (1957) Carbon dioxide exchange between atmosphere and ocean and the question of an increase of atmospheric CO_2 during the past decades. *Tellus*, **9**, 18–27.

Riederer M, Schreiber L (2001) Protecting against water loss: analysis of the barrier properties of plant cuticles. *Journal of Experimental Botany*, **52**, 2023–2032.

Riley W (2005) A modeling study of the impact of the $\delta^{18}O$ value of near-surface soil water on the $\delta^{18}O$ value of the soil-surface CO_2 flux. *Geochimica et Cosmochimica Acta*, **69**, 1939–1946.

Riley W, Still C, Helliker BR, Ribas Carbo M, Berry JA (2003) ^{18}O composition of CO_2 and H_2O ecosystem pools and fluxes in a tallgrass prairie: Simulations and comparisons to measurements. *Global Change Biology*, **9**, 1567–1581.

Riley W, Still C, Torn M, Berry JA (2002) A mechanistic model of $H_2{}^{18}O$ and $C^{18}OO$ fluxes between ecosystems and the atmosphere: Model description and sensitivity analyses. *Global Biogeochemical Cycles*, **16**, 1095.

Rouse JW, Haas RH, Schell JA, Deering DW (1973) Monitoring vegetation systems in the Great Plains with ERTS. In: *Third ERTS Symposium*, pp. 309–317. NASA.

Rowlett RS (2010) Structure and catalytic mechanism of the β-carbonic anhydrases. *BBA - Proteins and Proteomics*, **1804**, 362–373.

Rowlett RS, Gargiulo NJ III, Santoli FA, Jackson JM, Corbett AH (1991) Activation and inhibition of bovine carbonic anhydrase III by dianions. *The Journal of biological chemistry*, **266**, 933–941.

Rowlett RS, Tu C, McKay MM et al. (2002) Kinetic characterization of wild-type and proton transfer-impaired variants of β-carbonic anhydrase from *Arabidopsis thaliana*. *Archives of biochemistry and biophysics*, **404**, 197–209.

Rozanski K, Araguás-Araguás L, Gonfiantini R (1992) Relation between long-term trends of oxygen-18 isotope composition of precipitation and climate. *Science*, **258**, 981–985.

Rusconi S, Innocenti A, Vullo D, Mastrolorenzo A, Scozzafava A, Supuran CT (2004) Carbonic anhydrase inhibitors. Interaction of isozymes I, II, IV, V, and IX with phosphates, carbamoyl phosphate, and the phosphonate antiviral drug foscarnet. *Bioorganic & Medicinal Chemistry Letters*, **14**, 5763–5767.

Ryu Y, Berry JA, Baldocchi DD (2019) What is global photosynthesis? History, uncertainties and opportunities. *Remote Sensing of Environment*, **223**, 95–114.

Sander R (2015) Compilation of Henry's law constants (version 4.0) for water as solvent. *Atmospheric Chemistry and Physics*, **15**, 4399–4981.

Sandoval-Soto L, Kesselmeier M, Schmitt V, Wild A, Kesselmeier J (2012) Observations of the uptake of carbonyl sulfide (COS) by trees under elevated atmospheric carbon dioxide concentrations. *Biogeosciences*, **9**, 2935–2945.

Sandoval-Soto L, Stanimirov M, Hobe MV, Schmitt V, Valdes J, Wild A, Kesselmeier J (2005) Global uptake of carbonyl sulfide (COS) by terrestrial vegetation: Estimates corrected by deposition velocities normalized to the uptake of carbon dioxide (CO_2). *Biogeosciences*, **2**, 125–132.

Sauze J, Jones SP, Wingate L, Wohl S, Ogée J (2018) The role of soil pH on soil carbonic anhydrase activity. *Biogeosciences*, **15**, 597–612.

Sauze J, Ogée J, Maron P-A et al. (2017) The interaction of soil phototrophs and fungi with pH and their impact on soil CO_2, $CO^{18}O$ and OCS exchange. *Soil Biology and Biochemistry*, **115**, 371–382.

Scanlon BR, Nicot JP, Massmann JW (2002) Soil gas movement in unsaturated systems. In: *Soil Physics Companion*, pp. 297–341. CRC Press: Boca Raton, FL.

Schenk S, Kesselmeier J, Anders E (2004) How Does the Exchange of One Oxygen Atom with Sulfur Affect the Catalytic Cycle of Carbonic Anhydrase? *Chemistry - A European Journal*, **10**, 3091–3105.

Schimel D, Pavlick R, Fisher JB et al. (2015) Observing terrestrial ecosystems and the carbon cycle from space. *Global Change Biology*, **21**, 1762–1776.

Schimel DS, Braswell BH, Holland EA et al. (1994) Climatic, edaphic and biotic controls over storage and turnover of carbon in soils. *Global Biogeochemical Cycles*, **8**, 279–293.

Seibt U, Kesselmeier J, Sandoval-Soto L, Kuhn U, Berry JA (2010) A kinetic analysis of leaf uptake of COS and its relation to transpiration, photosynthesis and carbon isotope fractionation. *Biogeosciences*, **7**, 333–341.

Seibt U, Wingate L, Berry JA (2007) Nocturnal stomatal conductance effects on the $\delta^{18}O$ signatures of foliage gas exchange observed in two forest ecosystems. *Tree Physiology*, **27**, 585.

Seibt U, Wingate L, Lloyd J, Berry JA (2006) Diurnally variable $\delta^{18}O$ signatures of soil CO_2 fluxes indicate carbonic anhydrase activity in a forest soil. *Journal of Geophysical Research*, **111**, G04005.

Sellers P, Sellers P, Dickinson RE et al. (1997a) Modeling the exchanges of energy, water, and carbon between continents and the atmosphere. *Science*, **275**, 502.

Sellers PJ, Berry JA, Collatz GJ, Field CB, Hall FG (1992) Canopy Reflectance, Photosynthesis,and Transpiration. III. A Reanalysis Using Improved Leaf Models and a New Canopy Integration Scheme. *Remote Sensing of Environment*, **42**, 187–216.

Sellers PJ, Hall FG, Kelly RD et al. (1997b) BOREAS in 1997: Experiment overview, scientific results, and future directions. *Journal of Geophysical Research-Atmospheres*, **102**, 28731–28769.

Serna-Chavez HM, Fierer N, Van Bodegom PM (2013) Global drivers and patterns of microbial abundance in soil. *Global Ecology and Biogeography*, **22**, 1162–1172.

Silverman DN (1973) Carbonic anhydrase catalyzed oxygen-18 exchange between bicarbonate and water. *Archives of biochemistry and biophysics*, **155**, 452–457.

Silverman DN (1982) Carbonic anhydrase: oxygen-18 exchange catalyzed by an enzyme with rate-contributing proton-transfer steps. *Methods in enzymology*, **87**, 732–752.

Sinclair TR, Murphy CE, Knoerr KR (1976) Development and Evaluation of Simplified Models for Simulating Canopy Photosynthesis and Transpiration. *Journal of Applied Ecology*, **13**, 813–829.

Skole D, Tucker C (1993) Tropical Deforestation and Habitat Fragmentation in the Amazon:

Satellite Data from 1978 to 1988. *Science*, **260**, 1905–1910.

Slocum G (1955) Has the amount of carbon dioxide in the atmosphere changed significantly since the beginning of the twentieth century? *Monthly Weather Review*, **10**, 225–231.

Smith K, Jakubzick C, Whittam T, Ferry J (1999) Carbonic anhydrase is an ancient enzyme widespread in prokaryotes. *Proceedings of the National Academy of Sciences of the United States of America*, **96**, 15184–15189.

So AKC, Espie GS, Williams EB, Shively JM, Heinhorst S, Cannon GC (2004) A Novel Evolutionary Lineage of Carbonic Anhydrase (Class) Is a Component of the Carboxysome Shell. *Journal of bacteriology*, **186**, 623–630.

Sonawane BV, Cousins AB (2018) Uncertainties and limitations of using ^{13}C and ^{18}O leaf isotope exchange to estimate the temperature response of mesophyll CO_2 conductance in C_3 plants. *New Phytologist*, **169**, 1850.

Stern L, Baisden W, Amundson R (1999) Processes controlling the oxygen isotope ratio of soil CO2: Analytic and numerical modeling. *Geochimica et Cosmochimica Acta*, **63**, 799–814.

Stern LA, Amundson R, Baisden WT (2001) Influence of soils on oxygen isotope ratio of atmospheric CO_2. *Global Biogeochemical Cycles*, **15**, 753–759.

Still CJ, Riley WJ, Biraud SC et al. (2009) Influence of clouds and diffuse radiation on ecosystem-atmosphere CO 2and CO 18O exchanges. *Journal of Geophysical Research*, **114**, G01018.

Stimler K, Berry JA, Yakir D (2012) Effects of Carbonyl Sulfide and Carbonic Anhydrase on Stomatal Conductance. *Plant Physiology*, **158**, 524–530.

Stimler K, Berry JA, Montzka SA, Yakir D (2011) Association between carbonyl sulfide uptake and $^{18}\Delta$ during gas exchange in C_3 and C_4 leaves. *Plant Physiology*, **157**, 509–517.

Stimler K, Montzka SA, Berry JA, Rudich Y, Yakir D (2010) Relationships between carbonyl sulfide (COS) and CO2 during leaf gas exchange. *New Phytologist*, **186**, 869–878.

Studer AJ, Gandin A, Kolbe AR, Wang L, Cousins AB, Brutnell TP (2014) A Limited Role for Carbonic Anhydrase in C_4 Photosynthesis as Revealed by a ca1ca2 Double Mutant in Maize. *Plant Physiology*, **165**, 608–617.

Sun W, Maseyk K, Lett C, Seibt U (2015) A soil diffusion-reaction model for surface COS flux: COSSM v1. *Geoscientific Model Development Discussions*, **8**, 5139–5182.

Svoronos PDN, Bruno TJ (2002) Carbonyl Sulfide: A Review of Its Chemistry and Properties. *Industrial & Engineering Chemistry Research*, **41**, 5321–5336.

Syrjänen L, Vermelho AB, de Almeida Rodrigues I et al. (2013) Cloning, Characterization, and Inhibition Studies of a β-Carbonic Anhydrase from Leishmania donovani chagasi, the Protozoan Parasite Responsible for Leishmaniasis. *Journal of Medicinal Chemistry*, **56**, 7372–7381.

Tang J, Riley WJ (2019) A Theory of Effective Microbial Substrate Affinity Parameters in Variably Saturated Soils and an Example Application to Aerobic Soil Heterotrophic Respiration. *Journal of Geophysical Research: Biogeosciences*, **124**, 918–940.

Tans P (1998) Oxygen isotopic equilibrium between carbon dioxide and water in soils. *Tellus B*, **50**, 163–178.

Tans PP, Fung IY, Takahashi T (1990) Observational contrains on the global atmospheric CO_2 budget. *Science*, **247**, 1431–1438.

Tholen D, Zhu X-G (2011) The Mechanistic Basis of Internal Conductance: A Theoretical Analysis of Mesophyll Cell Photosynthesis and CO_2 Diffusion. *Plant Physiology*, **156**, 90–105.

Ubierna N, Gandin A, Cousins AB (2018) The response of mesophyll conductance to short-term variation in CO_2 in the C_4 plants *Setaria viridis* and *Zea mays*. *Journal of Experimental Botany*, **69**, 1159–1170.

Ubierna N, Gandin A, Boyd RA, Cousins AB (2017) Temperature response of mesophyll

conductance in three C_4 species calculated with two methods: ^{18}O discrimination and *in vitro* V_{pmax}. *The New phytologist*, **214**, 66–80.

Uchikawa J, Zeebe RE (2012) The effect of carbonic anhydrase on the kinetics and equilibrium of the oxygen isotope exchange in the CO_2–H_2O system: Implications for $\delta^{18}O$ vital effects in biogenic carbonates. *Geochimica et Cosmochimica Acta*, **95**, 15–34.

Uedan K, Sugiyama T (1976) Purification and Characterization of Phosphoenolpyruvate Carboxylase from Maize Leaves. *Plant Physiol.*, **57**, 906.

Van Diest H, Kesselmeier J (2008) Soil atmosphere exchange of carbonyl sulfide (COS) regulated by diffusivity depending on water-filled pore space. *Biogeosciences*, **5**, 475–483.

Wehr R, Commane R, Munger JW et al. (2017) Dynamics of canopy stomatal conductance, transpiration, and evaporation in a temperate deciduous forest, validated by carbonyl sulfide uptake. *Biogeosciences*, **14**, 389–401.

Wehr R, Munger JW, Nelson DD, McManus JB, Zahniser MS, Wofsy SC, Saleska SR (2013) Long-term eddy covariance measurements of the isotopic composition of the ecosystem–atmosphere exchange of CO_2 in a temperate forest. *Agricultural and Forest Meteorology*, **181**, 69–84.

Welp LR, Keeling RF, Meijer HAJ et al. (2011) Interannual variability in the oxygen isotopes of atmospheric CO_2 driven by El Niño. *Nature*, **477**, 579–582.

Wenzel S, Cox PM, Eyring V, Friedlingstein P (2016) Projected land photosynthesis constrained by changes in the seasonal cycle of atmospheric CO_2. *Nature*, 1–9.

Whelan ME, Rhew RC (2015) Carbonyl sulfide produced by abiotic thermal and photodegradation of soil organic matter from wheat field substrate. *Journal of Geophysical Research: Biogeosciences*, **120**, 54–62.

Whelan ME, Hilton TW, Berry JA, Berkelhammer M, Desai AR, Campbell JE (2016) Carbonyl sulfide exchange in soils for better estimates of ecosystem carbon uptake. *Atmospheric Chemistry and Physics*, **16**, 3711–3726.

Whelan ME, Lennartz ST, Gimeno TE et al. (2018) Reviews and syntheses: Carbonyl sulfide as a multi-scale tracer for carbon and water cycles. *Biogeosciences*, **15**, 3625–3657.

Williams M, Rastetter EB, Fernandes DN, Goulden ML, Shaver GR, Johnson LC (1997) Predicting gross primary productivity in terrestrial ecosystems. *Ecological Applications*, **7**, 882–894.

Williams T, Flanagan LB, Coleman J (1996) Photosynthetic gas exchange and discrimination against $^{13}CO_2$ and $C^{18}O^{16}O$ in tobacco plants modified by an antisense construct to have low chloroplastic carbonic anhydrase. *Plant Physiology*, **112**, 319.

Williams TG, Flanagan LB (1996) Effect of changes in water content on photosynthesis, transpiration and discrimination against $^{13}CO_2$ and $C^{18}O^{16}O$ in *Pleurozium* and *Sphagnum*. *Oecologia*, **108**, 38–46.

Wingate L, Ogée J, Burlett R, Bosc A (2010) Strong seasonal disequilibrium measured between the oxygen isotope signals of leaf and soil CO_2 exchange. *Global Change Biology*, **16**, 3048–3064.

Wingate L, Ogée J, Cuntz M et al. (2009) The impact of soil microorganisms on the global budget of $\delta^{18}O$ in atmospheric CO_2. *Proceedings of the National Academy of Sciences of the United States of America*, **106**, 22411–22415.

Wingate L, Seibt U, Maseyk K et al. (2008) Evaporation and carbonic anhydrase activity recorded in oxygen isotope signatures of net CO_2 fluxes from a Mediterranean soil. *Global Change Biology*, **14**, 2178–2193.

Wohlfahrt G, Gu L (2015) Opinion: The many meanings of gross photosynthesis and their implication for photosynthesis research from leaf to globe. *Plant Cell and Environment*.

Wong S-C, Cowan IR, Farquhar GD (1979) Stomatal conductance correlates with photosynthetic capacity. *Nature*, **282**, 424–426.

Yakir D, Wang X-F (1996) Fluxes of CO_2 and water between terrestrial vegetation and the atmosphere estimated from isotope measurements. *Nature*, **380**, 515–517.

Yakir D, Berry JA, Giles L, Osmond C (1994) Isotopic heterogeneity of water in transpiring leaves: identification of the component that controls the $\delta^{18}O$ of atmospheric O_2 and CO_2. *Plant Cell and Environment*, **17**, 73–80.

Yi Z, Wang X, Sheng G, Zhang D, Zhou G, Fu J (2007) Soil uptake of carbonyl sulfide in subtropical forests with different successional stages in south China. *Journal of Geophysical Research*, **112**, D08302.

Yonemura S, Sandoval-Soto L, Kesselmeier J, Kuhn U, Hobe von M, Kawashima S (2005) Uptake of Carbonyl Sulfide (COS) and Emission of Dimethyl Sulfide (DMS) by Plants. *Phyton*, **45**, 17–24.

Zscheischler J, Mahecha MD, Avitabile V et al. (2017) Reviews and syntheses: An empirical spatiotemporal description of the global surface–atmosphere carbon fluxes: opportunities and data limitations. *Biogeosciences*, **14**, 3685–3703.

Zscheischler J, Mahecha MD, Buttlar von J et al. (2014) A few extreme events dominate global interannual variability in gross primary production. *Environmental Research Letters*, **9**, 035001.